



Politecnico di Torino

Master's degree in Aerospace Engineering A.a. 2024/2025 Graduation Session October 2025

Design of test benches for cryogenic hybrid rocket engines

Supervisors:

Candidate:

Andrea Ferrero

Dario Pastrone

Filippo Masseni

Tutor:

Vincenzo Mazzella

Marco Prodan



Abstract

This manuscript is the result of a 6 months internship in the French startup Alpha Impulsion, that is currently developing hybrid autophage rocket propulsion; in particular, the focus is on the design and development of test benches peculiar to this kind of motors, that have some specific requirements. In such a context of the development of new technologies, the capability to test new designs is essential, both to prove functionality and to explore new technical solutions; therefore, in the context of space propulsion, test benches are developed to study and improve the engine before performing flight tests. The design process of a generic test bench will be investigated, starting from the base requirements from the development team to the design of the facility in all its subsystems, like cryogenic (and not) fluid system, control systems, valves, actuation, measurement and acquisition systems, support structure, safety systems. This method will then be applied to two case studies: a generic autophage launcher (like the company's Grenat 200 kN obital satellite launcher) rocket motor and the slab burner test bench (10 kN test rig to investigate the regression rate in HRE). The preliminary design of each subsystem will be explained, integration and interfaces will be discussed, to conclude with a comparison between the two cases.

Acknowledgements

I want to thank my tutor, Vincenzo Mazzella and the whole Alpha Impulsion team for hosting me in Toulouse during the realization of this work. It was a very valuable learning experience. Thanks also to Prof. Andrea Ferrero for following me in this thesis work and helping me to realize my internship in Toulouse. Thanks to my Family, who supported me in these years of university with all themselves.

Table of Contents

Lis	st of	Tables	;	VIII
Lis	st of	Figure	es	X
1	Intr	oducti	on	1
	1.1	Overvi	ew of the history and current technology	. 1
	1.2	Introd	uction to hybrid rocket engine and autophage propulsion	. 5
		1.2.1	Hybrid rocket engine technology	. 5
		1.2.2	Hybrid autophage propulsion	. 7
	1.3	A prof	essional point of view: reference to kitsche's book	. 8
2	Des	ign pro	ocess of a test bench	11
	2.1	Overvi	ew of the design process	. 11
	2.2	Config	uration and preliminary concept of the structure	. 12
	2.3	Design	methods and softwares used	. 14
	2.4	Subsys	stems	. 16
	2.5	Struct	ure	. 16
	2.6	Fluids		
		2.6.1	Gases or cryogenic propellants?	. 18
		2.6.2	Introduction to cryogenics	. 19
	2.7	Main e	elements of a cryogenic system	. 19
		2.7.1	Material behavior at cryogenic temperatures	. 20
	2.8	Cryoge	enic tanks, Gas tanks and pressurization	. 24
		2.8.1	Overview of pressurization methods and design trade-offs .	
		2.8.2	Campaign-driven storage: number of tests and total volume	
		2.8.3	Blowdown-only sizing (no active regulation)	
		2.8.4	External-gas pressurization (inert pressurant)	
		2.8.5	Self-pressurization (autopressure by evaporation)	
		2.8.6	Pump-fed operation	
		2.8.7	Pressurant and purge gas selection	
		2.8.8	Purge sizing and dedicated storage	. 31

		2.8.9	Safety, codes and allowable stresses (overview)	31
		2.8.10	Trade-off summary and recommended workflow	32
	2.9	Pipes :	for cryogenic and gas application, feed lines sizing	33
		2.9.1	Insulation Strategies and Pipe Typologies	33
		2.9.2	Thermal Performance and Heat Leak	35
		2.9.3	Fluid Behaviour and Flow Regimes	35
		2.9.4	Pipe Coupling Methods	36
		2.9.5	Determination of pipe diameter	37
		2.9.6	Pressure loss estimation	38
		2.9.7	Normative and safety references	39
	2.10	Valves	and Line Components	41
		2.10.1	Cryogenic Control Valves	41
			Safety and Overpressure Components	42
		2.10.3	Placement and Sizing of Safety Devices	43
		2.10.4	Special Considerations for Oxygen Service	44
		2.10.5	Valve Sizing and Flow Coefficient Fundamentals	44
	2.11	Sensor	S	47
		2.11.1	Temperature Measurement	47
		2.11.2	Pressure Measurement	48
			Flow Measurement	48
			Liquid Level Measurement	49
			Sensor Placement Summary	49
		-	sition and control	51
			onmental considerations: noise reduction and exhaust dumping	53
	2.14	Integra	ation of the test bench	55
3	Car	4	1. Autoubono lourobon toet bonob	59
3	3.1		y n.1: Autophage launcher test bench	59 59
	3.1		o de la companya de l	59 60
	ე.∠	3.2.1	cations and Operative Requirements	60
		3.2.1 $3.2.2$	-	60
	3.3	-	Engine Configuration	61
	5.5	3.3.1	Benchmark of Existing Test Bench Configurations	62
		3.3.2	Preliminary Dimensional Estimation of the Test Stand Height	68
		3.3.3	Width of the Test Stand	69
		3.3.4	Mounting Platform	73
	3.4		stems	73
	3.5	Struct		73
	5.5	3.5.1	Second iteration of platform design	73
		3.5.1	Finite Element Analysis (FEM) of the Platform	74
		3.5.2 $3.5.3$	Auxiliary Elements and Ground Support	78
		0.0.0	ruxmary Elements and Ground Support	10

		3.5.4	Preliminar CAD model of the test bench structure		81
	3.6	Fluids			82
		3.6.1	Pressurizing and Purge Gas		82
		3.6.2	Fluid Path and Line Configuration		84
		3.6.3	Pressure Losses and System Evaluation		85
		3.6.4	Sizing of the pressurization system		85
		3.6.5	Feed System Design Choice and Preliminary P&ID $$		90
	3.7	Acquis	sition and Control		95
	3.8	Final (Considerations		97
4	Case	e study	y n.2: the Slab Burner test bench		99
	4.1	Overvi	iew of the project		99
	4.2		cations and operative requests		99
	4.3	Config	uration and preliminary concept of the structure		100
		4.3.1	Structure weight estimation		101
	4.4	Subsys	stems		102
	4.5	Fluids	feed system		102
		4.5.1	Specific subsystem considerations		107
		4.5.2	GOX and GN_2 storage system		107
		4.5.3	LOX storage and implementation for cooling		110
		4.5.4	Pipes, valves, and sensors		113
		4.5.5	Valve Sizing		117
		4.5.6	Ignition line		119
		4.5.7	Acquisition System interfaces		120
		4.5.8	Water Deluge System		120
		4.5.9	Final Configuration of the Feed System		121
	4.6	Acquis	sition System		123
		4.6.1	Control and Data Flow Architecture		123
		4.6.2	Measurement and Video Equipment		123
		4.6.3	Standard Sensors and Outputs		124
	4.7	Integra	ation and final considerations		127
5	Con	npariso	on between the two case studies		129
6	Con	clusio	ns and Future Developments		133
Bi	bliog	graphy			136

List of Tables

2.1	Thermophysical properties of selected cryogenic fluids	19
2.2	Comparison of typical pressurant and purge gases	31
2.3	Summary of recommended sensors and placement for the cryogenic	
	test bench	50
2.4	Comparison of main communication protocols for test bench applications	52
3.1	General specifications for the autophage launcher test bench 6	60
3.2	1 0	51
3.3	ı ı ı ı ı	76
3.4	1	30
$3.4 \\ 3.5$	v 1	31
3.6	Summary of self-pressurization calculations for the single-tank con-) Т
5.0	•	36
3.7	8	38
3.8	· · · · · · · · · · · · · · · · · · ·	90
3.9	Main feed system components (blowdown configuration; alternative	,0
J.9		95
4.1	Estimated component masses for the slab burner test bench 10	
4.2	Operating configurations of the slab burner fluid subsystem 10	
4.3	Estimated nitrogen volume required for purging operations 10	
4.4	Storage and operating parameters for oxygen and nitrogen systems 11	
4.5	Estimated LOX and GOX volumes required for weekly test operations 11	
4.6	Pressure losses and flow velocity in candidate LOX lines 11	
4.7	Summary of feed line sizing for gaseous systems (GOX and GN_2) . 11	
4.8	Summary of feed line sizing for liquid oxygen (LOX)	
4.9	Required C_v for pressure regulators	
4.10	Reference C_v values for valve and component sizing	
4.11	Calculated C_v for liquid oxygen components	7
4.12	Summary of required components for each fluid line	8

4.13	Direct-injection pump types for ignition fuel systems	119
4.14	Summary of transducers and signal types in the acquisition system	124

List of Figures

1.1	Historical rocket test stands	2
1.2	Modern liquid rocket engine test firing on small test bench (credits:	
	launcher space/NASA)	3
1.3	NASA A-2 test stand (credits: NASA)	3
1.4	Schematic diagram of a hybrid rocket engine showing oxidizer tank, injector, ignition system and solid fuel grain. (credits: CIAS/UNIPD)	5
1.5	details of the working principle of Alpha Impulsion's first HARE integrated within the launcher (credits:Alpha Impulsion)	7
2.1	Variation of Young's modulus and yield strength with decreasing temperature for typical structural metals [15]	21
2.2	Ultimate strength and fracture toughness curve for steels and austenitic stainless steels [15]	22
2.3	Thermal expansion coefficients of typical sealing polymers versus temperature [15]	23
2.4	Schematic cross-section of a typical cryogenic dewar tank showing the double-wall structure, vacuum insulation, and MLI layers (credits: Learn Pick)	24
2.5	Examples of commercial cryogenic storage tanks and internal vessel design (credits: Linde Engineering product catalogue)	26
2.6	Flexible vacuum-jacketed cryogenic pipe: internal section (courtesy	
	of Cryogas)	34
2.7	Rigid vacuum-jacketed cryogenic pipe (courtesy of Cryogas)	34
2.8	Typical heat leak values for vacuum-jacketed cryogenic piping (data courtesy of Cryogas, based on PHPK standards)	35
2.9	Typical two-phase flow patterns observed in cryogenic lines (adapted from Flow Studies)	36
2.10	Examples of cryogenic line couplings: quick-release (left) and bolted flange (right) (courtesy of Cryonorm)	37

2.12 2.13	Typical impingement velocity curve for gaseous oxygen, showing increasing ignition risk above 30 m/s. Adapted from EIGA Document 13/20, "Oxygen pipeline and piping systems", European Industrial Gases Association, 2020. Source: https://www.eiga.eu/uploads/documents/DOC013.pdfschematics of a typical Data Acquisition System (credits: Studytronics) water deluge system on a launchpad (credits: NASA)	39 51 53 54
3.1	Test bench of company RFA — Credits: RFA	63
3.2	Test bench of company ISAR Aerospace — Credits: ISAR Aerospace	
3.3	Test bench of company HY Impulse — Credits: HY Impulse	64
3.4	Test bench of company Latitude — Credits: Latitude	64
3.5	Test bench of company Opus Aerospace — Credits: Opus Aerospace	65
3.6	Test bench of company Orbex Aerospace — Credits: Orbex Aerospace	65
3.7	Test bench of company Skyrora — Credits: Skyrora	66
3.8	Test bench of company PLD Space — Credits: PLD Space	66
3.9	Test bench of company Arkadia Space — Credits: Arkadia Space .	67
3.10	Test bench of company Stoke Space — Credits: Stoke Space	67
3.11	Test bench of company ABL Space Systems — Credits: ABL Space	
	Systems	68
3.12	Constraints on height of the test stand (Credits: Alpha Impulsion) .	69
3.13	Example of container platforms used as structural load distribution	
	elements (Credits: Hacon Containers)	71
3.14	Different configurations of the thrust measurement system and motor	
	mount (Credits: Alpha Impulsion)	72
3.15	Preliminary configuration of the engine mounting base and support	
	platform (Credits: Alpha Impulsion)	74
3.16	CAD of the mounting platform with a grid paving to allow operator	
0.15	activity on top (Credits: Alpha Impulsion)	75
3.17	Dimensional details of the selected H-beam section (DIN 1025) —	
9 10	(Credits: Alpha Impulsion)	75
5.18	Mesh of the FEM model with refined zones near load application	77
9 10	points (Credits: Alpha Impulsion)	77 77
	Combined stress field at room temperature (Credits: Alpha Impulsion)	78
	Displacement field at room temperature (Credits: Alpha Impulsion) Combined stress distribution at 800°C (Credits: Alpha Impulsion).	79
	/	79
	Displacement field at 800°C (Credits: Alpha Impulsion)	81
	CAD model (Credits: Alpha Impulsion)	82
	CAD model (Credits: Alpha Impulsion)	83
5.40	orizo modor (orogios, riipiio impubitor)	-00

3.26	CAD model of the main fluid line placement (Credits: Alpha Impulsion)	84
3.27	Estimated fluid line pressure losses (Credits: Alpha Impulsion)	85
3.28	Density of oxygen at varying temperature and pressure (Credits:	
	The Engineering ToolBox)	87
3.29	Pressure variation versus time for different ullage fractions during	
	blowdown (Credits: Alpha Impulsion)	88
3.30	Pressure decay during blowdown for various tank capacities (Credits:	
	Alpha Impulsion)	89
3.31	CAD model including fluids feed system tanks and piping (Credits:	
	1 /	91
3.32	CAD model including fluids feed system tanks and piping (Credits:	
	1 1 /	92
3.33	PFD of the self pressurized tanks feed system (Credits: Alpha	
	1 /	93
3.34	PFD of the pump pressurized feed system (Credits: Alpha Impulsion)	94
4.1	preliminary CAD model of the configuration for the thest bench	
		.00
4.2	PFD diagram of the GOX-water configuration (credits: Alpha Im-	
		04
4.3	PFD diagram of the GOX-LOX configuration (credits: Alpha Im-	
		.05
4.4	PFD diagram of the LOX-LOX configuration (credits: Alpha Impul-	
	sion)	06
4.5	results of calculations for the quantity choice of 200 bar GOX cylinders 1	.08
4.6	CAD model of a preliminary configuration of LOX dewar, GOX and	
	GN2 tanks (credits: Alpha Impulsion)	12
4.7	Preliminary schematic of the fluid feed system, including control	
	and measurement components (Credits: Alpha Impulsion) 1	13
4.8	Preliminary schematic of the ignition fuel line with tank, high-	
	pressure pump, flow meter, injector, and non-return valve (Credits:	
	Alpha Impulsion)	20
4.9	PID diagram of the feed system preliminary design (credits: Alpha	
	1 /	22
4.10	O I	
	1 1 /	25
4 11	breakdown of input/output of the system (credits: Alpha Impulsion) 1	26

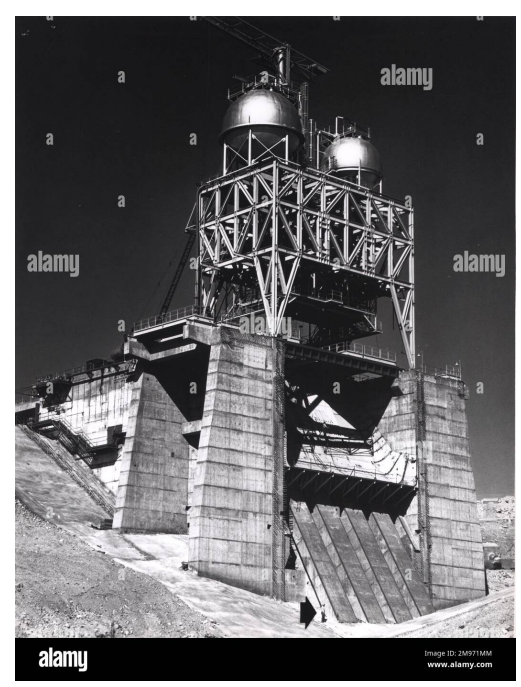
Chapter 1

Introduction

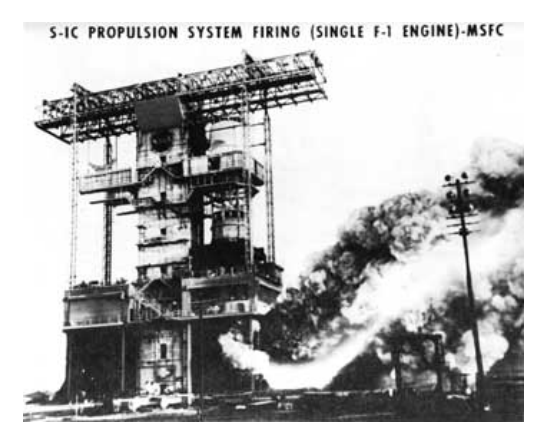
1.1 Overview of the history and current technology

The development of rocket propulsion systems has always been intrinsically linked to the capability of testing them on the ground under controlled and repeatable conditions. Since the first experimental rockets of the twentieth century, test benches have served not only as static structures to hold engines during firing but as complex systems that allow engineers to validate performance, analyze failures, and refine designs before flight. The first significant test facilities appeared in the 1930s and 1940s, with pioneers such as Robert Goddard in the United States and the German team at Peenemunde. These early facilities were rudimentary, often consisting of open-air concrete slabs with minimal measurement capabilities. The focus was primarily on containing the engine and observing basic thrust and combustion characteristics. However, even at this stage, the importance of safe and repeatable test conditions was evident. With the rapid evolution of liquidpropellant engines during World War II, exemplified by the V-2 rocket program, the need for more sophisticated test facilities became apparent. Large static test stands were constructed to support engines producing tens of kilonewtons of thrust. Instrumentation, although still basic by modern standards, began to include pressure and temperature sensors, as well as mechanical thrust measurement systems. Postwar, with the advent of the Cold War and the space race, rocket engine test benches underwent a significant transformation. The United States established dedicated test centers, such as NASA's Stennis Space Center in Mississippi, designed specifically for large-scale propulsion testing. In the Soviet Union, extensive facilities were developed in locations like Khimki and Baikonur. These infrastructures featured high-capacity propellant systems, advanced data acquisition equipment, and reinforced structures capable of withstanding the intense mechanical and

acoustic loads generated by engines exceeding 1 MN of thrust. [1, 2]



(a) Early Rocketdyne test stand (credits: Alamy)



(b) S-1C Propulsion System Firing, 1966 (credits: NASA/MSFC)

Figure 1.1: Historical rocket test stands.

The technological progression of test benches continued through the 1960s and 1970s with the introduction of cryogenic propellants (liquid hydrogen and liquid oxygen) and complex staged combustion cycles. This era necessitated the development of test systems capable of managing cryogenic fluid dynamics, high-precision measurement instrumentation, and real-time control architectures. Facilities such as the DLR's Lampoldshausen test center in Germany [3] became critical assets for European propulsion programs, notably for Ariane launchers. In contemporary aerospace engineering, test benches have evolved into highly integrated, modular platforms designed to accommodate a wide range of propulsion technologies. Modern facilities combine advanced Measurement, Control, and Command (MCC) systems with digital twin simulation models, allowing engineers to predict and analyze engine behavior with unprecedented accuracy. Data acquisition systems now operate at high sampling rates, interfacing with complex control loops to ensure both safety and fidelity of test operations. [4]

Furthermore, the trend towards reusable launch vehicles and innovative propulsion cycles (such as hybrid engines, autophage concepts, and electric propulsion) is driving a shift towards more flexible and reconfigurable test infrastructure.



Figure 1.2: Modern liquid rocket engine test firing on small test bench (credits: launcher space/NASA)



Figure 1.3: NASA A-2 test stand (credits: NASA)

Test benches today are often designed with modular architectures, enabling rapid adaptation to different engine configurations and test scenarios. Facilities now incorporate environmental control measures, such as sound suppression systems and emissions management, reflecting increased regulatory and societal awareness. Major aerospace companies and space agencies maintain dedicated test centers NASA's Stennis Space Center, SpaceX's McGregor site, Blue Origin's West Texas facilities, ESA's Lampoldshausen DLR, and Roscosmos' extensive test facilities. Alongside these, an increasing number of private companies and new space actors are developing bespoke test benches tailored to their specific propulsion technologies.[1]

In summary, test benches have transitioned from simple static platforms to highly engineered systems that are integral to the propulsion development process. The continuous drive for innovation in rocket engine technologies, particularly in hybrid and advanced cycle propulsion, ensures that the evolution of test infrastructure remains a critical focus for the aerospace community.

1.2 Introduction to hybrid rocket engine and autophage propulsion

1.2.1 Hybrid rocket engine technology

Hybrid rocket engines are propulsion systems that utilize a combination of solid fuel and liquid or gaseous oxidizer. This configuration bridges the gap between the simplicity and storability of solid rockets and the controllability of liquid propulsion systems. The typical arrangement involves a solid fuel grain, often composed of polymers like hydroxyl-terminated polybutadiene (HTPB) or high-density polyethylene (HDPE), and a liquid oxidizer such as liquid oxygen (LOX), nitrous oxide (N2O), or hydrogen peroxide (H2O2).[5]

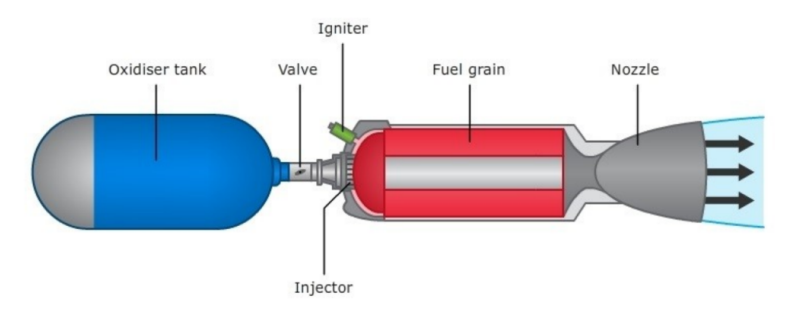


Figure 1.4: Schematic diagram of a hybrid rocket engine showing oxidizer tank, injector, ignition system and solid fuel grain. (credits: CIAS/UNIPD)

The fundamental operation of a hybrid rocket involves the injection of the oxidizer into a combustion chamber where it reacts with the surface of the solid fuel grain. The combustion process is governed by the regression rate of the solid fuel, which defines how quickly the fuel surface recedes during burning. The regression rate \dot{r} is often expressed as [6]:

$$\dot{r} = a G^n \tag{1.1}$$

where:

- a is an empirical constant dependent on the fuel-oxidizer combination,
- G is the oxidizer mass flux (kg/m²/s),
- n is the pressure exponent, typically ranging between 0.3 and 0.5 for most hybrid systems.

One of the primary engineering challenges in hybrid propulsion is achieving high regression rates to maximize thrust output. Several techniques have been explored to enhance regression rates, including:

- use of fuel additives,
- grain geometries with increased surface area (e.g., star or helical ports),
- active boundary layer manipulation techniques.

Hybrid engines inherently provide throttling capability by adjusting the oxidizer flow rate, a significant advantage over solid motors. Additionally, they offer improved safety compared to fully liquid systems, as the solid and liquid propellants are stored separately, reducing the risk of catastrophic failure due to leaks or handling mishaps.

However, hybrid systems face challenges related to combustion efficiency and stability. The diffusive mixing of oxidizer and fuel in the combustion chamber can result in incomplete combustion, leading to lower specific impulse compared to conventional liquid engines. Engineers mitigate these issues through optimized injector designs, turbulent flow enhancement, and secondary injection strategies. [6, 2]

Several hybrid propulsion variants have been developed, including:

- classical hybrid engines (separate solid fuel and liquid oxidizer),
- hybrid engines with paraffin-based fuels to increase regression rates,
- autophage hybrid engines, where the fuel casing itself is consumed during combustion, providing structural efficiency,
- hybrid-augmented liquid engines (HAL), utilizing hybrid stages as boosters.

Recent advancements in additive manufacturing have enabled complex grain geometries that optimize surface area exposure and flow dynamics, significantly enhancing performance characteristics. Moreover, modern hybrid engines are increasingly designed with modular configurations, allowing for flexible adaptation to various mission profiles and scalability in thrust levels.

The development cycle of hybrid engines typically involves iterative testing on ground-based test benches, with a strong emphasis on empirical validation due to the complexity of combustion physics. Test infrastructure must accommodate the dual-phase nature of the propellants, precise flow control mechanisms, and robust measurement systems capable of capturing transient combustion behaviors.

As aerospace industries seek cost-effective and safer propulsion alternatives, hybrid rocket engines continue to represent a promising technology, balancing performance, simplicity, and operational flexibility.[6]

1.2.2 Hybrid autophage propulsion

This particular innovative propulsion technology for space launchers is currently being pioneered by few realities in Europe, one of the main developers of this technology is the French startup Alpha Impulsion. The term 'hybrid' refers to the combination of a solid fuel grain, typically a cylindrical structure made of polymers such as Polyethylene, ABS, or PMMA, with a liquid oxidizer, which may include substances like hydrogen peroxide (H2O2), liquid oxygen (LOX), or nitrous oxide (N2O). These fuel-oxidizer combinations are inherently safer than conventional propellant mixtures, as they do not react spontaneously under normal conditions. Combustion occurs only when both components are introduced into a high-temperature and pressurized environment, thereby offering significant operational safety advantages. The 'autophage' concept signifies that the rocket progressively reduces its structural length during flight by consuming its own body as propellant. In this architecture, the solid fuel grain simultaneously functions as the structural support for the launcher. This design philosophy eliminates the need for additional metallic tanks, which otherwise contribute non-propulsive mass, resulting in an overall increase in mass efficiency and payload capability.

A schematic representation of the general autophage principle is provided for conceptual reference, while a dedicated diagram detailing the hybrid autophage configuration will be presented subsequently.

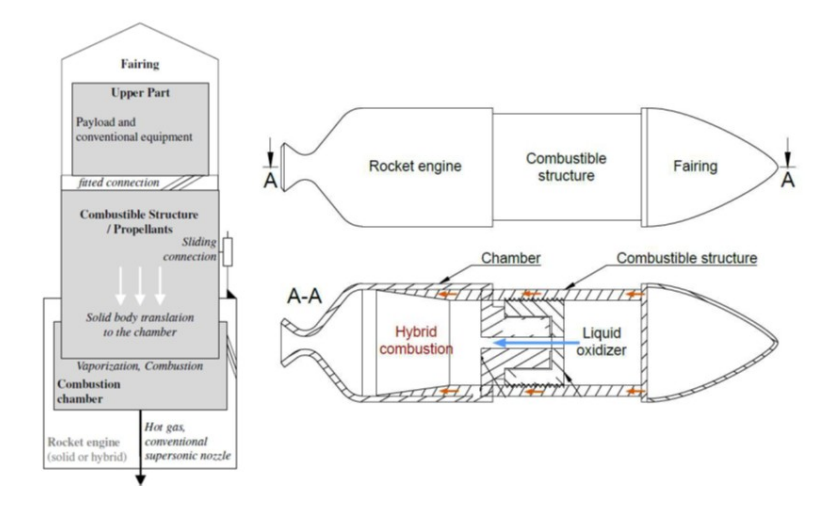


Figure 1.5: details of the working principle of Alpha Impulsion's first HARE integrated within the launcher (credits:Alpha Impulsion)

One of the primary differences between classical hybrid engines and autophage engines lies in the approach to static fire testing. For autophage engines, the test bench must accommodate a tall vertical stack of propellant structure to feed the combustion chamber continuously during firing. Each second of combustion demands a corresponding additional length of fuel casing to be mechanically inserted into the combustion zone. This requirement introduces specific challenges in the design of the test infrastructure, notably in terms of vertical space, feed mechanisms, and structural integration. Alpha Impulsion's strategy to address these challenges involves decoupling the combustion performance studies from the structural autophage behaviour during the initial testing phases. As such, the test campaigns will alternate between classical hybrid engine tests, where oxidizer injection is performed directly through the test bench to simulate nominal combustion conditions, and autophage tests that incrementally incorporate structural consumption dynamics. This approach enables a progressive validation of combustion parameters—such as pressure, mass flow rate, and regression behaviour—before engaging in full-scale autophage operational scenarios. [7, 8]

1.3 A professional point of view: reference to kitsche's book

While developing this thesis work, one of the main references literature-wise was the work of the german engineer Wolfgang Kitsche: In his seminal work 'Operation of a Cryogenic Rocket Engine', Kitsche provides a comprehensive perspective on the pivotal role of test benches in the development and validation of propulsion systems. According to Kitsche, a test bench is not merely a static structure for engine restraint but a fully integrated system that replicates the environmental and operational conditions the engine will encounter during flight. This philosophy elevates the test facility to a critical component of the propulsion system's development cycle, where design assumptions are empirically verified, and system-level interactions are meticulously analyzed. Kitsche emphasizes that the primary purpose of a test bench is to provide a safe, controlled, and instrumented environment to evaluate engine performance, characterize combustion stability, and validate the interaction between subsystems such as feed lines, pressurization systems, and thrust measurement devices. In particular, cryogenic propulsion systems impose stringent requirements on the test infrastructure, including precise temperature management, robust fluid handling capabilities, and high-fidelity data acquisition systems. The evolution of test benches, as described by Kitsche, follows the progression of propulsion technologies themselves. As engines have grown in complexity, introducing advanced cycles like staged combustion and expander cycles, test facilities have had to evolve in parallel, incorporating modular architectures, flexible control systems, and comprehensive safety frameworks. Kitsche notes that the operational cycle of a test bench encompasses preparation, hot-fire testing, and post-test analysis, each requiring meticulous planning and execution to ensure data reliability and operational safety. One of the key concepts introduced by Kitsche

is the Measurement, Control, and Command (MCC) system. He describes the MCC as the 'nerve center' of the test facility, responsible for orchestrating test sequences, monitoring real-time system states, and executing emergency shutdown procedures if anomalies are detected. The MCC's integration with data acquisition networks enables engineers to capture critical parameters such as thrust, chamber pressure, flow rates, and thermal profiles with high temporal resolution. Kitsche also underscores the importance of designing test benches with scalability and adaptability in mind. Given the iterative nature of engine development, test facilities must accommodate evolving engine configurations, allowing for incremental upgrades without necessitating complete infrastructural overhauls. This modularity is particularly relevant in the context of emerging propulsion concepts, including hybrid and autophage engines, where the interplay between engine structure and propellant behavior introduces new testing requirements. Furthermore, Kitsche discusses the operational challenges inherent to cryogenic testing, such as managing boil-off losses, ensuring proper insulation of feed systems, and maintaining accurate instrumentation calibration across a wide range of operating conditions. His methodology advocates for a holistic design approach, where mechanical, thermal, and fluidic subsystems are developed concurrently with a focus on system-level integration. In summary, Kitsche's professional insights establish a robust framework for the conceptualization and implementation of rocket engine test benches. His work serves as a foundational reference for engineers aiming to design test facilities that not only withstand the physical demands of propulsion testing but also deliver precise, repeatable, and actionable data to support the development of next-generation aerospace propulsion systems.[4]

Chapter 2

Design process of a test bench

2.1 Overview of the design process

The design process for a rocket engine test bench begins with a systematic definition of specifications and operational requests provided by the client or propulsion development team. These requirements form the foundation on which the entire test infrastructure is conceptualized, ensuring that the facility is tailored to the specific characteristics of the engine under evaluation and the objectives of the test campaign.

In the context of hybrid rocket engines, particularly those with autophage capabilities, the specification phase involves a detailed collection of technical parameters such as:

- Maximum and minimum thrust levels
- Chamber pressure range and expected transients
- Oxidizer type, storage requirements, and flow rate profiles
- Fuel grain dimensions and consumption behavior
- Thrust vectoring and gimbal requirements
- Desired test duration and firing cadence

These parameters dictate critical aspects of the test bench, including structural load paths, fluidic system capacities, thermal management strategies, and data acquisition needs. Operational requests also include logistical and regulatory considerations, such as:

- Safety distance from populated areas
- Environmental impact constraints (acoustic emissions, effluents)
- Availability of utilities (electricity, water, inert gases)
- Integration with existing site infrastructure
- Access requirements for personnel and equipment

An essential aspect of this phase is the iterative dialogue between the design team and the propulsion engineers. As described in the design methodology applied to Alpha Impulsion's test bench development, the specification phase is not a one-time deliverable, but an evolving dataset, refined through technical reviews, risk assessments, and trade-off analyses.

Kitsche emphasizes in his work that alignment of test facility capabilities with the operating cycle of the propulsion system is paramount. The test bench must replicate, as closely as possible, the conditions the engine will face during flight, both in terms of mechanical loads and fluidic dynamics. This necessitates a holistic evaluation of the engine's behavior, including start-up and shut-down transients, steady-state performance, and off-nominal scenarios.

In addition to technical specifications, operative requests often include tests of flexibility considerations. For emerging propulsion technologies, the test bench must be able to adapt to design evolutions, supporting modular upgrades to fluid circuits, instrumentation, and structural components.

Ultimately, the outcome of this phase is a comprehensive requirements matrix that serves as the reference framework for all subsequent design activities. This matrix defines the performance envelope of the test bench and ensures that every subsystem is developed in accordance with the operational demands of the propulsion system it will serve.

2.2 Configuration and preliminary concept of the structure

The configuration and preliminary concept of the test bench structure represent the first step in translating test requirements into an engineering design. This phase is critical, as it defines the overall architecture of the facility and establishes the constraints for subsequent subsystems. The methodology relies on an iterative process that integrates operational objectives, structural choices, subsystem integration, and cost considerations into a coherent and flexible concept [6].

The process begins with the operational definition of the test campaign: what needs to be tested, and under which conditions. The disposition of the engine—whether vertically or horizontally mounted—emerges directly from this decision:

- Vertical configurations: often adopted for hybrid engines, require tall supporting structures and flame deflectors to redirect exhaust gases.
- Horizontal configurations: emphasize containment and shielding, with easier access for personnel and instrumentation.

The choice strongly influences the dimensions of the test stand, the design of its foundation, and accessibility.

Once the orientation is defined, preliminary dimensions are derived from thrust level, chamber pressure, and expected flame length. Typical considerations include:

- additional clearances for thermal effects,
- vibration damping and structural stiffness,
- space for gimbal or thrust vectoring systems.

The selection of structural materials and construction methods is then addressed. Common options include:

- Reinforced concrete: robust and durable, but with limited adaptability once built.
- Steel frame structures: modular and strong, but subject to higher cost and corrosion.
- Container-based modular structures: cost-effective, deployable, and relocatable, though they may require reinforcement for high thrust loads.

The choice among these solutions depends on expected test campaign duration, scalability, regulatory compliance, and budget:

- long-term, high-power campaigns → permanent reinforced concrete facilities,
- flexible or evolving programs \rightarrow container-based modular systems.

Beyond structural considerations, integration of the subsystem must be anticipated early. The routing of feed lines, the placement of cryogenic tanks, flame deflectors, data acquisition racks, and operator platforms impose spatial constraints that directly influence the architecture. Neglecting these aspects can lead to costly redesigns later in the process.

Additional requirements may include:

- Thrust vector control: clearance and stiffness must be ensured if nozzle deflection is to be measured or actuated.
- Rapid interchangeability: enabling efficient replacement of engines or fuel grains across multiple campaigns.

The methodology is inherently iterative: initial layouts are drafted, reviewed, and refined through trade-offs between cost, adaptability, and performance. As Kitsche emphasizes in his work [4], the ability of a test bench to replicate flight conditions while maintaining flexibility is central to its effectiveness. This requirement is particularly relevant in the case of hybrid propulsion, where the uncertainties of the regression rate and the evolving designs demand adaptability [5].

At the end of this phase, the design team should have developed a preliminary concept with:

- defined orientation and estimated dimensions,
- identified material options,
- initial integration scheme for critical subsystems.

This concept provides the framework for detailed design activities while preserving flexibility to evolve with propulsion development needs [6].

2.3 Design methods and softwares used

The development of a rocket engine test bench requires the use of systematic design methods [9] supported by appropriate software tools. In the preliminary phase, the objective is not to produce a detailed design but rather to establish the viability of the configuration, confirm the adequacy of the structure under expected loads, and provide a framework for the integration of subsystems. For this reason, the methods employed are often simplified, using conservative assumptions and large safety margins, while more detailed analyses are left to subsequent design stages. The design process begins with preliminary hand calculations. These calculations include static load evaluations based on the thrust to be sustained, estimates of pressure and thermal loads on the structure, and approximate sizing of critical components such as beams or mounting plates. Although approximate, these evaluations are essential to provide a first-order validation of the design before moving to numerical simulations. Factors of safety are introduced at this stage to compensate for the uncertainties typical of early design, often with values in the range of 2 to 3 for structural elements and higher margins for cryogenic or pressurized subsystems. [4] The creation of a preliminary CAD model represents another key step. At this stage, the model is not meant to capture all engineering details but rather

to visualize the overall configuration of the test bench, including its dimensions, clearances, and integration of major subsystems. The CAD model allows the design team to identify potential clashes, confirm that accessibility requirements are satisfied, and communicate the concept to stakeholders. In addition, CAD representations serve as the basis for iterative design reviews and later integration with more detailed subsystem models. Finite Element Method (FEM) simulations are employed in the preliminary phase to evaluate the structural behavior of the test bench. Simplified FEM models, often using beam or shell elements, are sufficient to provide insight into stress distribution and deformation under static and dynamic loads. These analyses enable the identification of weak points and the validation of design choices without requiring detailed geometrical models. As the project progresses, the FEM simulations are refined with increasingly accurate representations, but their early use ensures that design iterations move in the right direction. For the fluid systems, simplified flow models are typically sufficient at this stage. One-dimensional analyses of oxidizer feed lines, pressurization circuits, and purge systems are performed using compressible flow equations and empirical correlations for pressure losses. These calculations confirm that the intended line diameters and tank pressurization strategies are adequate before considering more advanced computational fluid dynamics (CFD) analyses. By focusing on flow network behavior rather than detailed local fluid dynamics, the methodology ensures efficiency while maintaining reliability. In contrast, electronic subsystems and sensors do not usually impose significant constraints during the preliminary design. Since these components mainly consist of cabling, connectors, and compact instrumentation devices, their integration is flexible and can be adapted later in the design process. Routing of cables and sensor placement can be managed once the structural and fluidic layout is defined, with little impact on the overall dimensions of the test bench. This reduces the number of constraints to be addressed at the preliminary stage, allowing focus on the more critical elements of the design.

An important feature of the methodology is its iterative nature. The design process alternates between hand calculations, CAD modeling, FEM analyses, and reviews of requirements. Each loop refines the concept, incorporating insights from simulations and stakeholder feedback. This iterative approach ensures that the preliminary design remains aligned with operational requirements while retaining the flexibility to evolve as propulsion technologies develop. In summary, the combined use of analytical methods, CAD tools, and FEM simulations provides a robust framework for the preliminary design of rocket engine test benches. Hand calculations ensure conservative validation, CAD models offer spatial and integration insight, FEM analyses highlight structural feasibility, and simplified flow models secure the adequacy of fluid systems. Together, these tools create a coherent methodology that balances accuracy with efficiency, setting the foundation for detailed design activities. Softwares like Solidworks for 3D modelling and

ANSA/META by BetaCAE Systems are employed in the analysis and design of the components

2.4 Subsystems

The main subsystems analyzed and developed throughout this work are presented in the following sections. Each subsystem has been studied with respect to its specific functional requirements, design constraints, and integration within the overall test bench architecture.

2.5 Structure

The structural subsystem of a rocket engine test bench provides the primary support for the engine and associated hardware, transmitting loads to the ground and ensuring mechanical stability during static firings. Its design methodology begins with a survey of existing solutions adopted by other organizations. Benchmarking the structural concepts used by agencies, established aerospace companies, and other private ventures allows engineers to identify recurring approaches, understand their strengths and limitations, and select candidate solutions for adaptation. Containerbased platforms, reinforced concrete stands, and modular steel frameworks have all been widely employed in the industry, and their analysis offers valuable insight into the trade-offs between robustness, flexibility, and cost. [4] From this comparative study, the design process proceeds with the identification of load conditions: the static weight of the motor, the dynamic thrust during operation, and possible additional forces from thrust vectoring or structural resonances. These inputs define the baseline structural requirements and guide the selection of the supporting architecture. Several structural solutions can be adopted, each with specific advantages and constraints. Reinforced concrete offers robustness and durability, making it suitable for permanent facilities, though at the cost of flexibility. Modular steel frames provide adaptability and ease of assembly, with the drawback of higher material costs and potential corrosion. Container-based solutions strike a balance by enabling rapid deployment, disassembly, and reconfiguration, although they may require reinforcement to sustain high dynamic loads. The choice among these options depends on test objectives, expected campaign duration, and the need for scalability. [2] In the preliminary phase, a mounting platform must also be defined to serve as the interface between the engine and the structural system. This platform distributes loads, provides anchoring points for load cells and sensors, and ensures accessibility for technicians. The geometry and stiffness of this platform directly affect measurement accuracy and operational safety. Iterative design, combining hand calculations with simplified finite element analyses, is essential to

refine its dimensions and validate its performance under representative conditions. Thermal effects also influence structural design, as high-temperature exhaust and acoustic loads can cause material degradation or resonance phenomena. For this reason, protective coatings, refractory materials, or deflectors are integrated into the structural concept from the early stages. Accessibility, operator safety, and integration with auxiliary systems (cryogenic feed lines, instrumentation racks, water deluge systems) are additional constraints that shape the configuration. While structural cost is not the primary driver in preliminary design, it remains a practical consideration. Some solutions, such as container-based systems, can reduce investment while providing sufficient robustness, whereas more permanent designs may involve higher costs but deliver greater long-term stability. These trade-offs are evaluated within the broader context of test facility objectives and expected operational lifespan. The methodology, therefore, is not to converge immediately to a final solution, but to iterate between benchmarking of existing designs, load definition, configuration options, subsystem integration, and cost constraints. This ensures that the structural subsystem evolves into a design that is both technically sound and operationally viable, while maintaining flexibility for future modifications and upgrades. [10]

2.6 Fluids

The definition of the fluid subsystem is one of the first steps in the configuration of a rocket engine test bench, as it dictates how the propellant and pressurant are supplied to the engine. The bench may operate with conventional gases at ambient conditions or with cryogenic liquids such as liquid oxygen or liquid nitrogen, which introduce additional requirements in terms of storage, insulation, and safety.

Before selecting components such as tanks, valves, or transfer lines, it is necessary to choose the working fluids and the pressurization strategy. Typical approaches include blowdown systems, where the pressurant expands directly into the propellant tank, pump-fed systems, or schemes based on gas evaporation to maintain pressure. This choice strongly influences the overall layout and complexity of the bench [4, 11, 12].

2.6.1 Gases or cryogenic propellants?

When operating with gases at ambient conditions, the design is generally simpler. Calculations are limited to pressures, flows, and valve sizing, while thermodynamic effects are minor and easier to handle. In such cases, the choice of tanks and piping materials is relatively straightforward, and the system can be assembled and operated with fewer risks and lower costs. For preliminary testing or low-power applications, this solution can be an efficient option.

In contrast, cryogenic propellants introduce a higher level of complexity. The use of liquids such as liquid oxygen requires the implementation of insulation systems to minimize boil-off, materials resistant to very low temperatures, and careful management of transients during chill-down and evaporation. The routing of lines and the design of valves and fittings must consider the risk of leaks and the need for precise sealing.

Despite these challenges, cryogenic systems are often preferred in advanced testing scenarios. The main reasons for this preference include their ability to store propellants with higher density, thereby allowing longer tests or higher thrust levels for the same storage volume, as well as the possibility of replicating flight conditions more accurately. Moreover, cryogenic oxidizers such as liquid oxygen provide higher specific impulse compared to storable oxidizers, making them the natural choice for most high-performance propulsion systems. For these reasons, the design of cryogenic feed systems becomes a central focus of test bench development, and the following sections will provide a more detailed analysis of their components and methodologies [4, 13].

2.6.2 Introduction to cryogenics

A gas or liquid is considered *cryogenic* when its temperature is lower than $123 \,\mathrm{K}$ ($-150\,^{\circ}\mathrm{C}$). In rocket propulsion, the most relevant cryogenic substances are helium, oxygen, and nitrogen, whose main thermophysical properties are reported in Table 2.1 [11, 14].

Property Helium-4 (He) Nitrogen (N₂) Oxygen (O_2) Gas density (0 °C, 1 bar) 0.176 kg/m^3 1.429 kg/m^3 1.250 kg/m^3 77.37 K (-195.8°C) Boiling temperature (1 atm) $4.224 \text{ K} (-268.9 \,^{\circ}\text{C})$ 90.18 K (-182.2 °C) 124.96 kg/m^3 1141.0 kg/m^3 808.6 kg/m^3 Liquid density (boiling) 4.475 kg/m^3 16.891 kg/m^3 4.614 kg/m^3 Vapor density (boiling) Latent heat of vaporization 4.878 kcal/kg50.87 kcal/kg47.46 kcal/kgGas volume from 1 L liquid 748 L 854 L691 L 5.20 K154.58 K $126.20 \ K$ Critical temperature 50.43 bar 33.99 bar 2.275 barCritical pressure Critical density 69.64 kg/m^3 436.1 kg/m^3 314.0 kg/m^3 54.35 K (-218.8 °C) 63.15 K (-210.0 °C) Triple point temperature Triple point pressure 0.00152 bar0.1253 bar

Table 2.1: Thermophysical properties of selected cryogenic fluids

When stored in liquid phase, gases such as oxygen, nitrogen, and helium are considered cryogenic. Among these, helium requires special attention: it is harder to employ in liquid form for test bench applications, as any phase transformation in which it is involved provides enough energy to rapidly vaporize it.

The choice of liquid oxygen (LOX) as oxidizer usually does not fall within the scope of the test bench design, since it is normally specified directly by the engine manufacturer. What can instead be selected at the facility level are the auxiliary fluids used for purging and cooling operations. In this context, helium and liquid nitrogen (LN_2) are suitable candidates for cooling down the feed lines and purging oxygen from the circuits. Each of these gases presents specific advantages and limitations, which must be carefully compared to identify the most appropriate solution for a given test campaign [12, 13].

2.7 Main elements of a cryogenic system

The principal elements of a cryogenic fluid system are:

- 1. Tanks
- 2. Pipes
- 3. Control valves

- 4. Relief valves and burst disks
- 5. Measurement system
- 6. Pressurization system
- 7. Gaskets

In a typical cryogenic test bench, these elements are arranged in a logical sequence that follows the flow of the propellant from storage to the engine. The tanks, located at the core of the facility, store the cryogenic fluids and feed them into insulated pipes that transport the liquids toward the combustion chamber. Along these lines, control valves regulate flow and pressure, while relief valves and burst disks provide essential safety functions. The pressurization system interfaces with the tanks to ensure the required operating pressure, and gaskets and seals are integrated throughout the system to guarantee tightness under cryogenic conditions. Finally, the measurement system is distributed across all these subsystems, acquiring data on temperature, pressure, and flow to enable safe and controlled operation.

Each component will be further investigated in the subsequent chapters. Before doing so, it is essential to understand the peculiar behaviour of materials under cryogenic conditions, as this governs the reliability and safety of the entire system [4, 11].

2.7.1 Material behavior at cryogenic temperatures

The understanding of material behavior at cryogenic temperatures is fundamental for the design of safe and reliable test benches operating with liquid oxygen, nitrogen, or other low-temperature propellants. As discussed by Polinski [15], cryogenic environments significantly affect the mechanical, thermal, and chemical properties of materials. The selection of metals and sealing materials must therefore be based on both their mechanical response and their compatibility with the working fluids.

From a design standpoint, two main categories of materials must be evaluated:

- **Metallic materials** used for tanks, piping, valves, and structural components;
- Sealing and polymeric materials used for gaskets, O-rings, and valve seats.

Metallic materials At cryogenic temperatures, the general trend for most metals is an increase in yield strength, ultimate tensile strength, and elastic modulus. This occurs because the movement of dislocations within the crystal lattice is restricted, making the material stiffer and stronger. However, toughness and ductility tend to

decrease as temperature drops, sometimes leading to a ductile-to-brittle transition. Materials exhibiting this transition, typically those with a body-centered-cubic (bcc) crystal structure (e.g., plain carbon steels), are unsuitable for cryogenic use. Conversely, face-centered-cubic (fcc) metals such as austenitic stainless steels (e.g., 304L and 316L), aluminum, and copper retain ductility and high impact resistance even at liquid helium temperature, and are therefore the preferred choice for cryogenic lines and pressure vessels.

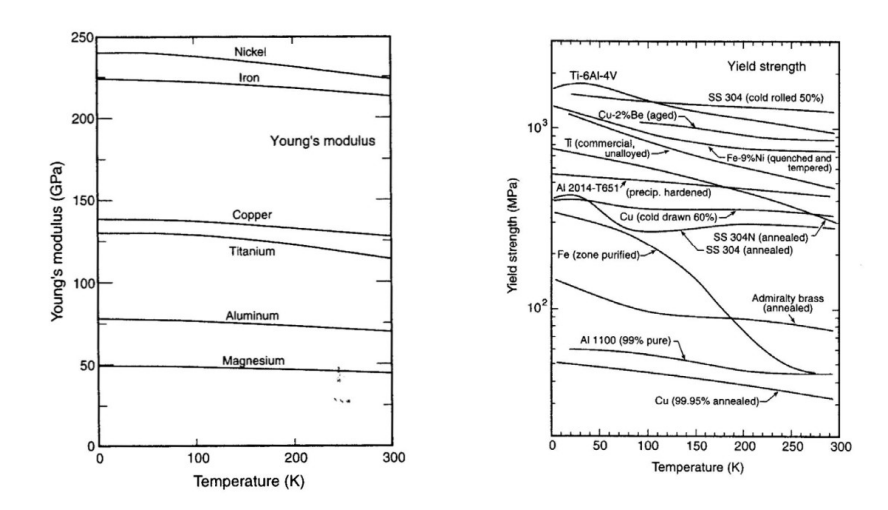
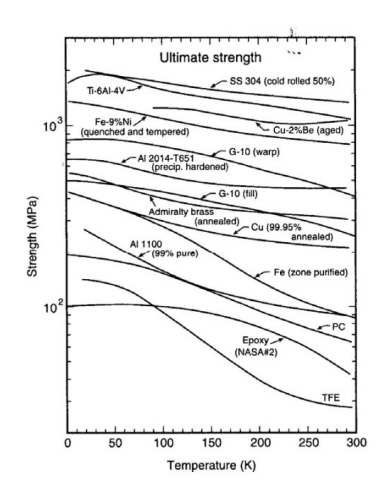


Figure 2.1: Variation of Young's modulus and yield strength with decreasing temperature for typical structural metals [15].

Impact energy and ductility can be further visualized through the Charpy impact test results, where a sharp decrease in absorbed energy marks the transition from ductile to brittle behavior. This transition temperature must always remain below the lowest expected operating temperature of the system.



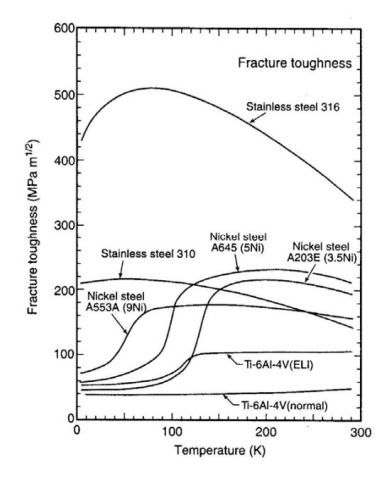


Figure 2.2: Ultimate strength and fracture toughness curve for steels and austenitic stainless steels [15].

In addition to mechanical behavior, differential thermal contraction must be accounted for. Each material exhibits a specific coefficient of thermal expansion, and differences among components can lead to the formation of stresses, leaks, or even structural failure. To mitigate this, flexible connections such as bellows, expansion joints, or compliant supports are commonly introduced in cryogenic systems.

Sealing and polymeric materials At low temperatures, most elastomers lose elasticity and become rigid or brittle, compromising sealing capability. Polinski [15] highlights that only certain fluoropolymers (e.g., PTFE, FKM, or specific cryogenic-grade perfluoroelastomers) maintain sufficient flexibility and low gas permeability under cryogenic conditions. The thermal contraction of these materials must be carefully evaluated to ensure proper compression in the sealing interface, avoiding both excessive deformation and loss of contact pressure. Figure 2.3 shows typical linear expansion data for selected polymeric materials used in cryogenic seals.

Chemical compatibility is equally critical: while helium and nitrogen are inert and pose no risk of reaction, liquid oxygen (LOX) is a strong oxidizer that can decompose or ignite organic materials. Therefore, all sealing elements in contact with LOX must be oxygen-certified, and lubricants must be fluorinated and non-flammable, such as the *Krytox* series of perfluoropolyether greases.

Overall, stainless steels 304L and 316L, combined with PTFE-based seals and oxygen-compatible greases, represent the most reliable configuration for the cryogenic fluid systems described in this work.

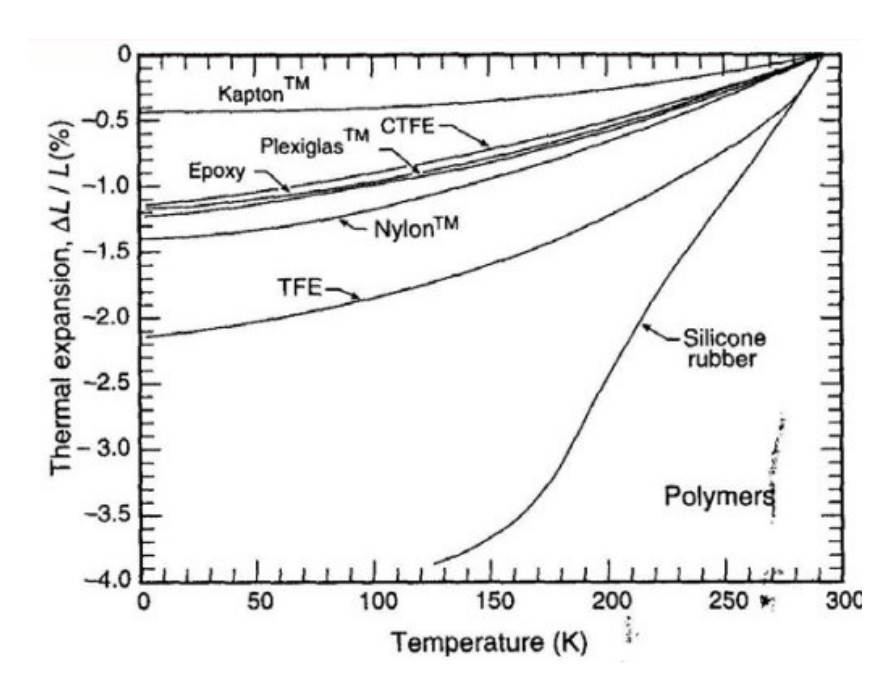


Figure 2.3: Thermal expansion coefficients of typical sealing polymers versus temperature [15].

2.8 Cryogenic tanks, Gas tanks and pressurization

Cryogenic storage tanks, commonly referred to as *dewars*, are pressure vessels specifically designed to store liquefied gases at very low temperatures. Their function is to maintain the stored fluid below its boiling point while minimizing thermal losses and ensuring operational safety [11, 16, 17].

Construction and materials A typical cryogenic tank consists of an inner and an outer vessel separated by an evacuated space that provides thermal insulation. The inner vessel is usually fabricated from austenitic stainless steels (such as 304L or 316L) or aluminum alloys, which retain ductility and toughness at cryogenic temperatures [4]. The outer shell is generally made of carbon steel or stainless steel, providing mechanical strength and protection against environmental effects. Between the two walls, multilayer insulation (MLI) composed of alternating reflective foils and spacer materials further reduces radiative heat transfer [18]. The inner tank is mechanically supported by low-thermal-conductivity structures—such as fiberglass-reinforced polymer struts or thin-walled supports—to minimize conductive heat paths, while accommodating differential thermal contraction.

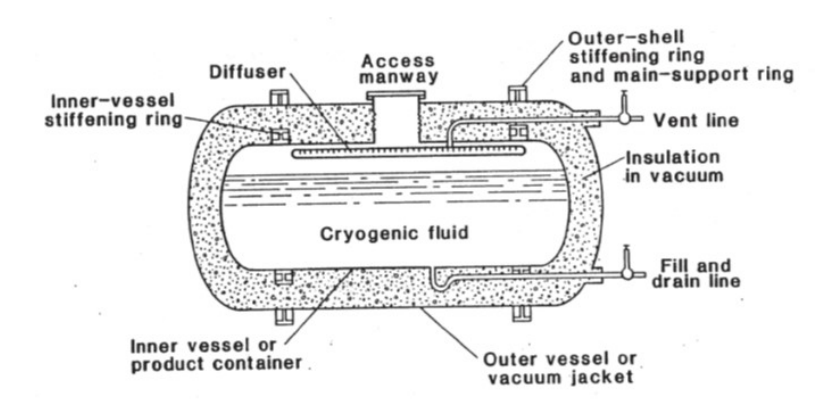


Figure 2.4: Schematic cross-section of a typical cryogenic dewar tank showing the double-wall structure, vacuum insulation, and MLI layers (credits: Learn Pick).

All tank penetrations, including fill and drain lines, are equipped with cryogenicrated valves and seals to ensure leak-tightness despite cyclic thermal contraction. Even with efficient insulation, a small amount of heat ingress is inevitable, leading to gradual evaporation of the stored liquid and consequent pressure rise inside the vessel. Therefore, venting systems are integral to tank safety [16]. **Operating principles** Cryogenic tanks are designed based on the required storage capacity, working pressure, and intended operational mode. Orientation (vertical or horizontal) is selected depending on available space and fluid management strategy [11].

Filling. Tanks can be filled using cryogenic pumps or by gravity feed from a higher reservoir. Flow rates and temperature gradients must be carefully controlled to prevent excessive thermal stress on internal components.

Pressure regulation. To maintain stable operating conditions, tanks are fitted with pressure control devices such as relief valves, burst disks, and in some cases active pressure regulators [17]. Boil-off gases resulting from liquid evaporation may either be vented to the atmosphere or recovered for reuse in pressurization or purge systems.

Temperature control. Continuous temperature monitoring is essential to detect any abnormal heat ingress or instability in the stored liquid. Sensors installed at multiple levels inside the tank allow precise detection of temperature gradients, ensuring that corrective measures (e.g., venting or re-cooling) can be taken promptly.

Safety features. Safety systems are fundamental to cryogenic tank design. Pressure relief valves and burst disks protect the vessel from overpressure, while flame arrestors are required for flammable fluids such as liquid hydrogen [16]. Emergency venting systems provide a controlled discharge path in the event of rapid pressure buildup.

Handling boil-off gases. Depending on the type of stored cryogen, the management of boil-off gases varies. For inert gases like nitrogen, venting is generally acceptable. For oxidizers such as oxygen, venting systems must ensure safe dispersion to avoid enrichment of the surrounding atmosphere. In the case of hydrogen, boil-off must be managed with special care, often through recovery or recondensation systems due to its high flammability [18].

Material compatibility. Material selection must prevent chemical reactions with the stored substance. In particular, hydrocarbons must not be used in contact with liquid oxygen due to the risk of spontaneous ignition. For hydrogen service, resistance to hydrogen embrittlement becomes a critical factor, influencing both alloy selection and fabrication techniques [11].

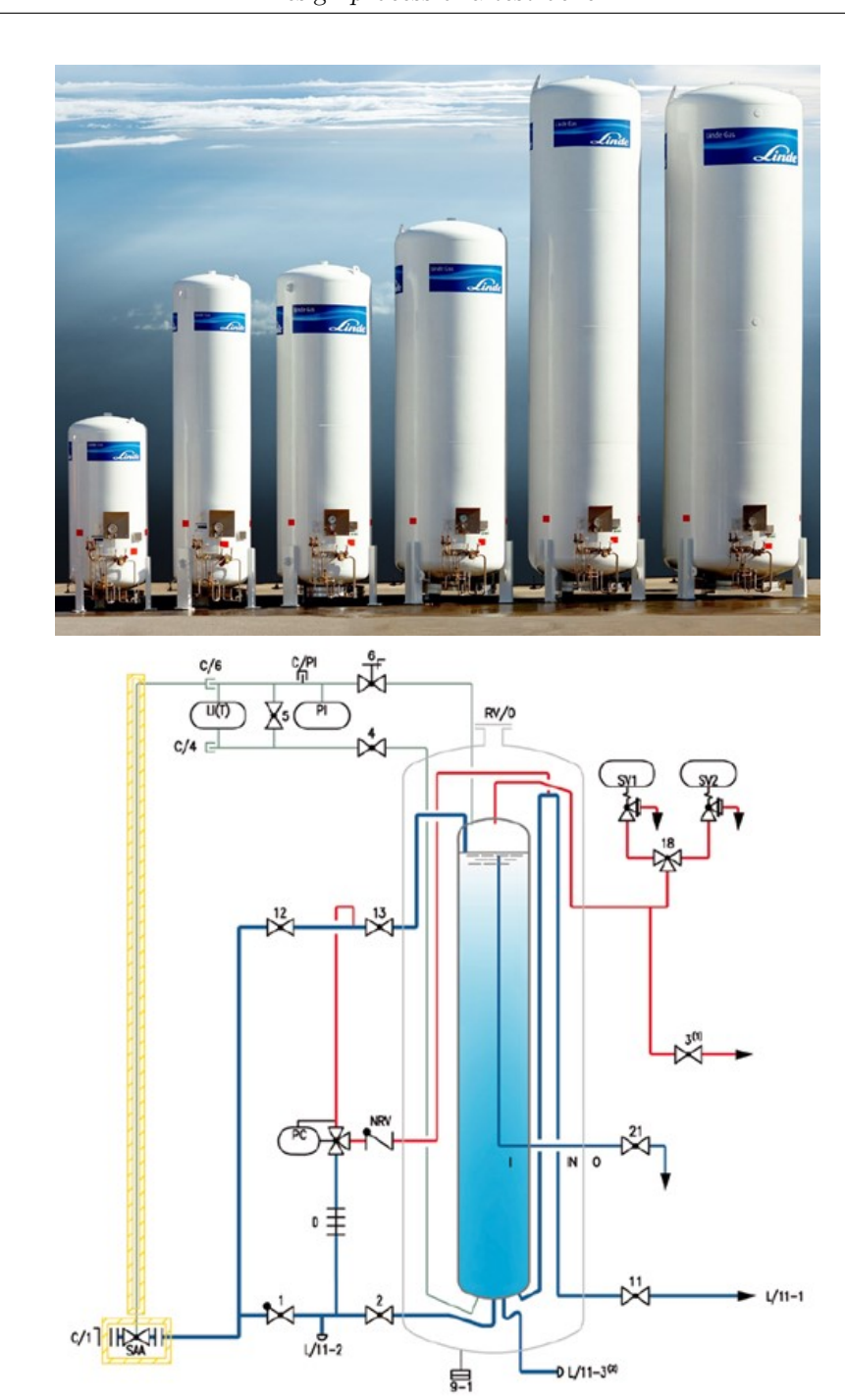


Figure 2.5: Examples of commercial cryogenic storage tanks and internal vessel design (credits: Linde Engineering product catalogue).

Cryogenic tanks represent one of the most safety-critical subsystems of the

feed architecture. Their design requires the integration of mechanical, thermal, and fluid-dynamic analyses to guarantee safe operation under all expected test conditions [4, 16, 11].

The sizing of cryogenic tanks and the choice of pressurization strategy are central to ensuring that the engine receives the required mass flow, pressure, and temperature, while maintaining safe and controllable operations. In this work we adopt a pragmatic, preliminary method—built from standard cryogenic practice and cross-checked against widely used references—that enables rapid early-phase trade-offs among storage volume, run time, allowable pressure drop, cost, and operational complexity [11, 19, 6, 20, 21, 22].

We distinguish three canonical feed architectures:

- 1. External-gas pressurization: an inert gas $(GN_2 \text{ or He})$ regulates the ullage pressure independently of liquid thermodynamics.
- 2. **Self-pressurization**: a controlled fraction of the cryogen is evaporated to set ullage pressure via $P_{\text{sat}}(T)$.
- 3. **Pump-fed operation**: pumps decouple line pressure from tank pressure, enabling lower storage pressure and tighter control.

In addition, purge requirements (GN_2/He) for safety and operability must be sized consistently with storage choices [23, 24, 25].

2.8.1 Overview of pressurization methods and design tradeoffs

External-gas pressurization. Using an external pressurant gas decouples pressure control from the cryogenic liquid, simplifying regulation and enabling rapid response to transient demands. It avoids heater power during steady delivery and preserves low liquid temperature, reducing boil-off. Trade-offs: added infrastructure (bottles, regulators, manifolds), contamination control in oxygen service (cleanliness per ASTM G93), and logistics/cost of the gas supply [21, 26]. This is preferred when stable feed pressure and agile control outweigh mass efficiency.

Self-pressurization. A fraction of the liquid is evaporated and reintroduced in ullage to regulate pressure along the saturation curve. Pros: full fluid compatibility and compact integration. Cons: continuous energy input and precise thermal management to avoid pressure run-up; robust relief and venting are mandatory [20, 22]. Attractive for steady, medium-duration tests with simple plant topology.

Pump-fed operation. Cryogenic pumps allow low tank pressure with high delivery pressure at the engine, eliminating blowdown decay and enabling flight-like conditions. They introduce CAPEX/OPEX, pre-chill procedures, NPSH and cavitation constraints, and maintenance [6]. Choice among centrifugal / reciprocating / submersible depends on $(\dot{m}, \Delta P)$ and duty cycle.

Cross-cutting trade-offs (summary).

- **Performance vs. simplicity:** pumps > external-gas > self-press. for pressure stability; the inverse for hardware simplicity/integration.
- Safety vs. efficiency: lower tank pressures reduce stored energy but may require pumps; higher pressures favor blowdown but increase wall thickness and test pressures.
- Logistics & cost: helium and pumps are costly; nitrogen-based systems and blowdown tanks minimize procurement and maintenance.
- **Flexibility:** external-gas offers fast set-point changes; self-press. is thermally coupled; pumps are most flexible but operationally heavier.

2.8.2 Campaign-driven storage: number of tests and total volume

Let one test require a liquid mass $m_{\ell}^{(1)}$ (or an equivalent injected gas mass). For a campaign of N_{tests} tests, the baseline liquid requirement is

$$m_{\ell}^{(\text{tot})} = N_{\text{tests}} m_{\ell}^{(1)}.$$
 (2.1)

The *storage* mass must include operational margins:

$$m_{\ell}^{(\text{stor})} = m_{\ell}^{(\text{tot})} \left[1 + \phi_{\text{bo}} + \phi_{\text{heel}} + \phi_{\text{press}} \right],$$
 (2.2)

where $\phi_{\rm bo}$ covers expected boil-off, $\phi_{\rm heel}$ the residual liquid that cannot be drained (heel), and $\phi_{\rm press}$ any liquid consumed for self-pressurization. The nominal tank volume (excluding ullage) follows from $V_{\ell} = m_{\ell}^{\rm (stor)}/\rho_{\ell}$ at the storage temperature. The geometric tank volume with ullage fraction β is

$$V_{\rm t} = \frac{V_{\ell}}{1-\beta}, \quad \beta \in [0.10, 0.35] \text{ typically, per handling/slosh/thermal margins [19, 11].}$$

$$(2.3)$$

When cylinder bundles are used for gases (GOX/GN₂), convert liquid-equivalent requirements to gas volume/mass using reference densities and compressibility factors for the storage state [19, 22, 27, 28].

2.8.3 Blowdown-only sizing (no active regulation)

A common early-phase approach feeds the engine by opening a valve and letting tank pressure decay as ullage expands. Two bounding models are used.

Isothermal blowdown (conservative for volume). With initial gas volume $V_{g,i} = \beta V_t$ and final gas volume $V_{g,f} = \beta V_t + \Delta V_\ell$, where $\Delta V_\ell = \dot{m}_\ell t/\rho_\ell$ is the liquid volume withdrawn in time t, the ideal-gas relation yields

$$P_f = P_i \frac{V_{g,i}}{V_{q,f}} = P_i \frac{\beta V_t}{\beta V_t + \dot{m}_\ell t / \rho_\ell}.$$
 (2.4)

Given $(P_i, P_f, \dot{m}_\ell, t, \rho_\ell)$, solve Eq. (2.4) for V_t :

$$V_{\rm t} \ge \frac{\dot{m}_{\ell}t}{\rho_{\ell}} \frac{P_f}{\beta \left(P_i - P_f\right)}. \tag{2.5}$$

Adiabatic blowdown (lower bound on volume). With $PV^{\gamma} = \text{const}$ for the ullage (diatomic vapor: $\gamma \simeq 1.3-1.4$),

$$P_f = P_i \left(\frac{V_{g,i}}{V_{g,f}}\right)^{\gamma} = P_i \left(\frac{\beta V_t}{\beta V_t + \dot{m}_{\ell} t/\rho_{\ell}}\right)^{\gamma}, \tag{2.6}$$

so that

$$V_{\rm t} \ge \frac{\dot{m}_{\ell}t}{\rho_{\ell}} \frac{P_f^{1/\gamma}}{\beta \left(P_i^{1/\gamma} - P_f^{1/\gamma}\right)}.$$
 (2.7)

Designers typically take the larger of Eqs. (2.5)–(2.7) and add margin for transients and uncertainties [19, 11]. Note that a *larger ullage* ($\beta \uparrow$) reduces pressure drop but decreases liquid capacity, increasing geometric volume and cost; this trade-off is central to blowdown tanks.

Hold-time and heat leak. Even in vacuum-MLI vessels, heat leak $Q_{\rm in}$ introduces a natural boil-off rate $\dot{m}_{\rm bo} \simeq Q_{\rm in}/h_{\rm lv}$, with $h_{\rm lv}$ latent heat. A coarse estimate is

$$Q_{\rm in} \approx \underbrace{\sum_{i} \frac{k_i A_i}{L_i} \Delta T}_{\text{supports, penetrations}} + \underbrace{\sigma \, \varepsilon_{\rm eff} \, A_{\rm rad} \, (T_{\rm amb}^4 - T_{\rm sh}^4)}_{\text{radiation}}, \tag{2.8}$$

where MLI reduces the effective emissivity ε_{eff} dramatically [11]. Hold-time constraints and allowed pressure rise (if unvented) may drive either larger volume or active vent/relief capacity [20].

2.8.4 External-gas pressurization (inert pressurant)

With an external pressurant, ullage pressure P_{set} is maintained by a regulator, decoupling pressure control from liquid thermodynamics and avoiding heater power during steady delivery [21, 20]. The required pressurant inventory (at storage conditions P_s, T_s) for a test of duration t and liquid outflow \dot{m}_{ℓ} is

$$n_{\text{req}} = \frac{P_{\text{set}}}{ZRT} \left(\beta V_{\text{t}} + \frac{\dot{m}_{\ell}t}{\rho_{\ell}} \right), \qquad m_{\text{req}} = n_{\text{req}} M_{p},$$
 (2.9)

and the equivalent bottle volume follows from the real-gas law at (P_s, T_s) [19, 22]. Cleanliness and compatibility are mandatory in oxygen service (materials, cleaning to ASTM G93; flow-velocity limits and ignition-risk mitigation per CGA G-4.4) [21, 26].

2.8.5 Self-pressurization (autopressure by evaporation)

Self-pressurization uses a controlled vapor mass flow \dot{m}_v via heaters/evaporators to lock pressure to the saturation curve $P_{\rm sat}(T)$ [11]. A steady energy balance gives a first sizing for heater power:

$$\dot{m}_v(h_v - h_\ell) \approx Q_{\rm in} + \dot{m}_\ell (h_\ell^{\rm out} - h_\ell^{\rm tank}), \tag{2.10}$$

with h_v, h_ℓ evaluated at tank conditions. Transient set-point changes and start-up require additional power margins. Relief and emergency venting must cover credible fault cases (heater run-away, valve failure) [20].

2.8.6 Pump-fed operation

Pumps enable high delivery pressure with modest tank pressure, improving storage efficiency and line control [6]. The tank still must prevent cavitation:

$$P_{\text{tank}} \ge P_{\text{sat}}(T) + \Delta P_{\text{inlet}} + \rho g \, \text{NPSH}_{\text{reg}}.$$
 (2.11)

Thermal conditioning of the inlet, avoidance of two-phase ingestion, and mechanical integration (contraction, vibration) are key. Relief/vent sizing must accommodate pump trip with continuing heat leak [20, 25]. While pumps reduce blowdown-induced ΔP , they introduce capital cost and maintenance; selection (centrifugal vs reciprocating vs submersible) depends on range $(\dot{m}, \Delta P)$ and duty cycle.

2.8.7 Pressurant and purge gas selection

Beyond tank pressurization, the same gas is often used for line cooldown, inerting, and post-test purging; logistics and compatibility therefore dominate the selection [23, 24, 25]. LN₂ is effective for cooling due to its boiling point proximity to

LOX, while He is superior for purging thanks to its lightness and non-condensability. A hybrid strategy (LN₂ for cooldown, He for final purge) balances cost, safety, and performance; this is consistent with practices at major cryogenic sites [2, 3].

Table 2.2: Comparison of typical pressurant and purge gases.

Gas	Main Advantages	Main Limitations
$\overline{ ext{LN}_2}$ He	Low cost and wide availability; boiling point close to LOX → efficient cooling; inert and safe in contact with oxygen. Completely inert and noncondensable; very effective purge gas; usable for leak detection; lightweight and diffusive.	ing risk; heavier vapor, less effective for purging; may freeze sensitive com- ponents. High cost and limited availability; poor cooling capability; supply-chain

2.8.8 Purge sizing and dedicated storage

Purge operations (cooldown, inerting, flame extinction, clearing LOX-rich volumes) define GN_2/He storage independent of propellant tanks [23, 24]. For a single purge, the required gas at 1 bar is

$$V_{\text{purge, 1bar}} = N_{\text{ex}} \left(V_{\text{pipes}} + V_{\text{chamber}} \right), \qquad N_{\text{ex}} \in [5,7],$$
 (2.12)

with conversion to storage conditions via real-gas scaling

 $V_s = V_{\text{purge, 1bar}}(P_{\text{1bar}}/P_s)(T_s/T_{\text{1bar}})/Z$ [19]. The campaign purge inventory multiplies this by the expected number of purges (including pre/post-test cycles and emergency inerting). Pressure level and timing are chosen to balance rapid dilution with mechanical/thermal constraints; moderate-pressure purge after a short natural decay is a robust baseline [25, 23].

2.8.9 Safety, codes and allowable stresses (overview)

Final wall thickness, joints and test pressures are governed by applicable vessel codes (e.g., EN/ASME), with allowable stresses at cryogenic temperature and weld efficiencies, plus proof and leak tests [11]. Oxygen service imposes additional constraints: material compatibility and cleaning (ASTM G93), flow-velocity limits and ignition-risk controls (CGA G-4.4) [21, 26]. Cryogenic vessel compatibility is addressed by ISO 21010 [20]. Relief and vent systems must be sized for worst-case credible scenarios (blocked-in heating, fire, loss of vacuum), consistent with facility standards and GSE rules [25].

2.8.10 Trade-off summary and recommended workflow

- Run-time vs. volume: longer tests at fixed ΔP demand larger tanks (Eqs. (2.5)–(2.7)); increasing β reduces ΔP but increases geometric volume and cost.
- Simplicity vs. control: self-press. is compact but couples pressure to $P_{\text{sat}}(T)$; external pressurant adds logistics but yields agile control; pumps add CAPEX/OPEX yet provide flight-like conditions.
- Campaign logistics: early decision on N_{tests} , refill cadence and on-site footprint avoids under/over-sizing; purge cycles often dominate GN_2/He requirements.
- Operability & safety: cleanliness and velocity limits in O₂ service (CGA G-4.4), materials per ISO 21010, and relief/vent design per facility standards are non-negotiable.

Recommended steps: (i) fix engine interface $(\dot{m}, P_{\rm in}, T_{\rm in}, t_{\rm run})$ and campaign $(N_{\rm tests})$; (ii) select strategy and targets (P_i, P_f) or $P_{\rm set}$; (iii) size $V_{\rm t}$ by blowdown bounds plus margins; (iv) compute pressurant or heater power; (v) size purge storage; (vi) verify code stresses, relief/vent capacity, and oxygen-service constraints [19, 11, 6, 21, 20, 22, 23, 24, 25].

2.9 Pipes for cryogenic and gas application, feed lines sizing

Cryogenic piping constitutes a core subsystem of any rocket engine test bench, as it ensures the controlled and safe transfer of cryogenic propellants such as liquid oxygen (LOX) or liquid nitrogen (LN₂) from storage tanks to the engine feed system or auxiliary components. The design of these lines must balance several critical requirements: minimization of heat inleak, mechanical stability under severe thermal contraction, structural support against pressure and vibration, and full material compatibility with cryogenic temperatures and the specific fluids involved [11, 19, 6, 20, 21, 22]. Furthermore, accessibility for maintenance, safety, and instrumentation routing must also be considered during the layout phase.

2.9.1 Insulation Strategies and Pipe Typologies

Cryogenic lines can be insulated through two main approaches:

- 1. External insulation cover, typically composed of foam or multilayer wraps.
- 2. Vacuum-jacketed (VJ) insulation, which uses a double-wall construction with a vacuum annulus and, in most cases, multilayer reflective insulation.

While externally insulated pipes provide an economical solution, vacuum-jacketed designs achieve far superior thermal performance, reducing heat leak by over an order of magnitude at the expense of higher cost and complexity. The choice between these solutions depends on system criticality, fluid boil-off tolerance, and mechanical integration constraints.

Cryogenic piping can further be classified as either **rigid** or **flexible**. In VJ lines, rigid pipes generally provide better thermal insulation—typically 2.5 to 3.5 times lower heat leak in terms of watts per meter dissipated—but they are unsuitable in areas where vibration, misalignment, or variable routing geometry are expected. Flexible VJ hoses, on the other hand, enable easier assembly and maintenance but with slightly higher heat losses.

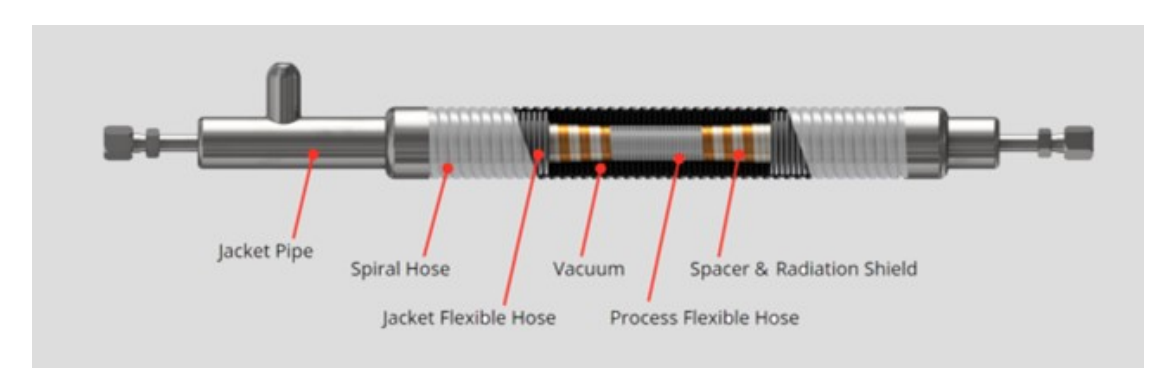


Figure 2.6: Flexible vacuum-jacketed cryogenic pipe: internal section (courtesy of Cryogas).



Figure 2.7: Rigid vacuum-jacketed cryogenic pipe (courtesy of Cryogas).

As visible from Figure 2.7, rigid VJ pipes are equipped with expansion compensators to absorb the axial contraction of the inner pipe occurring at cryogenic temperatures. Each pipe section includes one or more vacuum valves used to establish and maintain the high vacuum in the annular space, typically on the order of 10 μ Hg and not exceeding 50 μ Hg. Standard manufacturing lengths seldom exceed 12–13 m, and longer runs are obtained by welding or by using mechanical couplings equipped with sealing gaskets rated for cryogenic service.

The lines are supported above ground by dedicated adjustable supports that allow for both expansion and contraction. For non-VJ pipes, an external insulation layer (foam or polyurethane) is applied to prevent atmospheric moisture condensation and subsequent ice formation on the external wall.

2.9.2 Thermal Performance and Heat Leak

HEAT LEAK in Btu/hr/ft and (Watts/ft)								
I DIE CIZE	LN ₂		LO ₂		LH ₂			
LINE SIZE	RIGID	FLEX	RIGID	FLEX	RIGID	FLEX		
3/4" OD x 1-1/4" NPS	0.37 (0.11)	0.97 (0.28)	0.37 (0.11)	0.96 (0.28)	0.40 (0.12)	1.05 (0.31)		
3/4" NPS x 2" NPS	0.43 (0.13)	1.21 (0.35)	0.42 (0.12)	1.19 (0.35)	0.46 (0.13)	1.29 (0.38)		
1" NPS x 2-1/2" NPS	0.47 (0.14)	1.43 (0.42)	0.47 (0.14)	1.41 (0.41)	0.51 (0.15)	1.54 (0.45)		
1-1/2" NPS x 3" NPS	0.58 (0.17)	1.74 (0.51)	0.57 (0.17)	1.71 (0.50)	0.63 (0.18)	1.89 (0.55)		
2" NPS x 4" NPS	0.79 (0.23)	2.37 (0.70)	0.65 (0.19)	1.95 (0.57)	0.85 (0.25)	2.56 (0.75)		
3" NPS x 5" NPS	0.98 (0.29)	2.95 (0.86)	0.84 (0.25)	2.52 (0.74)	1.08 (0.32)	3.24 (0.95)		
4" NPS x 6" NPS	1.28 (0.38)	3.85 (1.13)	1.01 (0.30)	3.03 (0.89)	1.40 (0.41)	4.22 (1.24)		
6" NPS x 8" NPS	1.65 (0.48)	4.97 (1.46)	1.36 (0.40)	4.10 (1.20)	1.83 (0.54)	5.50 (1.61)		

Figure 2.8: Typical heat leak values for vacuum-jacketed cryogenic piping (data courtesy of Cryogas, based on PHPK standards).

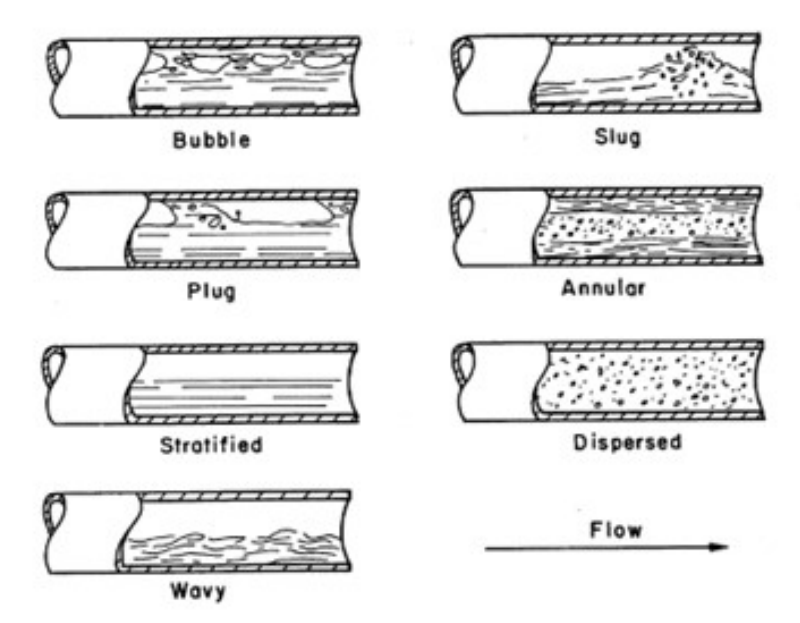
The table in Figure 2.8 shows typical heat leak values for PHPK vacuum-jacketed piping. These conservative figures already include minor components such as elbows and tees and are suitable for preliminary system heat-budget estimation. Additional contributions from valves, bayonets, and quick-disconnects must be added to determine the total heat load of the complete transfer line.

2.9.3 Fluid Behaviour and Flow Regimes

Cryogenic fluids inside transfer lines are frequently in a *two-phase* condition, where both liquid and vapour coexist due to heat input and pressure variations. This multiphase behaviour significantly affects pressure drop and flow stability, which are governed by:

- 1. Wall friction losses, dependent on line roughness, flow velocity, and Reynolds number.
- 2. **Thermal input**, resulting from the imperfect insulation and leading to partial evaporation of the fluid.

Different two-phase flow regimes may occur—bubbly, slug, annular, or mist—depending on mass flux and vapour quality. Each regime requires specific empirical or semi-empirical correlations to estimate frictional pressure losses and void fraction [11, 6].



All these flow regimes may occur in a horizontal pipe flow.

Figure 2.9: Typical two-phase flow patterns observed in cryogenic lines (adapted from Flow Studies).

2.9.4 Pipe Coupling Methods

Cryogenic pipes can be interconnected using different coupling systems depending on service conditions, maintenance frequency, and required tightness:

- 1. **Welded joints**, offering the best tightness and structural strength for permanent connections.
- 2. **Bolted flanged connections**, suitable for rigid assemblies where disassembly may occasionally be required.
- 3. Quick-release couplings, enabling fast and secure connection or disconnection without tools, typically used for flexible or mobile sections.





Figure 2.10: Examples of cryogenic line couplings: quick-release (left) and bolted flange (right) (courtesy of Cryonorm).

Proper selection of coupling type directly impacts not only ease of maintenance but also the overall reliability of the cryogenic feed system. All joints and fittings must be leak-tested using methods compliant with the applicable cryogenic and pressure-equipment standards [20, 22].

2.9.5 Determination of pipe diameter

The sizing of feed lines is based on the balance between flow capacity, cost, and safety constraints. The internal diameter D of a pipe can be determined directly from the mass flow rate \dot{m} , the fluid density ρ , and the desired flow velocity v, according to the continuity equation:

$$D = \sqrt{\frac{4\dot{m}}{\pi\rho v}} \tag{2.13}$$

Alternatively, the flow velocity can be estimated for a given pipe diameter:

$$v = \frac{4\dot{m}}{\pi\rho D^2} \tag{2.14}$$

Both expressions are useful for performing trade-off analyses between system cost and hydraulic performance. Larger diameters reduce flow velocity and pressure losses, improving safety but increasing material and fitting costs. Conversely, smaller diameters reduce cost and weight but lead to higher velocities and friction losses.

These calculations are fundamental in determining the optimal pipe size for each subsystem and were applied in Chapter 4, where specific values for gaseous oxygen (GOX), gaseous nitrogen (GN₂), and liquid oxygen (LOX) were evaluated.

Consideration on impingement velocity and material compatibility

An essential aspect of gaseous oxygen line design is the *impingement velocity*, which defines the maximum safe gas velocity at which oxygen can impact metallic or polymeric surfaces without causing spontaneous ignition. The phenomenon is driven by the heat generated by particle impact, friction, or adiabatic compression in oxygen-rich environments, where ignition thresholds of common materials are drastically reduced.

Standards such as ASTM G88 [29], NASA technical memoranda [30], and CGA G-4.4 [21] provide empirical and experimental data establishing recommended velocity limits. Typical safety ranges for gaseous oxygen at ambient temperature and 40 bar are:

- $v < 20 \,\mathrm{m/s}$ considered fully safe for clean, oxygen-certified systems (ASTM G93| ISO 15001);
- $20\,\mathrm{m/s} < v < 30\,\mathrm{m/s}$ acceptable under strictly controlled conditions, with oxygen-cleaned components and verified absence of contaminants;
- $v > 30 \,\mathrm{m/s}$ high ignition risk due to impact heating and compression effects; such velocities are discouraged in all oxygen service applications.

This behaviour is described by the impingement velocity curve (Figure 2.11), which shows a sharp increase in ignition probability beyond 30 m/s. These limits serve as critical design constraints when dimensioning oxygen feed lines, ensuring that selected diameters maintain flow velocities within the low- to medium-risk range.

2.9.6 Pressure loss estimation

Once a preliminary diameter has been identified, pressure losses are evaluated using the Darcy–Weisbach formulation:

$$\Delta P = f \frac{L}{D} \frac{\rho v^2}{2} \tag{2.15}$$

where f is the friction factor, obtained from the Swamee–Jain correlation for turbulent flow in rough pipes:

Pressure (psi absolute)

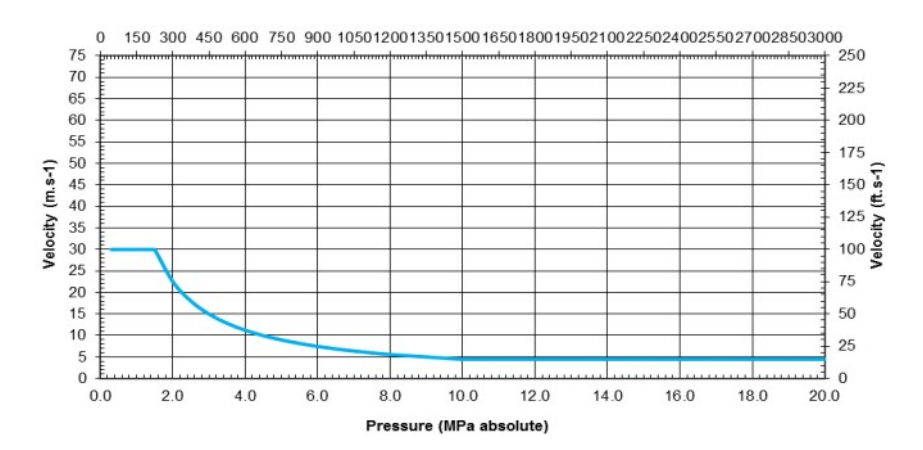


Figure 2.11: Typical impingement velocity curve for gaseous oxygen, showing increasing ignition risk above 30 m/s. Adapted from EIGA Document 13/20, "Oxygen pipeline and piping systems", European Industrial Gases Association, 2020. Source: https://www.eiga.eu/uploads/documents/DOC013.pdf.

$$f = \frac{0.25}{\left[\log_{10}\left(\frac{\varepsilon}{3.7D} + \frac{5.74}{Re^{0.9}}\right)\right]^2}$$
 (2.16)

Here ε represents the pipe roughness, and Re the Reynolds number, calculated as:

$$Re = \frac{\rho v D}{\mu} \tag{2.17}$$

These relationships allow the determination of pressure losses per unit length and their influence on system performance.

2.9.7 Normative and safety references

In the design and operation of gaseous oxygen systems, adherence to established standards is mandatory. The primary references are:

• CGA G-4.4: "Oxygen Pipeline and Piping Systems" — comprehensive design and safety guidelines for oxygen handling, covering material compatibility, cleaning, velocity limits, and commissioning practices [21].

- ISO 7291:2010: "Gas cylinders Refilling stations and bundles for compressed gases Inspection and testing" expands CGA principles internationally, addressing periodic inspection, bundle design, and safety management [28].
- ASTM G93: "Standard Practice for Cleaning Methods and Cleanliness Levels for Material and Equipment Used in Oxygen-Enriched Environments" defines oxygen-cleaning procedures and contamination limits [26].

Compliance with these standards ensures that all oxygen-handling subsystems maintain safe operational limits, avoiding ignition hazards caused by particle impact, adiabatic compression, or contamination.

2.10 Valves and Line Components

In cryogenic feed systems, valves and ancillary components play a critical role in controlling, regulating, isolating, and protecting the system. Their design and selection must ensure reliability, tightness, minimal heat leak, and compatibility with extremely low temperatures.

2.10.1 Cryogenic Control Valves

Cryogenic control valves are engineered with specific features to operate safely under cryogenic conditions. Material selection is crucial: bodies and internals are typically made from stainless steel or nickel alloys that retain toughness at temperatures below -150 °C, avoiding embrittlement. Seal and seat materials often involve PTFE or specially formulated elastomers capable of functioning at low temperatures [31, 32].

A common architectural feature is the *extended bonnet*, a long-stem housing that increases the distance between the actuator and the cryogenic fluid, thus reducing heat conduction into the fluid and preventing icing or actuator freezing. This design is typical in valves for cryogenic service according to manufacturer catalogs and cryogenic valve design guides [32, 31]. Actuators (pneumatic, electric, or hydraulic) are selected for low-temperature performance; pneumatic actuators are popular due to their simplicity and robustness in cryogenic service.

The internal trim (plug, seat, passages) is also optimized to reduce turbulence, cavitation, or flashing phenomena, which are particularly problematic in cryogenic flows. Proper design ensures stable operation amid rapid temperature changes. For safety, it is critical to prevent ingress of moisture or liquid water, since ice formation in the valve internals can compromise sealing or movement.

Below are some of the common valve types used in cryogenic systems. Each type is associated with distinct advantages and limitations, and a figure should accompany each description (place figure showing that valve type, with caption and credit).

Globe Valve

Description: A globe valve features a spherical or cylindrical body with an internal baffle that guides flow along two paths. The valve's plug (or disc) moves linearly up and down to modulate flow.

Applications: Often used when precise control of flow or pressure is required—common in cryogenic control lines, pressure regulation, or instrumentation.

Advantages: High accuracy in throttling, stable control behavior, suitable for fine adjustments.

Disadvantages: Generates higher pressure drop compared to other valve types (e.g. ball valves). Manufacturers like Parker produce globe valves with bolted bonnets and loose-flange designs to accommodate thermal expansion in cryogenic environments [32].

Ball Valve

Description: Flow is controlled by a rotating ball with a central bore. In the open position, the bore aligns with the flow path; in closed, the bore is turned perpendicular and blocks flow.

Applications: Often used as isolation valves (on/off control). Some specialized designs allow limited throttling.

Advantages: Rapid opening/closing, low pressure drop, well-suited for larger diameters and cryogenic service. Parker's cryogenic ball valves are designed for tight sealing at very low temperatures and minimal leakage [32].

Disadvantages: Less precise for fine flow control compared to globe valves.

Butterfly Valve

Description: This valve uses a disc that rotates about an axis perpendicular to flow. In open position, the disc is aligned to allow flow; when closed, it blocks flow.

Applications: Larger pipelines where isolation or regulation is needed, when space or weight is a concern.

Advantages: Compact, lightweight, fast operation, cost-effective.

Disadvantages: Lower precision in flow control; may have sealing challenges in cryogenic service if not designed appropriately.

Check Valve

Description: Unlike other valves, a check valve does not regulate flow; it allows flow in one direction only, shutting off flow if reverse pressure occurs.

Applications: Protects against reverse flow in pump discharge lines, prevents backflow in feedlines or cryogenic circuits.

Advantages: Simple design, automatic action, essential safety component. Parker's range of cryogenic lift and swing check valves are explicitly designed for cryogenic pipelines with low leakage [33].

Disadvantages: Does not provide flow control—only direction enforcement.

2.10.2 Safety and Overpressure Components

Beyond control and isolation valves, cryogenic systems require safety devices to guard against overpressure or failure modes.

Relief Valves

Relief valves are designed to open when system pressure exceeds a preset threshold, thereby venting excess fluid to maintain safe pressure levels. They may be springloaded or pilot-operated. In cryogenic systems, they often operate between 90 % and 105 % of the maximum allowable working pressure. Parker offers cryogenic safety relief valves designed for static and transport storage applications [34].

Burst Disks

Burst disks (rupture disks) are non-reclosing devices that rupture at a designated pressure (often 110% of design pressure) to allow rapid, high-volume venting. They are typically used in applications where rapid action is essential and where valve actuation may be too slow.

Other Safety Devices: Flashback Arrestors

Especially in systems handling flammable gases, a flashback arrestor combines a non-return element and a flame arresting media to prevent flame propagation into supply lines. Their design and certification follow standards like ISO 5175.

2.10.3 Placement and Sizing of Safety Devices

Correct positioning of overpressure and control devices is essential for system integrity:

- Upstream and downstream of pressure regulators: Relief valves or burst disks should be placed as close as possible to regulator outlets to protect downstream components from regulator failure.
- On high-pressure storage systems: Relief valves or burst disks are often integrated into cylinder valves or located on near manifold lines, protecting against heating-induced pressure rise.
- On closed or dead-end piping sections: To prevent trapped gases from heating and overpressurizing, safety vents or relief devices should be placed at the end of dead legs.
- In vacuum-jacketed systems: In VJ lines (for example for LOX), devices may be needed in the annular vacuum space to relieve pressure if air or water vapor intrudes and condenses.
- On test benches or experimental setups: Safety devices are placed on feed lines, between valves and test articles, and on vent lines to protect equipment and personnel.

In choosing between burst disks and relief valves: use burst disks when a onetime, fast, high-integrity venting is needed and valve response might be too slow; use relief valves when repeated overpressure events or adjustable settings are required.

2.10.4 Special Considerations for Oxygen Service

For cryogenic oxygen systems, all materials and components must be oxygenclean and compatible (free of hydrocarbons, oils, or combustible residues). Avoid materials that may react under high-pressure O_2 . Oxygen-cleaning of valves is critical to avoid ignition risks; this process is typically governed by EIGA and ASTM standards (e.g. EIGA doc 33/18, ASTM G93) [35]. ISO 21010 also provides guidelines for gas/material compatibility in oxygen-enriched environments [20].

2.10.5 Valve Sizing and Flow Coefficient Fundamentals

The correct sizing and selection of valves in a propulsion test bench is critical to ensure proper flow regulation, minimize pressure losses, and maintain safety margins under various operating conditions. The design process generally starts by defining the desired mass flow rate, inlet and outlet pressures, and the thermodynamic properties of the working fluid.

Flow Coefficient Definition

The fundamental parameter governing valve selection is the flow coefficient (C_v) , which quantifies the capacity of a valve to pass a fluid for a given pressure drop. The relationship between the volumetric flow rate, the pressure differential across the valve, and the specific gravity of the fluid is expressed as:

$$C_v = \frac{Q}{\sqrt{\Delta P/SG}} \tag{2.18}$$

where:

- $C_v = \text{Flow coefficient (dimensionless)}$
- Q = Flow rate, typically in gallons per minute (GPM)
- ΔP = Pressure drop across the valve (psi)
- SG = Specific gravity of the fluid (dimensionless; water = 1)

In SI units, the equation can be rewritten as:

$$C_v = 1.17 \times 10^{-5} \cdot Q_{SI} \sqrt{\frac{SG}{\Delta P_{SI}}} \tag{2.19}$$

where Q_{SI} is in m³/s and ΔP_{SI} in Pa.

Design Procedure

The valve sizing process involves:

- 1. Determining the required mass or volumetric flow rate for the system.
- 2. Estimating the allowable pressure drop across the valve (typically 5–10 % of total line pressure).
- 3. Computing the required C_v using Eq. (1) or Eq. (2).
- 4. Comparing the obtained C_v value with manufacturer data (e.g. Parker, Cryocomp) to select a valve with an equal or slightly higher nominal C_v [31, 32].
- 5. Verifying compatibility with fluid, temperature, and pressure limits.

Material and Safety Considerations

For oxygen and cryogenic systems, valves must be manufactured and cleaned according to stringent standards to avoid ignition or contamination risks. Typical reference standards include:

- ASTM G93 Standard Practice for Cleaning Methods and Cleanliness Levels for Material and Equipment Used in Oxygen-Enriched Environments.
- ISO 21010:2017 Cryogenic Vessels Gas/Materials Compatibility [iso21010].
- CGA G-4.4 Oxygen Pipeline and Piping Systems.

Valves exposed to cryogenic fluids (e.g. liquid oxygen) should use soft-seated materials such as PTFE or PCTFE only where thermal contraction is limited, and preferably employ metal-to-metal seals for long-term durability. Thermal expansion, cavitation risk, and potential for phase change (flashing) must also be accounted for in sizing and material selection [31].

Pressure Loss Estimation

Given a flow coefficient, the pressure drop across the valve can be estimated by rearranging Eq. (1):

$$\Delta P = \left(\frac{Q}{C_v}\right)^2 SG \tag{2.20}$$

This relation helps verify that the selected valve meets both flow and pressure constraints without introducing excessive loss.

Control and Actuation Aspects

In automated test benches, control valves are typically actuated via electric or pneumatic servos. Selection criteria include:

- Response time and precision (especially for oxidizer injection valves)
- Compatibility with control signals (4–20 mA, digital, etc.)
- Leak-tightness class (ISO 5208)

The combined use of manual isolation valves, solenoid-actuated valves for fast switching, and proportional control valves for fine regulation offers both flexibility and redundancy during test campaigns.

2.11 Sensors

In a cryogenic test bench, the measurement system represents one of the most critical subsystems, providing the data necessary for both control and safety. Key physical quantities to be continuously monitored include temperature, pressure, mass flow rate, and the residual volume of cryogenic liquids within storage tanks. Proper sensor selection and positioning are fundamental to guarantee measurement accuracy, minimize heat inleak, and ensure compatibility with the harsh cryogenic environment [11, 19, 6, 20, 22].

2.11.1 Temperature Measurement

Accurate temperature monitoring is essential for safe handling of cryogenic fluids such as liquid oxygen (boiling point 90 K) and liquid nitrogen (77 K), both during operation and during purging procedures. Sensors must withstand operating pressures up to 50 bar, maintain accuracy down to at least 77 K, and resist stresses induced by thermal contraction and cycling.

The most commonly used technologies are platinum resistance thermometers (RTDs), silicon diode thermometers, and thermocouples. Each solution offers a different trade-off between accuracy, cost, and response time. Calibrated RTDs and diodes can achieve accuracies of a few tenths of a kelvin, with high reproducibility and minimal thermal loading. Commercial devices such as the Lake Shore DT-670 diode sensor and Omega PR-10 RTD are widely used due to their reliability and availability [36, 37].

Dynamic measurements impose stricter requirements. Most cryogenic thermometers have time constants of several seconds, unsuitable for transient phenomena. Faster response can be obtained using sensors with low thermal mass and high thermal conductivity—such as thin-wire or thin-film thermocouples—achieving time constants in the millisecond to microsecond range. Advanced technologies such as silicon-on-sapphire (SOS) thermometers or carbon film sensors can reach sub-microsecond responses in helium environments [11]. However, these devices are fragile and complex to install, so they are mainly used in research contexts.

Recommended Sensor Types and Placement

- Silicon diode sensors (e.g. Lake Shore DT-670): excellent accuracy (±0.25 K at 90 K), minimal self-heating, suitable for high-pressure systems.
- Platinum RTDs (e.g. Omega PR-10-3-100): linear response, high stability, four-wire configuration recommended for precision (± 0.1 K typical).

Typical placement: inside LOX and LN_2 tanks to monitor bulk temperature, and along feed lines near the engine inlet to verify propellant conditions before injection.

2.11.2 Pressure Measurement

Pressure measurement in cryogenic systems must ensure high accuracy while minimizing thermal drift. One common approach is to connect the measurement point to an ambient-temperature transducer through a capillary tube, enabling the use of conventional sensors while isolating them from cold regions. However, this method introduces thermal gradients and response delays. For direct cryogenic use, sensors based on capacitance, variable reluctance, strain-gauge, or piezoresistive technologies are preferred [20, 22].

Recommended Sensor Types

- Strain-gauge pressure sensors: robust, cost-effective, and capable of measuring up to several hundred bar; widely adopted for cryogenic liquids. Example: Setra Model 209 (up to 70 bar, ±0.25% FS accuracy).
- Capacitive pressure sensors: higher accuracy and long-term stability, minimal drift with temperature. Example: Kistler Type 4260 (up to 100 bar, $\pm 0.1\%$ FS accuracy).

Typical placement: at tank outlets and along feed lines to monitor injection pressure stability and detect pressure oscillations during tests.

2.11.3 Flow Measurement

Cryogenic flow measurement is crucial for verifying mass flow rates and ensuring safe operation of both propellant and purge systems. Different principles are used depending on accuracy, cost, and flow regime: Coriolis, Venturi, and vortex flowmeters are the most common [19, 20].

Recommended Sensor Types

- Coriolis flowmeters: directly measure mass flow and fluid density with high accuracy ($\pm 0.1\%$). Example: Emerson Micro Motion ELITE CMF300, compatible with LOX and LN₂.
- Venturi flowmeters: simpler and economical solution, suitable for steady-state flows; accuracy typically ±1%, may require density compensation. Example: Yokogawa Vortex Flowmeter.

Typical placement: on main LOX feed lines to measure propellant delivery to the combustion chamber, and on purge or vent lines to monitor nitrogen mass flow.

2.11.4 Liquid Level Measurement

Accurate liquid-level measurement in cryogenic tanks is essential for managing propellant inventory and planning refills. Measurement systems must be non-intrusive when possible, minimizing heat input and avoiding disturbance of the cryogenic liquid surface.

Recommended Sensor Types

- Load cells: measure total tank weight to infer liquid mass from density; provide high precision ($\pm 0.1\%$) and avoid direct contact with cryogen. Example: Interface load cells.
- Capacitance probes: measure level by detecting changes in capacitance as the liquid level varies; suitable for both stationary and pressurized tanks. Example: Cryomagnetics level sensors.

Typical placement: load cells installed beneath each tank for continuous level estimation; capacitive probes can be used inside tanks as a redundant or localized measurement.

2.11.5 Sensor Placement Summary

Accurate sensor selection and calibration, combined with proper wiring, thermal anchoring, and signal conditioning, ensure reliable data acquisition for both safety and performance analysis of the cryogenic test bench.

Table 2.3: Summary of recommended sensors and placement for the cryogenic test bench.

Location	Sensor Type	Purpose	Example Model / Accuracy
LOX Tank	RTDs, strain-gauge pressure sensor, load cells	Temperature, pressure, and level monitoring	Omega PR-10-3 (± 0.1 K); Setra 209 ($\pm 0.25\%$); Interface LC ($\pm 0.1\%$)
LN_2 Tank	RTDs, strain-gauge pressure sensor, load cells	Temperature and purge system monitoring	$ \begin{array}{cccc} \text{Lake} & \text{Shore} & \text{DT-670} \\ (\pm 0.25 & \text{K}); & \text{Setra} & 209; \\ \text{Interface LC} \end{array} $
Feed Line	Coriolis flowmeter, RTDs, pressure sensor	Mass flow, temperature, and injection pressure con- trol	Emerson CMF300 ($\pm 0.1\%$); Kistler 4260 ($\pm 0.1\%$)
Purge Lines	Venturi flowmeter, thermocouples	Verification of LN_2 or GOX purge efficiency	Yokogawa Vortex $(\pm 1\%)$; Type-K TC $(\pm 0.5 \text{ K})$

2.12 Acquisition and control

The acquisition and control subsystem of a rocket engine test bench provides the critical interface between the test article, its environment, and the operators. In essence, it performs two complementary functions: (i) acquiring and processing measurement data from the engine and the facility, and (ii) executing control actions on valves, actuators, and auxiliary devices. Together, these tasks ensure that the test can be monitored in real time, operated safely, and recorded for later analysis [6].

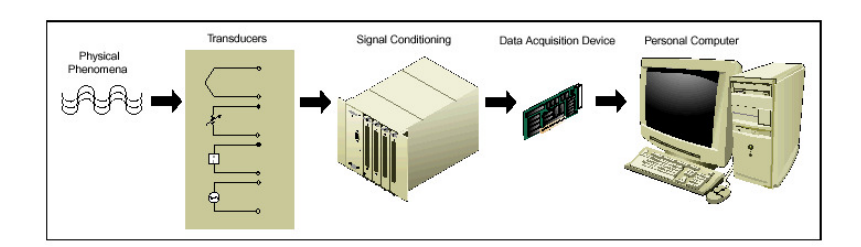


Figure 2.12: schematics of a typical Data Acquisition System (credits: Studytronics)

From a functional standpoint, data acquisition follows the classical measurement chain:

Sensor \rightarrow A/D conversion \rightarrow data logging \rightarrow processing \rightarrow output.

Conversely, control tasks can be represented as:

Input command \rightarrow processing routines \rightarrow D/A conversion \rightarrow actuator signal.

A dedicated data acquisition software is required to manage both chains: it processes sensor outputs for monitoring, while simultaneously handling operator commands to actuators (e.g., valves, pumps). Commercial solutions such as *Syclone* by Clemessy integrate software and hardware into unified platforms, but the selection is strongly driven by the adopted communication protocol.

For test bench applications, the choice of protocol is critical: it must guarantee deterministic timing, low latency, and reliability in safety-critical operations. Widely used real-time Ethernet-based protocols include **EtherCAT**, with sub-microsecond cycle times and distributed clock synchronization, and **PROFINET IRT**, suited for deterministic control in industrial automation [38, 39]. Other options include **CANopen** and **PROFIBUS DP**, still used when Ethernet-based solutions are not feasible, and specialized motion control protocols such as **SERCOS** and **POWERLINK** [40].

Table 2.4: Comparison of main communication protocols for test bench applications

Protocol	Туре	Key Features	Typical Applications
EtherCAT	Real-Time Ethernet	$<1 \mu s$ cycle times, distributed clock synchronization, ultra-low latency	High-speed valve actuation, real- time feedback loops
PROFINET IRT	Real-Time Ethernet	Deterministic performance, synchronization, standard in industrial automation	Actuators and sensors requiring strict timing
CANopen	Fieldbus (Serial)	Message prioritization, widely supported, real-time capable	•

In practice, protocol selection depends on test objectives, timing requirements, and integration with existing infrastructure. For high-thrust hybrid propulsion tests, where valves must be actuated in the millisecond range, real-time Ethernet tends to dominate. In contrast, smaller-scale benches or auxiliary subsystems may still rely on simpler fieldbus implementations. Ultimately, this phase of the design leads to a preliminary control architecture, identifying how many subsystems must be monitored, how many must be actively controlled, and which operational requirements will drive actuator selection in later design steps.

2.13 Environmental considerations: noise reduction and exhaust dumping

Static rocket engine testing produces significant environmental impacts, chiefly related to acoustic emissions and exhaust management. These aspects are not only a matter of minimizing nuisance but represent key requirements for safety, facility durability, and compliance with environmental regulations. Addressing them from the design phase ensures that the test bench can be operated both safely and sustainably [4, 2].

Noise generated during test firings originates primarily from the supersonic exhaust jet, which can reach levels above 180 dB, but also from secondary sources such as combustion instabilities and structural vibrations. If untreated, such levels can damage equipment and create disturbances several kilometers from the site. To mitigate these effects, several methodologies are employed. Large-scale sound suppression systems, usually based on water deluge or spray injection, are among the most effective: the injected water absorbs acoustic energy, cools exhaust gases, and reduces shock wave intensity. At NASA facilities such as Stennis Space Center, similar systems handle extremely high water flow rates during static firings [2]. In smaller test benches, misting or localized spray can provide a reduced but significant effect.



Figure 2.13: water deluge system on a launchpad (credits: NASA)

Complementary noise reduction strategies include the use of acoustic deflectors and baffles. These structures, often made of reinforced concrete or refractory material, redirect shock waves and attenuate their propagation. Experimental studies show that deflector geometry strongly influences the acoustic load distribution, highlighting the need for tailored designs depending on thrust level and nozzle orientation [41]. In addition, earthen berms or barriers can be employed as passive shields, while siting and orientation of the exhaust plume away from populated

areas remain essential planning measures.

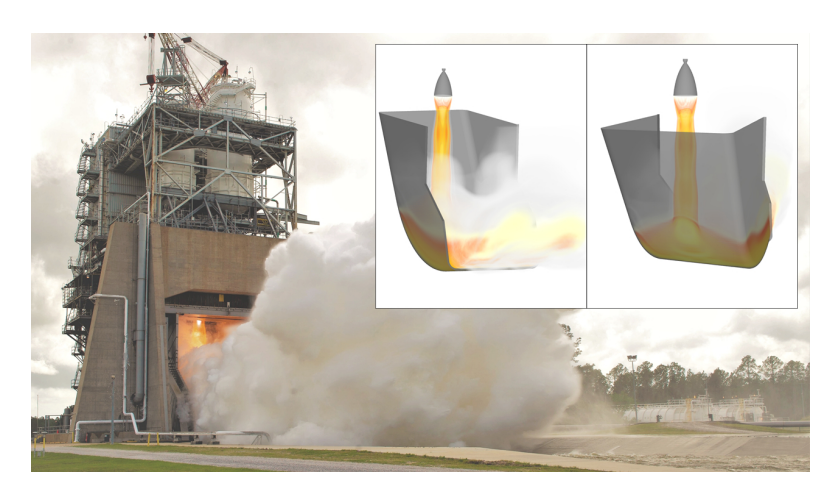


Figure 2.14: flame trench at the NASA Stennis test center (credits: NASA)

Exhaust management is equally critical, as rocket plumes involve extreme temperatures, mechanical loads, and effluents such as water vapor, carbon dioxide, nitrogen oxides, and, in the case of hybrid propulsion, particulates from solid fuel regression. Test benches therefore integrate flame trenches or deflectors to redirect exhaust gases away from sensitive structures and instrumentation. Their design typically minimizes plume impingement and avoids recirculation phenomena, thereby protecting sensors and improving measurement accuracy [4]. For enclosed or shielded facilities, ducts or exhaust silos may be added to guide gases, sometimes combined with water cooling or scrubbing systems to reduce local environmental impact.

Thermal protection of the structural subsystem must also be considered. Exhaust gases exceeding 3000 K and strong acoustic resonances can degrade materials over repeated firings. Protective coatings, refractory linings, and sacrificial inserts are often applied to trenches and deflectors, while water-cooled panels may be adopted for long-duration or high-power tests.

In conclusion, noise reduction and exhaust dumping form a central part of test bench design. By combining water suppression, structural shielding, optimized siting, and controlled exhaust management, facilities achieve safer operation and reduced environmental impact. The outcome of this preliminary phase is the definition of acoustic and exhaust requirements, which later serve as the basis for actuator selection, suppression equipment, and auxiliary infrastructure design.

2.14 Integration of the test bench

The integration of a rocket engine test bench extends beyond the standalone design of its subsystems. It requires a holistic view of how structural, fluidic, control, and safety elements interface with one another, with the surrounding environment, and with auxiliary infrastructure. Considering integration from the earliest design stages is essential to avoid conflicts, ensure operational efficiency, and comply with safety and regulatory requirements.

A fundamental aspect is the definition of spatial envelopes and mechanical interfaces. Each subsystem—cryogenic storage, fluid distribution lines, instrumentation racks, and structural supports—occupies physical volume and requires defined routing. Improper allocation of space may cause conflicts during assembly or limit the accessibility of critical components. Accessibility must therefore be prioritized according to operational needs: components that are subject to frequent maintenance or reconfiguration, such as valves, sensors, or modular fuel holders, should be positioned for easy access, while more permanent elements such as reinforced foundations can be located in less accessible areas [4].

The assembly sequence also constrains integration. Large elements such as the engine mounting frame, flame trench, or deflectors must typically be installed before ancillary instrumentation. Likewise, cryogenic lines and manifolds often dictate the spatial layout, since their geometry is tightly constrained by safety distances and thermal requirements. Integration points where high loads converge, for instance at thrust frame connections or valve clusters, must be reinforced and validated with structural and thermal analyses [6].

Integration also extends to site-level considerations. The placement and orientation of the test bench influence acoustic impact, exhaust dispersion, and compliance with environmental and safety regulations. Facilities such as NASA's Stennis Space Center demonstrate how site planning and integration of subsystems ensure safe operation while minimizing environmental impact [2]. Similarly, European facilities such as the DLR Lampoldshausen test benches highlight the importance of harmonizing subsystem design with local standards and permitting processes [3].

Finally, auxiliary infrastructure must be incorporated into the integration plan. Beyond the engine support structure and fluid systems, a complete test facility requires control rooms with protected operator access, redundant power supply, water for cooling and acoustic suppression, and inert gas networks for purging. These auxiliary services are integral to safe operation and must be located and routed consistently with the primary subsystems. Their integration defines not only functionality but also the scalability and adaptability of the test bench to future propulsion programs.

In summary, integration is not limited to combining subsystems, but encompasses assembly sequencing, accessibility planning, site-level constraints, and auxiliary

infrastructure. Addressing these aspects from the start of the design ensures that the test bench evolves into a coherent facility capable of safe, efficient, and adaptable operation.

Chapter 3

Case study n.1: Autophage launcher test bench

3.1 Overview of the Project

The autophage launcher investigated in this design study utilizes its structural material as fuel. Once orbit is reached, only the payload and the main engine remain, resulting in a fully consumable and highly efficient system.

The launcher has an overall height of approximately 25 m and a diameter of 1 m, with an estimated payload capability of 1 ton to low Earth orbit (LEO). Propulsion is provided by a hybrid combination of liquid oxygen (LOX) as oxidiser and high-density polyethylene (HDPE) as solid fuel.

The principal advantage of this architecture lies in its potential to reduce manufacturing and operational costs by nearly 80% through simplification of the propulsion system and a reduction in the number of components. The overall structural mass is expected to decrease by about 40% compared to a conventional multistage launcher configuration. Additionally, being a single-stage-to-orbit (SSTO) vehicle, it significantly mitigates the generation of orbital debris, as no stages are jettisoned during flight.

3.2 Specifications and Operative Requirements

The following information was extracted from the technical request provided by Alpha Impulsion for the design of a test bench intended for the hot-fire development testing of the autophage launcher engines. The company aims to design and manufacture a modular test bench capable of accommodating two engine classes—an initial hybrid configuration and a subsequent autophage version—while progressively scaling thrust capacity.

3.2.1 General Requirements

Table 3.1: General specifications for the autophage launcher test bench

Parameter	Specification
Thrust range	75–100 kN (2027) — up to 200 kN (2029)
Oxidiser	Liquid Oxygen (LOX, ~90 K), maximum storage capacity
	$\approx 5 \text{ tonnes}$
Fuel	Solid fuel based on HDPE or equivalent thermoplastic poly-
	mer
Firing cadence	Maximum 2 tests per week, each with duration up to $60 \mathrm{\ s}$

3.2.2 Engine Configuration

The engine Alpha Impulsion intends to test is a hybrid rocket engine, using a solid fuel and a liquid oxidiser (LOX). The test bench developed within this work must be capable of testing two different configurations:

- 1. Classical Hybrid Rocket Engine (HRE)
- 2. Autophage variant of the engine

Table 3.2: Main parameters of the hybrid and autophage engines

Parameter	Value / Description
Thrust	75–100 kN (2027) — up to 200 kN (2029)
Feed pressure	40–60 bar
Combustion chamber length	$\sim 2 \text{ m}$
Engine diameter	$\sim 0.8 \text{ m}$
Fuel	Solid HDPE or similar thermoplastic
Oxidiser	Liquid Oxygen (LOX)
Oxidiser mass-flow rate	30 kg/s
Stored LOX quantity	5 tonnes (safety-limited)
Pressurizing gas	Nitrogen or Helium (also used for post-firing purging)
Test duration	10–60 s (extendable up to 250 s after 2029)
Throttle capability	Down to 1/7 nominal mass flow; engine restart capability
Test rig orientation	Vertical
Flame deflector	Required (subject to detailed analysis)
Firing cadence	Approx. 2 firings per week (to be refined)
Thrust vectoring control	Measurement via lateral load cell
Assembly	Engine to be erected vertically (either lifted
	by crane or tilted from horizontal assembly)
Autophage configuration	Total engine $<$ 10 ton, overall length $<$ 10 m

3.3 Structural Configuration and Preliminary Concept

Following the design process described in Chapter 2, an assessment of existing cryogenic and hybrid rocket test infrastructures was conducted to identify reference architectures and design practices applicable to the Alpha Impulsion system.

A comparative review of medium-to-large-scale test benches was performed, focusing on European and North-American facilities operating in the 50-250 kN thrust range. The designs analysed include:

- RFA
- ISAR Aerospace
- HY Impulse
- Latitude

- Opus Aerospace
- Orbex
- Skyrora
- PLD Space
- Arkadia Space
- Stoke Space
- ABL Space Systems

This benchmarking served to identify common design philosophies, modular approaches, and safety layouts that would guide the conceptualization of the new test bench configuration presented in the following sections.

3.3.1 Benchmark of Existing Test Bench Configurations

A preliminary survey of existing hybrid and cryogenic rocket engine test benches was carried out to identify relevant design approaches, structural arrangements, and facility typologies. The following examples illustrate the diversity of solutions adopted by European and American companies operating in comparable thrust ranges.

RFA

Located in Kiruna, Sweden, the RFA test bench employs a modular container-based ahielding structure and a metal main support structure.





Figure 3.1: Test bench of company RFA — Credits: RFA

ISAR Aerospace

Also situated in Kiruna, Sweden, ISAR Aerospace operates a facility featuring an excavated test area. This semi-buried configuration naturally shields surrounding installations and personnel from acoustic and blast effects.



Figure 3.2: Test bench of company ISAR Aerospace — Credits: ISAR Aerospace

HY Impulse

HY Impulse tests hybrid rocket motors with thrust levels around 75 kN. The setup adopts a horizontal firing configuration, using containers as shielding and service structures for instrumentation and fluid handling.



Figure 3.3: Test bench of company HY Impulse — Credits: HY Impulse

Latitude

Latitude employs a compact vertical test arrangement hosted inside a modified container. The setup integrates a deflector shield at the base and is tailored for small-scale propulsion units.



Figure 3.4: Test bench of company Latitude — Credits: Latitude

Opus Aerospace

The Opus Aerospace test bench is constructed primarily from reinforced concrete blocks, with a flame deflector integrated at the lower section of the test cell.



Figure 3.5: Test bench of company Opus Aerospace — Credits: Opus Aerospace

Orbex Aerospace

Orbex Aerospace utilizes a horizontally oriented testing configuration enclosed within a containerized structure. The layout differs substantially from the vertical configuration considered in this work.



Figure 3.6: Test bench of company Orbex Aerospace — Credits: Orbex Aerospace

Skyrora

Skyrora has conducted 70 kN hybrid engine tests using a facility composed of stacked containers arranged vertically. The test stand is positioned in a partially excavated area, providing natural shielding and improved acoustic damping. The company reportedly operates another similar installation at a different site.





Figure 3.7: Test bench of company Skyrora — Credits: Skyrora

PLD Space

PLD Space employs a concrete foundation combined with a superstructure made of metallic beams, optimized for reusability and modular access to the engine and instrumentation.



Figure 3.8: Test bench of company PLD Space — Credits: PLD Space

Arkadia Space

Arkadia Space performs small-scale hybrid tests using container-based test benches. These configurations are designed for horizontal testing and differ significantly from

the vertical, large-scale layout investigated in the present study.



Figure 3.9: Test bench of company Arkadia Space — Credits: Arkadia Space

Stoke Space

The test facility of Stoke Space consists of a concrete base structure topped with a metallic roof. The system supports horizontal engine firings and includes dedicated exhaust management infrastructure.





Figure 3.10: Test bench of company Stoke Space — Credits: Stoke Space

ABL Space Systems

ABL Space Systems operates a robust test installation based on a metallic framework anchored to a concrete foundation. The bench integrates a flame deflector and is built along the carved side of a hill to provide natural containment and noise shielding.



Figure 3.11: Test bench of company ABL Space Systems — Credits: ABL Space Systems

3.3.2 Preliminary Dimensional Estimation of the Test Stand Height

From the comparative analysis above and considering the main dimensional and operational requirements of the Alpha Impulsion project, an initial estimation of the test stand height can be defined.

The combustion chamber of the target engine measures approximately 2.5 m in length. Downstream of the nozzle, the exhaust plume develops along the vertical axis, featuring a core region with temperatures reaching 2000–2500 K, decreasing to approximately 1500 K beyond the central zone. Based on empirical data and visual analyses of comparable test campaigns, the high-temperature core length can be approximated to 2 m for this engine scale.

To safeguard both the facility and the test article, a flame deflector must be implemented. Its primary function is to redirect the exhaust jet, preventing the supersonic and thermally destructive gases from directly impinging on structural elements. The redirected exhaust also mitigates the formation of standing shockwaves and excessive acoustic loads (see the analysis by Sachdev et al. on deflector thermal loading) [42].

Several design configurations are available, including fixed flame trenches or inclined deflectors. To reduce construction complexity and avoid excavation, the present concept adopts an inclined steel deflector—potentially arranged in two stages to gradually decelerate the exhaust and distribute loads more evenly.

Material selection is a critical aspect:

- Steel provides ease of fabrication, assembly, and replacement, with high-temperature resistance (melting point > 1700 K). However, it requires protective coatings against corrosion and oxidation (e.g. as used in test-stand deflectors at NASA's E-2 facility) [43].
- Refractory concrete or brick linings offer improved resistance to oxidation and thermal degradation but add weight and are less adaptable for modular maintenance.

Given the expected nozzle exit diameter of 0.3 m and typical plume divergence, a deflector surface of approximately 1×1 m is estimated to be sufficient for full jet interception. The vertical extension of the deflector should exceed the visible flame by 1-1.5 m, accounting for thrust vector control movements.

Combining these factors, the overall test stand height—from the base of the deflector to the top of the combustion chamber—is preliminarily estimated between 5.5 m and 6 m. This value serves as the initial design reference and will be refined during the integration phase with the full fluid and structural layout.

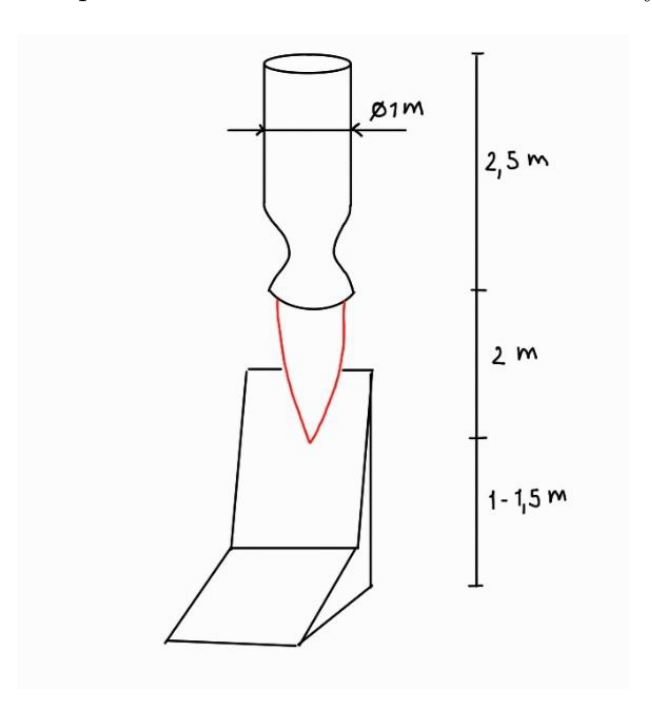


Figure 3.12: Constraints on height of the test stand (Credits: Alpha Impulsion)

3.3.3 Width of the Test Stand

The internal width of the test stand depends both on thermal protection requirements and on the space necessary for engine integration. Adequate clearance must

be provided to separate the structural walls from the exhaust plume, allowing airflow for convective cooling and reducing thermal stresses on the load-bearing elements.

Materials respond differently to elevated temperatures: concrete begins to degrade irreversibly above approximately 300 °C, while steel maintains structural integrity at higher temperatures but undergoes thermal expansion that can affect dimensional stability and the accuracy of thrust measurements (as discussed in structural design guidelines for protected facilities) [44]. Additional clearance is also needed to accommodate gimbaling of the combustion chamber for thrust vector control and to house the arms and load cells used for thrust measurement (as in common test-stand layouts) [45].

Considering these factors, a clearance of about 1 m around the engine is deemed appropriate, resulting in an estimated internal width of approximately 3 m.

External Width and Structural Typologies

The external width is dictated primarily by the construction method. Two design options are under evaluation:

- Modular container-based structures
- Reinforced concrete block assemblies

Both concepts can provide adequate robustness and stability, but container structures offer standardization, transportability, and ease of disassembly—important features during the development phase of a launcher program.

From a structural standpoint, the test stand must withstand both the static load of the engine and the dynamic loads generated during operation. For instance, an engine weighing approximately 20 t represents a purely compressive load at rest. During firings, however, thrust levels up to 100–200 kN may locally offset or even invert the static load, creating transient tensile forces. Consequently, the overall structure must be securely bolted and adequately weighted—either through ballast (e.g., sandbags, water tanks) inside the containers, or via reinforced tie-downs and anchoring elements in concrete implementations (analogous to bolted modular test facilities) [46].

Container-Based Structural Considerations

Two standardized modular elements are considered: **containers** and **container platforms**.

Container Platforms Container platforms are specialized flat modules designed to sustain distributed loads over their entire surface and perimeter. Thanks to their standardized geometry, they can transfer loads efficiently to the corner castings of ISO containers. When stacked at the top or bottom of a container assembly, they provide uniform load distribution and structural continuity, enabling the installation of beams or mounting frames above the test cell.



Figure 3.13: Example of container platforms used as structural load distribution elements (Credits: Hacon Containers)

Containers Standard ISO shipping containers are available in two main sizes:

- 20 ft container: 6.0 m \times 2.4 m \times 2.6 m (L×W×H); empty weight 2.2 t; max gross weight 24 t.
- 40 ft container: 12.2 m \times 2.4 m \times 2.6 m (L×W×H); empty weight 3.7 t; max gross weight 30.4 t.

Their standardized stacking capacity allows for vertical compressive strengths on the order of 192 t under ideal conditions—consistent with structural blast-load simulations on steel ISO containers [47]. When arranged in two parallel rows, the resulting external width is about 7 m, providing sufficient base area for both static and dynamic stability.

Concrete alternatives would fall in a similar dimensional range, since the surface area required for load support is smaller than that for structural stability. Thus, an external width between 6–7 m is identified as a practical design baseline for either container or concrete-based configurations.

Container platforms may also be integrated at both the top and bottom levels of the assembly to ensure uniform load transfer between stacked modules and to host additional structural components.

Influence of the Thrust Measurement System on Structural Height

The interface method between the combustion chamber and the test stand significantly affects the required structural height. Two primary design philosophies are identified:

- 1. **Bottom-supported configuration:** the combustion chamber is held from below using inclined braces or struts.
- 2. **Top-suspended configuration:** the chamber is suspended from upper beams or crossbars.

The bottom-supported concept requires a shorter structure, as the chamber is partially elevated by its own supports, but it limits operator accessibility and restricts instrumentation placement beneath the engine. Conversely, the top-suspended configuration offers improved accessibility and easier maintenance of the upper grain section, at the cost of a taller structural frame.

When these concepts are applied to a container-based architecture:

- The bottom-supported design would require two stacked containers, yielding a total structure height of approximately 5.2 m—consistent with previous flame-deflector clearance estimates.
- The top-suspended configuration would require three stacked containers (around 7.8 m total height) or two containers plus a steel extension frame to achieve the necessary attachment height.

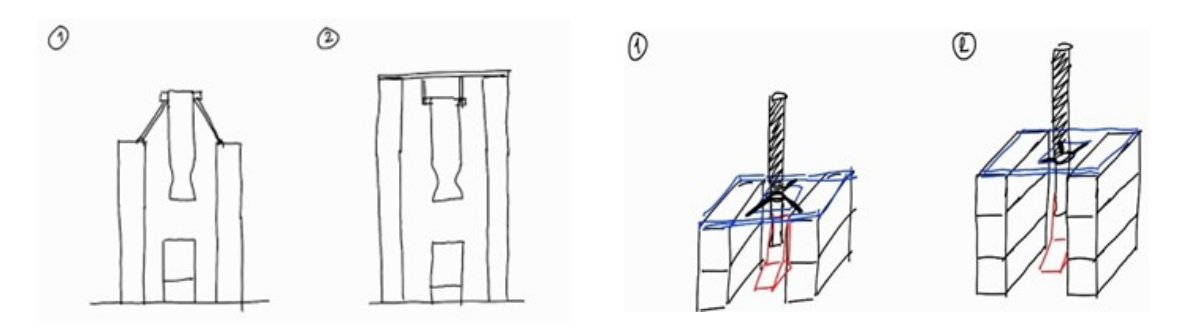


Figure 3.14: Different configurations of the thrust measurement system and motor mount (Credits: Alpha Impulsion)

A reinforced concrete structure offers greater geometric flexibility, as height can be tailored during construction; however, the same design trade-offs between accessibility and overall footprint remain valid.

In summary, depending on the selected configuration, the total height of the supporting structure is expected to range between approximately 5.2 m and 7.8 m.

3.3.4 Mounting Platform

With the preliminary configuration defined as two container stacks supporting a platform, the focus shifts to the design of the platform itself — the key interface between the engine and the supporting structure. Its role is to ensure proper engine mounting, operator accessibility, and safe load transfer to the base structure.

The platform must: (i) provide secure fixing points for the motor and load cells; (ii) allow access for integration and testing; (iii) transmit compressive and tensile loads to the container or concrete base; and (iv) host auxiliary systems such as sensors, feed lines, and safety equipment.

Structurally, it will be built from bolted steel profiles (e.g., H-beams) to ensure strength, modularity, and ease of assembly. Steel plates or gratings will cover the frame, offering a safe working surface and space for fences or enclosures. This modular design simplifies maintenance and allows future adaptations to different engine sizes.

The engine location on the platform remains a design variable. A central position provides balanced load distribution, whereas an offset placement toward one edge may improve heat dissipation by increasing the open area below the exhaust plume. The final layout will depend on the chosen thrust-support concept and the integration requirements of adjacent systems.

3.4 Subsystems

Following the workflow introduced in the previous chapter, the various subsystems will be designed around the structural concept presented in the first iterations.

3.5 Structure

3.5.1 Second iteration of platform design

After the evaluation and definition of other design aspects, several features of the platform have been refined:

• The engine mount is located near the platform edge;

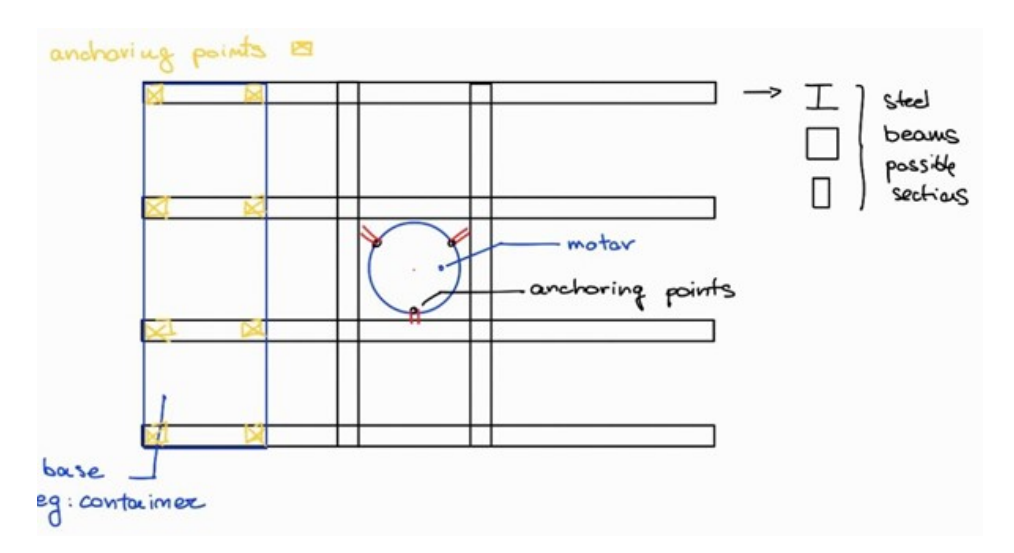


Figure 3.15: Preliminary configuration of the engine mounting base and support platform (Credits: Alpha Impulsion)

- The supporting structure consists of H-beam profiles;
- A mounting support for a vertical support structure is required or at least the corresponding load must be considered in the analysis.

This leads to a more defined configuration, which will be developed through a detailed CAD model in *SolidWorks* and verified using a finite-element analysis (FEA) in *Nastran* to evaluate structural deformation under both static and high-temperature operating conditions. As seen in the picture the structure is a semi-symmetrical 3x3 configuration with a larger box in the position where the motor will be installed.

3.5.2 Finite Element Analysis (FEM) of the Platform

A preliminary FEM analysis was carried out to size the structural elements of the mounting platform and select a suitable beam configuration. The analysis workflow included: (i) selection of an appropriate H-beam section and material; (ii) model setup and meshing; (iii) static load simulation; (iv) evaluation and refinement of results; and (v) a thermal performance check under high-temperature conditions. The approach followed standard practice for structural steel design and finite element verification, as outlined in [48, 49].

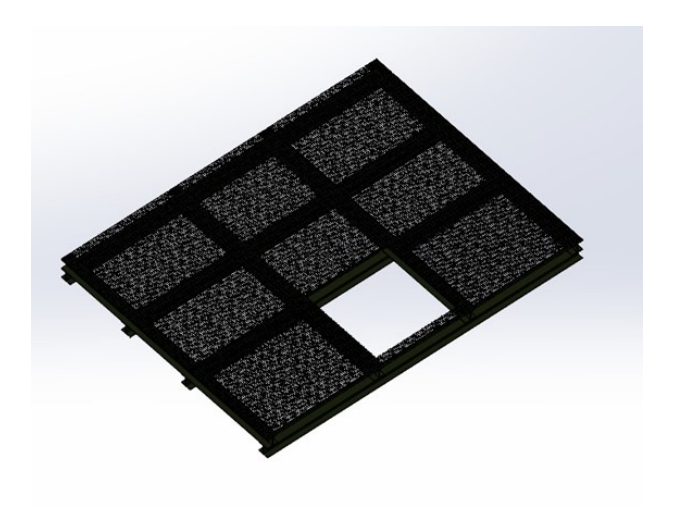


Figure 3.16: CAD of the mounting platform with a grid paving to allow operator activity on top (Credits: Alpha Impulsion)

Beam Selection and Material

The beams were chosen according to DIN 1025 standard dimensions (see Figure 3.17) [50].

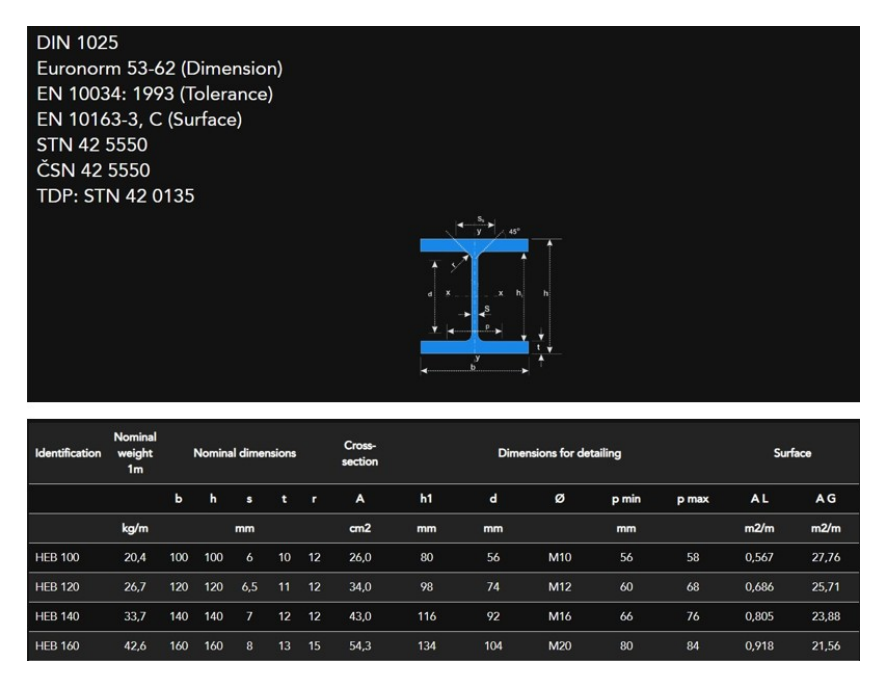


Figure 3.17: Dimensional details of the selected H-beam section (DIN 1025) — (Credits: Alpha Impulsion)

An initial analysis with 25×250 mm profiles showed that a smaller section would suffice. The selected configuration adopts **HEB 160** (160×160 mm) beams made of **S235 structural steel**, characterized by:

$$E = 210 \text{ GPa}, \quad \nu = 0.3, \quad \rho = 7850 \text{ kg/m}^3, \quad \sigma_y = 235 \text{ MPa}$$

Thermal expansion was included with $\alpha = 12 \times 10^{-6}$ °C⁻¹. The mechanical and thermal properties were derived from Eurocode 3 [51] and data sheets from Arcelor-Mittal and ThyssenKrupp [52, 53]. Although several materials were evaluated, S235 was retained for its wide availability and low cost. Table 3.3 compares alternative materials and their behavior at elevated temperatures based on [54, 55].

Table 3.3: Comparison of structural steels for the test bench platform

	S235	Corten (A242)	HSLA (A588)	AISI 304
Yield Strength (MPa)	235	235	345	215
$\rm Yield~@800^{\circ}C~(MPa)$	15	20	25	35
Thermal Expansion α (10 ⁻⁶ /°C)	12	11	11	17
Density (kg/m^3)	7850	7850	7850	8000
Cost (€/m)	60	65	67	200
Availability	High	High	High	Limited

Model Setup

The structure was simulated using NASTRAN, with the following boundary conditions:

- Fixed supports at the container interfaces and beam junctions, replicating bolted/flanged joints.
- Denser mesh around load application zones to capture peak stresses accurately (Figure 3.18), following meshing guidelines in [56].

Loads included a 20 t distributed weight (representing the engine) applied on the four corners of the motor base and an additional 1 t tower load to simulate the cryogenic pipe support and operator access structure. This represents the maximum static case before engine ignition. Such load assumptions are consistent with test-stand scaling methodologies found in [46, 57].

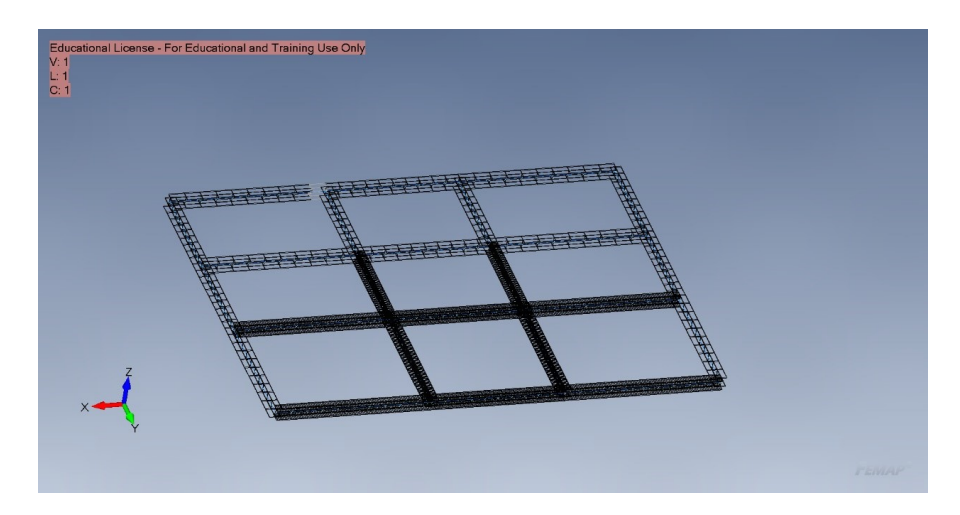


Figure 3.18: Mesh of the FEM model with refined zones near load application points (Credits: Alpha Impulsion)

Results at Room Temperature

The combined stress distribution is shown in Figure 3.19, expressed in Pascals. Peak stresses reached approximately **33 MPa**, well below the S235 yield limit, ensuring a high safety margin, in accordance with the safety factors recommended by Eurocode 3 [48].

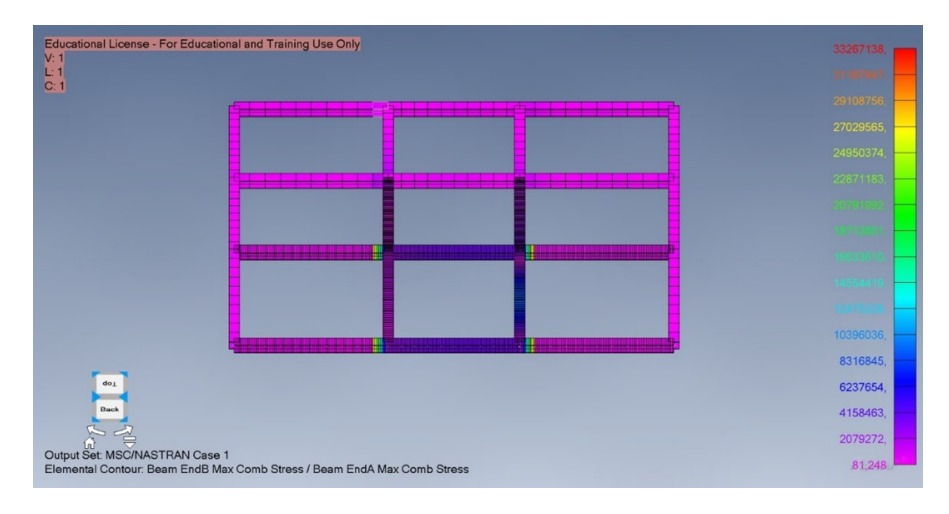


Figure 3.19: Combined stress field at room temperature (Credits: Alpha Impulsion)

The maximum displacement (Figure 3.20) was about **0.6 mm**, occurring on the beam supporting both the engine and tower loads. Deflections are compatible with

Educational License - For Educational and Training Use Only
V: 1
C: 1

0.0005601

0.0005601

0.00052

0.00048

0.00044

0.00044

0.00016

0.00016

0.00016

0.00016

0.00016

0.00016

0.00016

0.00016

0.00016

0.00016

0.00016

0.00016

0.00016

0.00016

0.00016

0.00017

Deformed(0.000401): Total Translation

the stiffness criteria defined for heavy steel platforms [48].

Figure 3.20: Displacement field at room temperature (Credits: Alpha Impulsion)

Results at High Temperature (800°C)

A second analysis considered reduced material properties at 800°C, based on experimental curves from [51, 54]:

$$E = 60 \text{ GPa}, \quad \nu = 0.3, \quad \rho = 7640 \text{ kg/m}^3, \quad \sigma_y = 20 \text{ MPa}$$

This represents a conservative case, since the structure will be water-cooled and only briefly exposed to exhaust heating [42]. Peak stresses reached about **47 MPa**, exceeding the reduced yield limit of S235, with maximum displacements around **1.8 mm**. Although such conditions are unlikely during normal operation, localized reinforcement with materials of better high-temperature performance (e.g., AISI 304) may be beneficial [55, 54].

3.5.3 Auxiliary Elements and Ground Support

The final part of the preliminary design includes an estimation of auxiliary structures and support elements, namely:

- 1. Protection against environmental conditions;
- 2. Accessibility and operator safety;
- 3. Ground foundation sizing and verification;
- 4. Preliminary structural cost estimation.

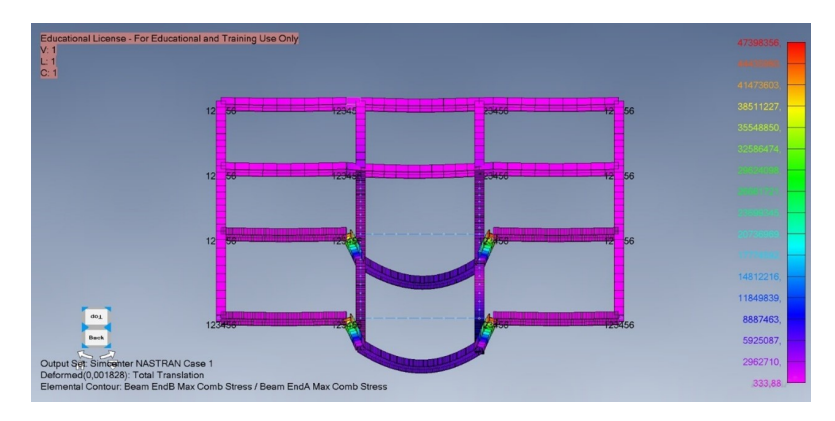


Figure 3.21: Combined stress distribution at 800°C (Credits: Alpha Impulsion)

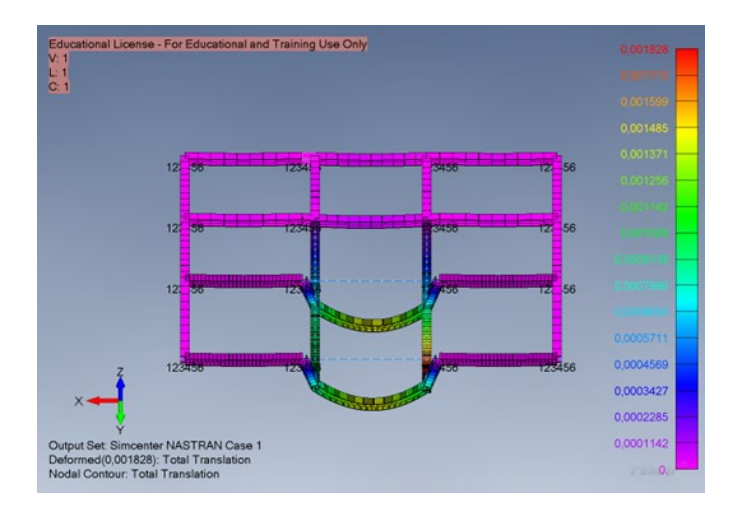


Figure 3.22: Displacement field at 800°C (Credits: Alpha Impulsion)

Environmental Protection

The potential need for a protective roof above the test stand must be carefully assessed. While a roof would shield the structure from rain and snow, it could limit the test height, particularly for autophage engines with variable grain length. To preserve flexibility, removable or retractable covers are preferred, offering weather protection during idle phases without constraining future test campaigns. Since hot-fire operations are planned only in favorable weather, a permanent roof is considered non-essential.

Accessibility

Safe access for operators is ensured through metallic stairs and protective railings integrated with the container frame. An auxiliary tower provides access to the

top of the motor and serves as an anchoring point for cryogenic feed lines, power cables, and instrumentation. The tower adopts a modular design—composed of 2 m segments (base, mid, and top)—to allow easy adjustment for different motor lengths or future reconfigurations.

Ground Support and Concrete Foundation

The static and dynamic loads of the test bench are transmitted to the ground through the container corner castings, which act as the main vertical load-bearing points. To ensure stability and durability, the installation is foreseen on a reinforced concrete slab designed to distribute these concentrated loads evenly.

Table 3.4 summarizes the load estimation used for preliminary dimensioning, based on the configuration with two container stacks supporting the platform.

Table 3.4: Summary of loads and pressures on the concrete foundation

Parameter	Value
Container casting area (per corner)	0.0225 m^2
Container self-weight	2.3 t
Ballast weight (per container)	2.0 t
Number of containers	6
Structure weight (platform + engine)	20 t
Stacks number	2
Total load	45.8 t
Load per stack	22.9 t
Load per corner	5.73 t
Pressure per corner	2.54 kPa
Soil bearing capacity	200 kPa
Concrete compressive strength (C25/30)	25,000 kPa

Even under conservative assumptions, the pressure transmitted to the soil remains well below the admissible bearing capacity, providing a large safety margin. A reinforced concrete slab of dimensions $10 \text{ m} \times 15 \text{ m}$ was adopted as baseline. Using the simplified bearing formula ([58, 59]):

$$h \ge k \cdot \sqrt{\frac{P}{\sigma_b}}$$

where h is the slab thickness, k a safety factor, P the load per corner, and σ_b the allowable soil pressure.

The calculation yields the values in Table 3.5.

Table 3.5: Preliminary results for the reinforced concrete foundation

Parameter	Result
Soil load capacity (σ_b)	200 kPa
Safety factor (k)	2
Equivalent slab thickness (reinforced)	$0.32 \mathrm{\ m}$
Concrete volume $(10 \times 15 \text{ m base})$	$48~\mathrm{m}^3$
Thickness at maximum load points (concrete only)	$1.06 \mathrm{m}$

The reinforced configuration, with approximately 0.3 m thickness, ensures adequate stiffness and load distribution while minimizing material use. Such a slab can be realized on compacted soil with proper formwork and reinforcement mesh, offering both stability and resilience to the mechanical and thermal stresses generated during firing.

3.5.4 Preliminar CAD model of the test bench structure



Figure 3.23: CAD model (Credits: Alpha Impulsion)

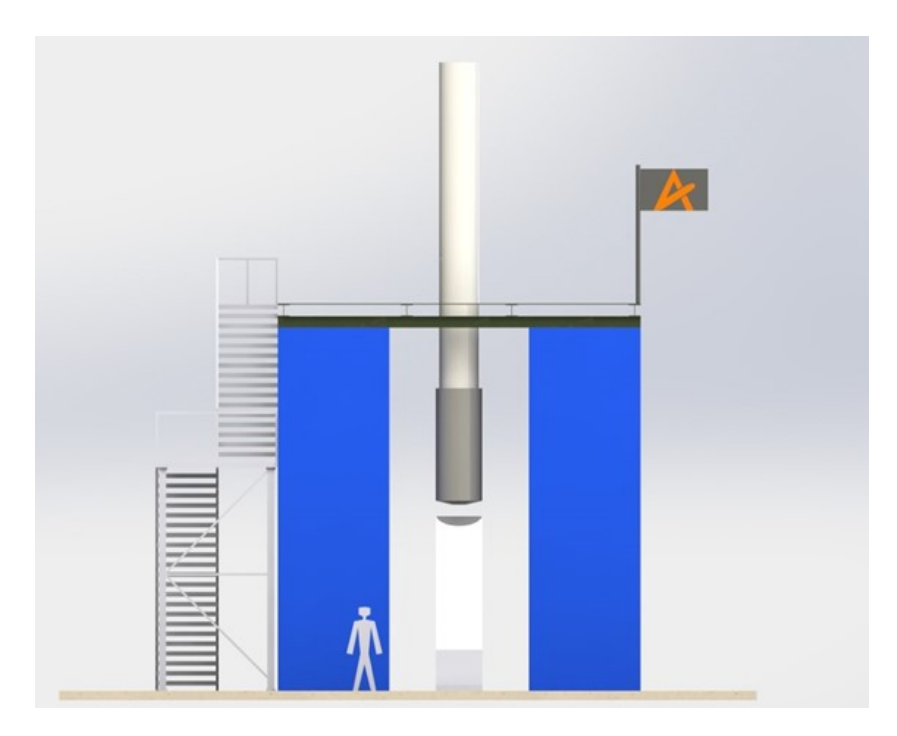


Figure 3.24: CAD model (Credits: Alpha Impulsion)

3.6 Fluids

The cryogenic feed system was preliminarily defined to ensure that liquid oxygen (LOX) can be delivered to the engine within the required parameters of 90 K, 30–50 bar pressure (up to 100 bar maximum), and 20–30 kg/s mass flow rate for test durations between 10 and 60 s, extendable to 250 s. The system must also allow throttling down to one-seventh of the nominal flow rate and support cooldown, pressurization, and purge operations.

3.6.1 Pressurizing and Purge Gas

Nitrogen was selected as the pressurizing and purge medium. Although helium offers superior purge efficiency and non-condensable behavior, its cost and limited availability make it impractical for routine operations. Nitrogen, in contrast, is inexpensive, abundant, and easy to handle, while liquid nitrogen can also be used for line cooldown before LOX transfer. This dual-purpose use provides both simplicity and cost efficiency. Proper venting procedures mitigate risks of oxygen condensation or icing during operations.

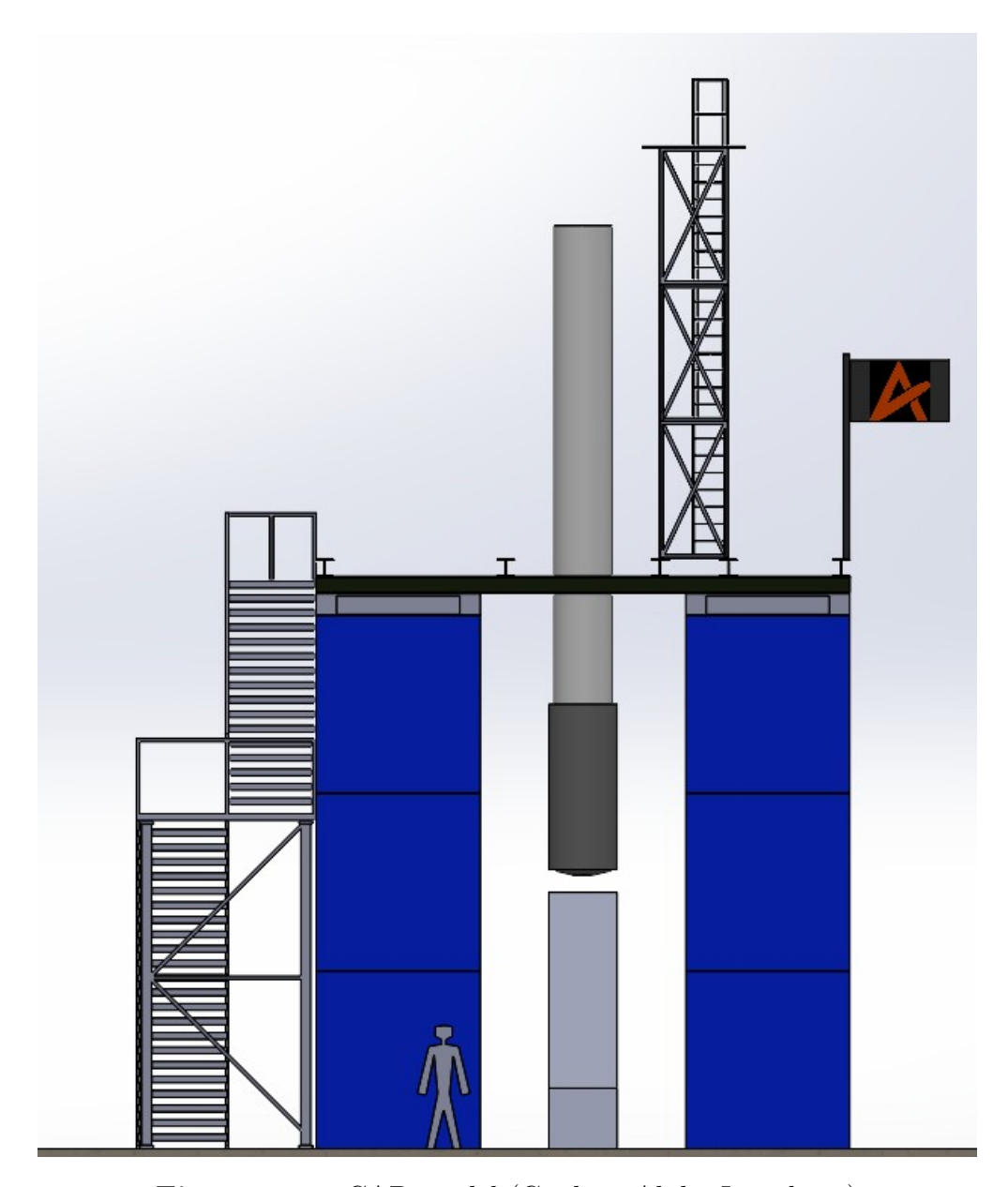


Figure 3.25: CAD model (Credits: Alpha Impulsion)

3.6.2 Fluid Path and Line Configuration

From the engine interface, a flexible cryogenic hose is foreseen to avoid transferring mechanical loads to the thrust measurement system. Downstream of this section, rigid vacuum-insulated pipes connect the feed line to the LOX tank, in accordance with typical cryogenic distribution practice for VIP/VJ lines [60, 61]. A Coriolistype mass flow meter, pressure and temperature sensors, and control valves are installed along the line, with Coriolis instrumentation selected for its accuracy and low temperature capability in LOX service [62]. The line includes approximately 30–40 m of piping, three 90° bends, and two 45° bends, with an elevation difference corresponding to the top of the combustion chamber (circa 6 m). The selected nominal pipe diameter is 8 inches, determined from the target flow rate and acceptable fluid velocity range.

The layout integrates:

- Three on/off valves of **ball** type for isolation and safety;
- One **globe** valve for flow regulation;
- One Coriolis mass-flow meter for precise flow measurement.

Valve selection follows cryogenic oxygen compatibility and tightness class guidance for pipeline components [63, 64].

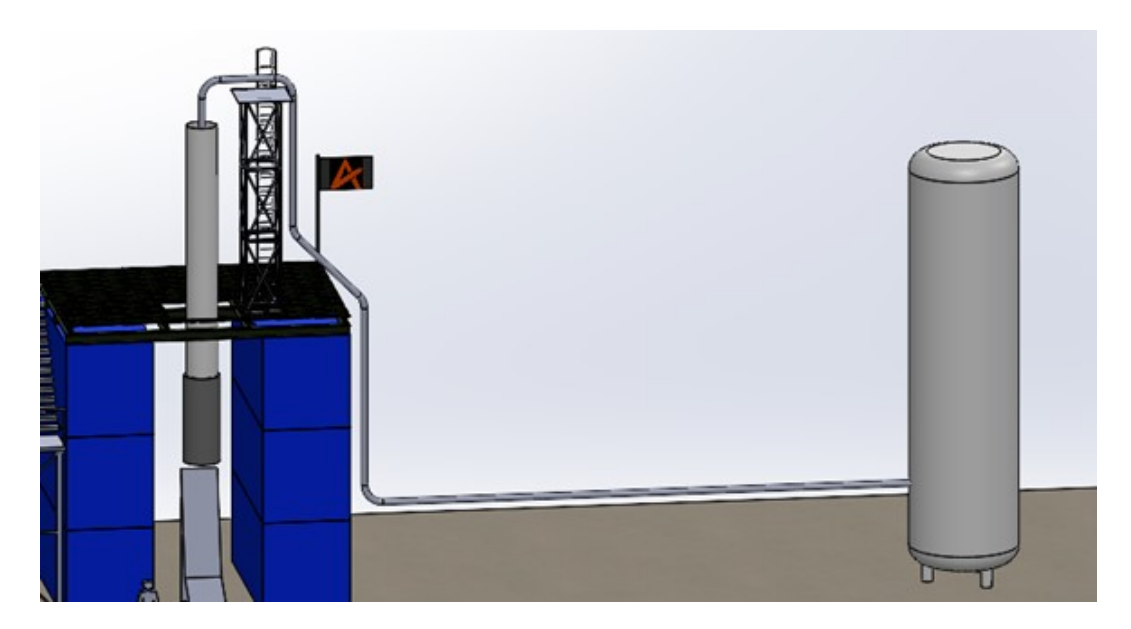


Figure 3.26: CAD model of the main fluid line placement (Credits: Alpha Impulsion)

3.6.3 Pressure Losses and System Evaluation

Using the Darcy-Weisbach correlation for cryogenic liquid flow, a pressure drop of approximately 0.037 bar/m was obtained, leading to total line losses of about 10–11 bar, including valves, elbows, sensors, and elevation head. Minor-loss coefficients and valve/bend contributions were estimated from standard data for piping components [65], while LOX properties versus temperature were taken from NIST data [66]. These results define the required operating margin for the tank pressurization system.

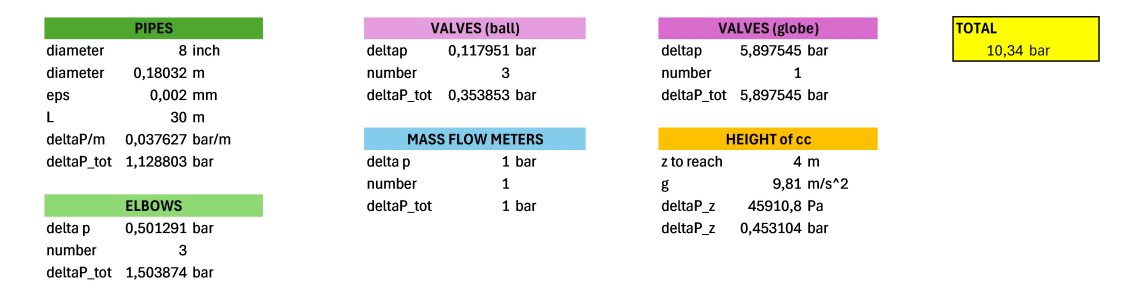


Figure 3.27: Estimated fluid line pressure losses (Credits: Alpha Impulsion)

3.6.4 Sizing of the pressurization system

Three potential pressurization concepts were evaluated to balance cost and operational complexity:

- 1. A single **self-pressurized tank**, simple but limited in control;
- 2. A dual-tank configuration, with a main storage tank and a smaller highpressure blowdown tank;
- 3. A **pressurized tank with cryogenic pump**, enabling continuous feeding and fine control of delivery pressure.

A trade-off analysis considering cost, maintainability, and test flexibility identified the third solution — pressurized tank plus cryogenic pump — as the most promising for achieving stable flow control and reusability in future campaigns [67, 19].

Option 1 – Single Auto-Pressurized Tank

This configuration relies on a self-pressurizing tank equipped with an internal evaporator coil. A controlled fraction of the liquid oxygen (LOX) is vaporized through a serpentine heat exchanger and recirculated into the tank ullage, maintaining

constant pressure during operation. The approach is mechanically simple and avoids the need for external high-pressure systems, though it demands a robust cryogenic tank capable of sustaining high pressures [61].

Design Basis The analysis was carried out assuming:

- 1. Negligible heat exchange between liquid and gaseous phases;
- 2. Incompressible LOX behavior;
- 3. Initial ullage fraction of 10%;
- 4. Vaporized LOX at the same temperature and pressure as the bulk liquid.

The tank must withstand internal pressures up to **61–65 bar**, requiring a custom-built cryogenic vessel. While feasible, the cost and safety constraints increase significantly for large storage volumes [22].

Table 3.6: Summary of self-pressurization calculations for the single-tank configuration

Parameter	Value
Feed pressure requirement	50 bar
Pressure losses in feed line	11 bar
Total required tank pressure	61 bar
Mass flow rate	30 kg/s
Test duration	60 s
Total LOX to engine	1800 kg
LOX evaporated for pressurization	530.8 kg (29.5 %)
Equivalent evaporated volume	$463.5~\mathrm{L}$
Total LOX consumption per test	2035.6 L (circa 2.3 t)
Available LOX per campaign	10 000 L
Number of tests possible	4
Required vaporizer mass flow	8.85 kg/s

Discussion The self-pressurization principle ensures automatic pressure control but requires precise management of the vaporization rate and ullage conditions during blowdown. The system's feasibility depends on the ability to operate the vaporizer safely and efficiently during transient conditions. Because of the high design pressure, this solution is better suited for short-duration tests and small-to-medium LOX volumes, rather than for large-scale continuous feeding.

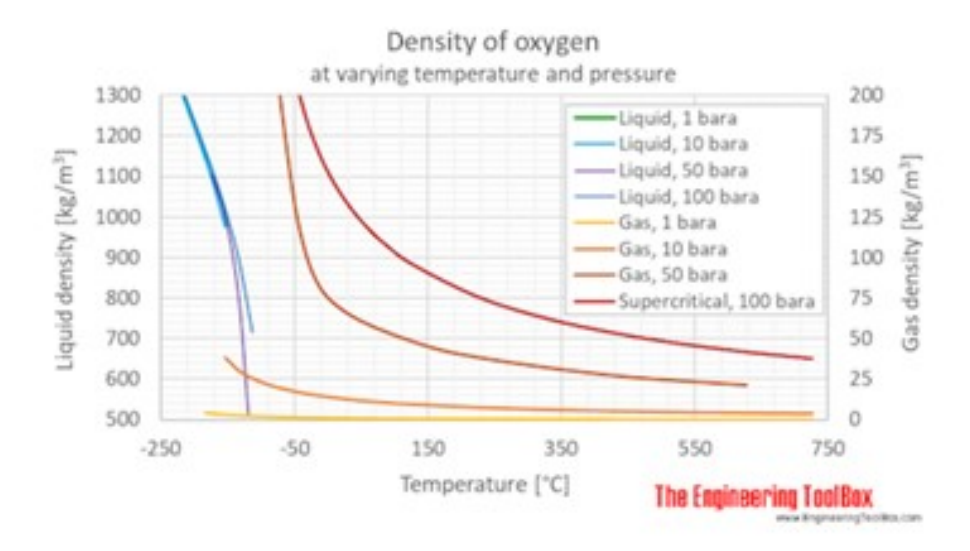


Figure 3.28: Density of oxygen at varying temperature and pressure (Credits: The Engineering ToolBox)

Option 2 – Normal Pressure Storage Tank + Self-Pressurized Blowdown Tank

This configuration combines a main storage tank operating near atmospheric pressure with a smaller, high-pressure self-pressurizing tank used during the firing phase. Once the required initial pressure is established, the feed valve opens and the system operates in a blowdown mode: the internal pressure gradually decreases as LOX is expelled. The design objective is to minimize this pressure drop during the test, maintaining acceptable engine feed conditions [19].

Assumptions

- 1. Adiabatic transformation of the ullage gas;
- 2. Fixed ullage fraction of 33%;
- 3. LOX mass flow rate of 30 kg/s.

A larger ullage fraction reduces pressure variation during blowdown but proportionally decreases the available liquid volume. An ullage of 33% was selected as a balanced compromise, corresponding to typical industrial LOX filling ratios [22].

Tank Sizing and Pressure Evolution The relationship between tank volume and pressure decay was evaluated for several capacities. Larger tanks exhibit slower

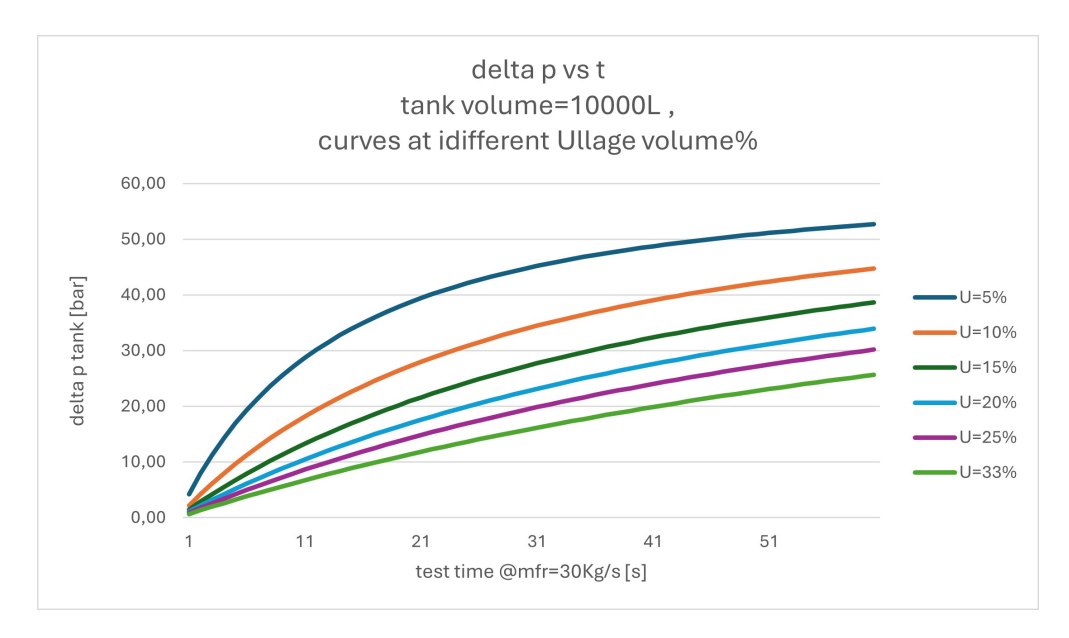


Figure 3.29: Pressure variation versus time for different ullage fractions during blowdown (Credits: Alpha Impulsion)

pressure loss but higher manufacturing and integration costs. A practical trade-off can be made between acceptable pressure decay (5–7 bar during one test) and tank cost, as summarized in Table 3.7.

Table 3.7: Estimated test durations versus tank volume for 5–7 bar pressure loss

Tank volume [L]	10,000	20,000	30,000	40,000	60,000	85,000
Test duration [s]	8–12	16-23	24–34	32-46	48-60+	60+

This configuration offers a balance between simplicity and control. The main storage tank can remain at low pressure, reducing safety requirements, while the smaller blowdown tank handles the high-pressure transient. However, the achievable test duration is limited by the tank's gas expansion capacity.

Option 3 – Pressurized Tank + Cryogenic Pump

In this configuration, the main LOX tank is maintained at a moderate pressure suitable for storage, while a cryogenic pump raises the liquid to the required feed pressure. This approach decouples storage and delivery functions, enabling long-duration tests and precise control of flow and pressure. Industrial cryogenic pumps

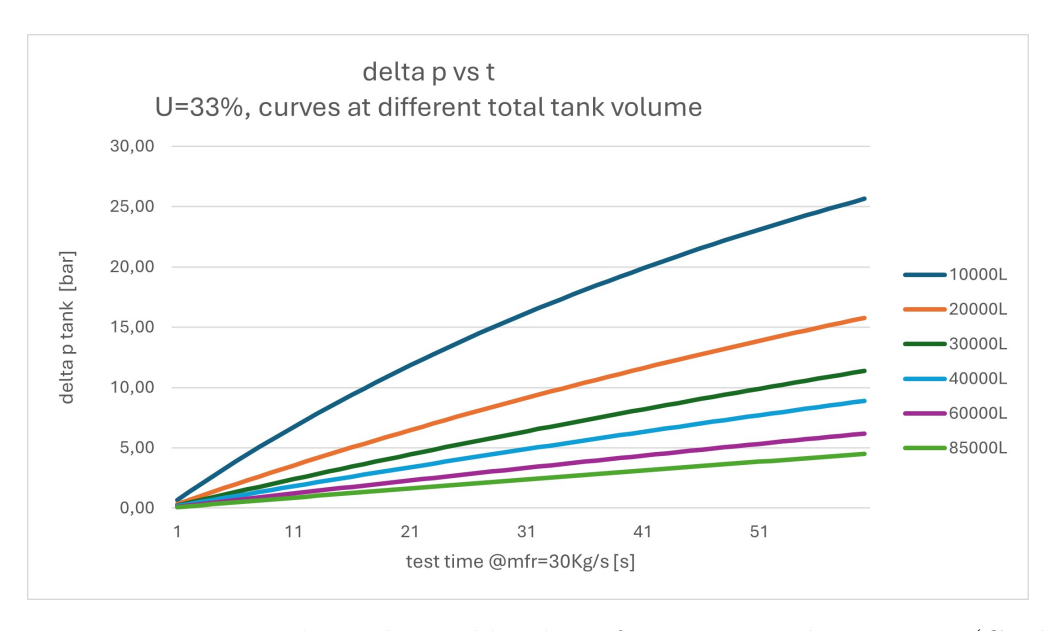


Figure 3.30: Pressure decay during blowdown for various tank capacities (Credits: Alpha Impulsion)

for LOX in this pressure/flow class are commercially available [68, 69].

Pump Requirements The cryogenic pump must be compatible with LOX and meet the following specifications:

• Mass flow rate range: 5–30 kg/s;

• Outlet pressure: 40–65 bar;

• Inlet pressure: 30–35 bar;

• Pressure differential (ΔP): 5–35 bar.

Discussion This configuration provides the most stable and controllable feed conditions, with minimal pressure decay and no need for large, high-pressure tanks. Its main drawback is the high cost of the pump, which may exceed €300,000. Nevertheless, the system offers scalability, reusability, and compatibility with future continuous-feed or regenerative pressurization architectures [67].

Main LOX and LN₂ Tanks

The sizing of the main oxidizer and auxiliary cryogenic tanks is determined by blowdown requirements and the number of consecutive tests. For liquid oxygen (LOX), a 20,000 L tank allows about 30 s of firing with a 5 bar pressure drop, or 60 s with a 15 bar loss, sustaining pressures from 15 to 60 bar depending on the configuration. After each test, the high-pressure tank is refilled from a larger low-pressure storage unit.

In the self-pressurizing configuration, the same capacity enables up to nine tests, considering evaporative losses. Liquid nitrogen (LN_2), used for pressurization, purge, and cooldown, operates at lower pressures but must also be stored in liquid form to reduce volume. A minimum of 2,500 L is required, while 10,000 L provides a safe operational margin. Both tanks are equipped with air evaporators for autonomous pressure maintenance between tests [22, 60].

Table 3.8: Summary of LOX and LN₂ tank requirements and calculated volumes

Parameter	Unit	LOX Tank	\mathbf{LN}_2 Tank	Notes
Operating pressure range	bar	15–65	2–20	$\begin{array}{ccc} LOX & pressurized & or \\ pumped; & LN_2 & for \\ purge/cooldown & \end{array}$
Nominal tank volume	L	20,000	10,000	Design reference volume
Minimum required volume	L	20,000	2,541	From purge/cooldown sizing
LOX/LN_2 per test campaign	L	20,000 (9 tests)	7,767 (gas) / 212 (liq.)	Includes purge and cooldown
Pressure loss (60 s blowdown)	bar	15	_	From blowdown analysis
Pressure loss (30 s blowdown)	bar	5	_	For steady tests
Evaporated mass flow	kg/s	8.85	_	Self-pressurization mode
Recommended safety margin	_	25%	50%	Operational allowance

3.6.5 Feed System Design Choice and Preliminary P&ID

Two configurations were considered for the feed system: the first employs a **blow-down LOX tank**, while the second uses a **cryogenic pump** to pressurize the line. The main distinction between the two lies in the maximum pressure required in the LOX tank.

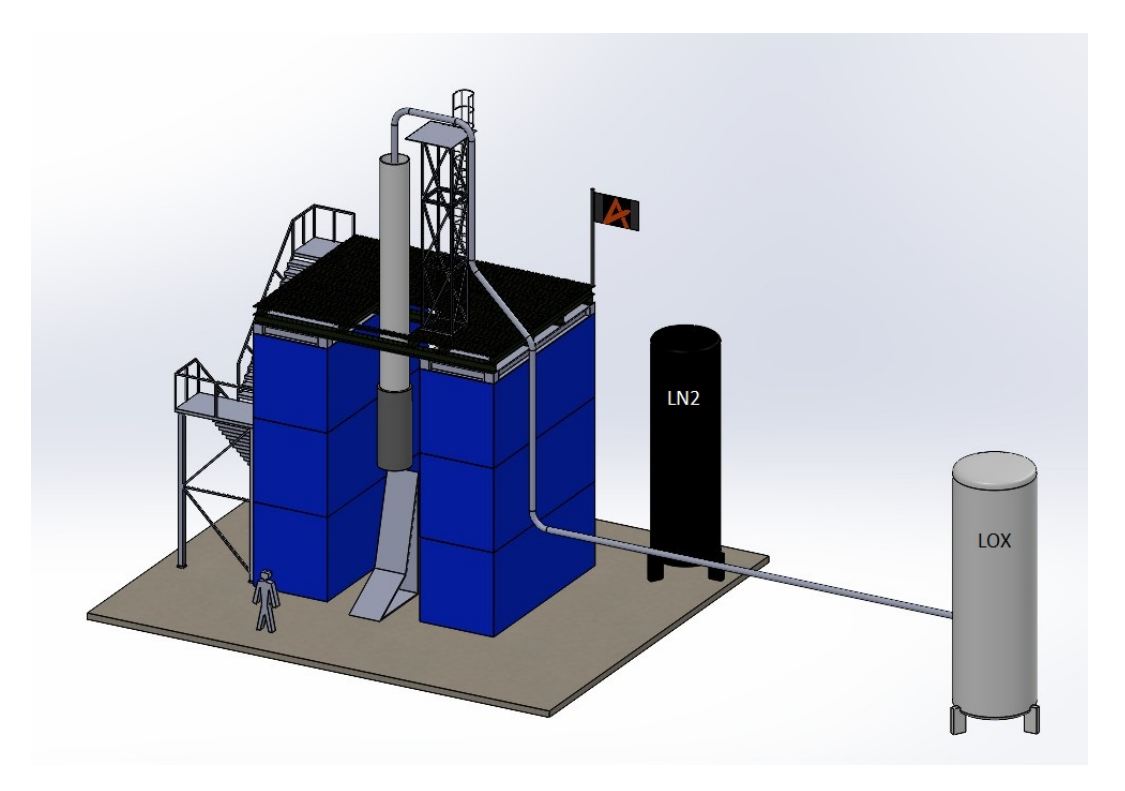


Figure 3.31: CAD model including fluids feed system tanks and piping (Credits: Alpha Impulsion)

Layout Considerations

The system was designed to support at least ten consecutive tests, with final storage capacity to be refined during the budgetary phase based on tank cost. At this stage, the trade-off between the two options is primarily economical: both are technically feasible, but the pump-based system introduces specialized and costly components. The next design phase will include supplier assessment to evaluate cost, manufacturability, and delivery time of each configuration.

Main Components

Pipes Two types of pipelines are foreseen: **vacuum-jacketed** (**VJ**) and non-insulated. VJ pipes—both rigid and flexible—will be used on the main LOX feed line to ensure minimal thermal losses, while other pipes may be foam-insulated to prevent ice formation. The total estimated pipe length, including elevation and safety distance, is approximately 25 m, with diameters between 6 and 8 inches.

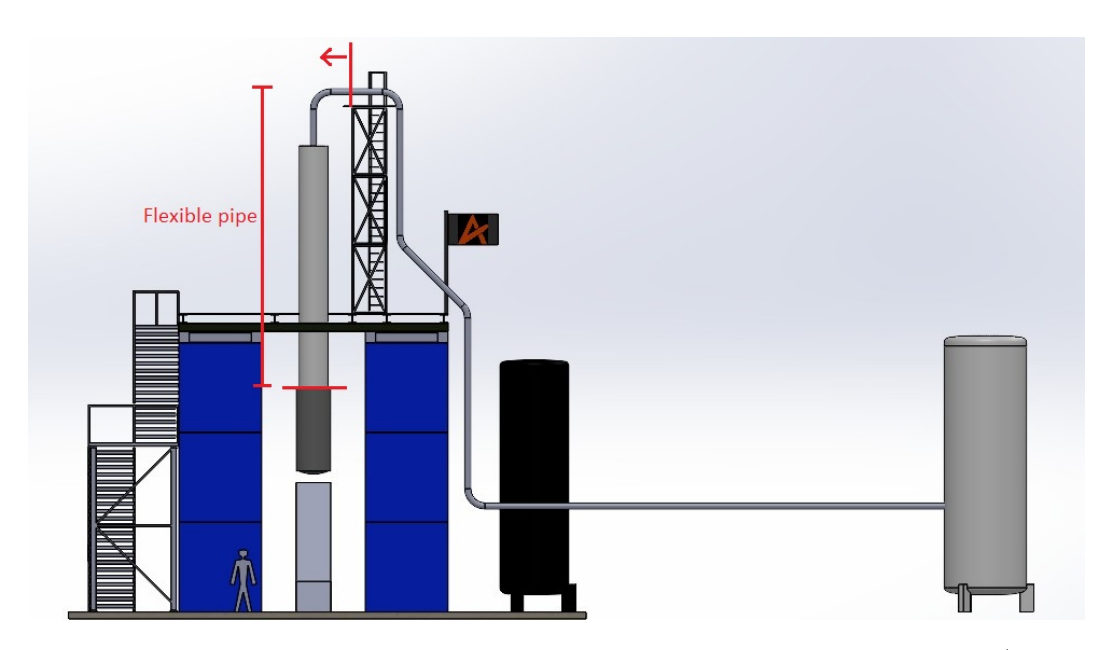


Figure 3.32: CAD model including fluids feed system tanks and piping (Credits: Alpha Impulsion)

Evaporators Air evaporators are required for both LOX and LN_2 systems. For LOX, they provide vaporization for cooldown and displacement during line operations; for LN_2 , they generate gaseous nitrogen for purge and pressurization cycles.

Pump The cryogenic pump (if adopted) must handle variable mass flow rates between 10 and 30 kg/s, raising pressure from 15–35 bar at the inlet up to 65 bar at the outlet. The expected ΔP range is 30–50 bar. While offering excellent control and reusability, the pump cost may exceed $\mathbf{\epsilon}$ 300,000 and will require dedicated procurement.

Valves Valve selection considers flow rate, operating pressure, and gas characteristics. In this preliminary phase, types and quantities are defined, while the specific models and manufacturers will be selected in later design iterations.

Feed System Components

The following table summarizes the main feed system components for the blowdown configuration, with alternative values in parentheses for the pump-based configuration.

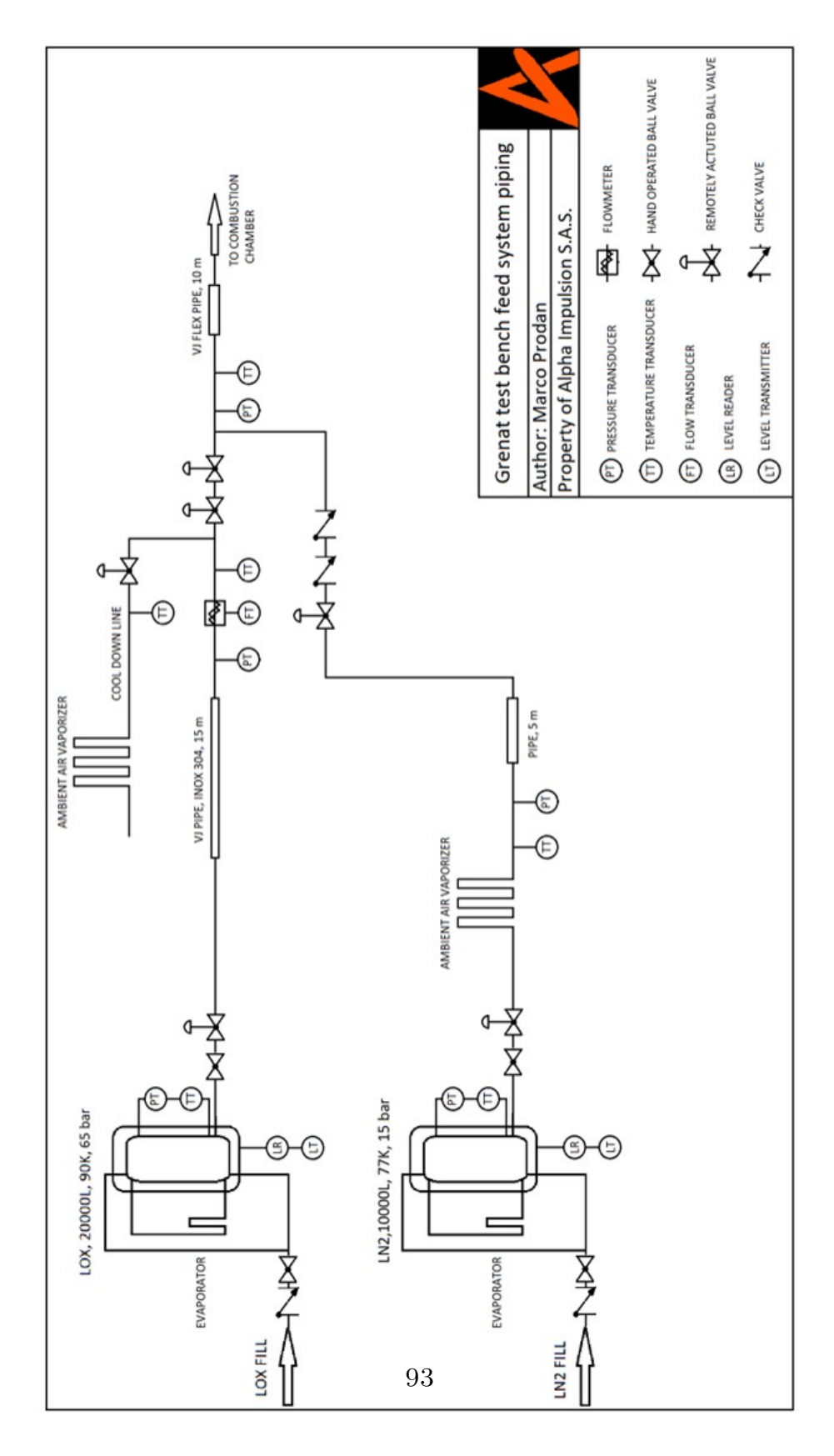


Figure 3.33: PFD of the self pressurized tanks feed system (Credits: Alpha Impulsion)

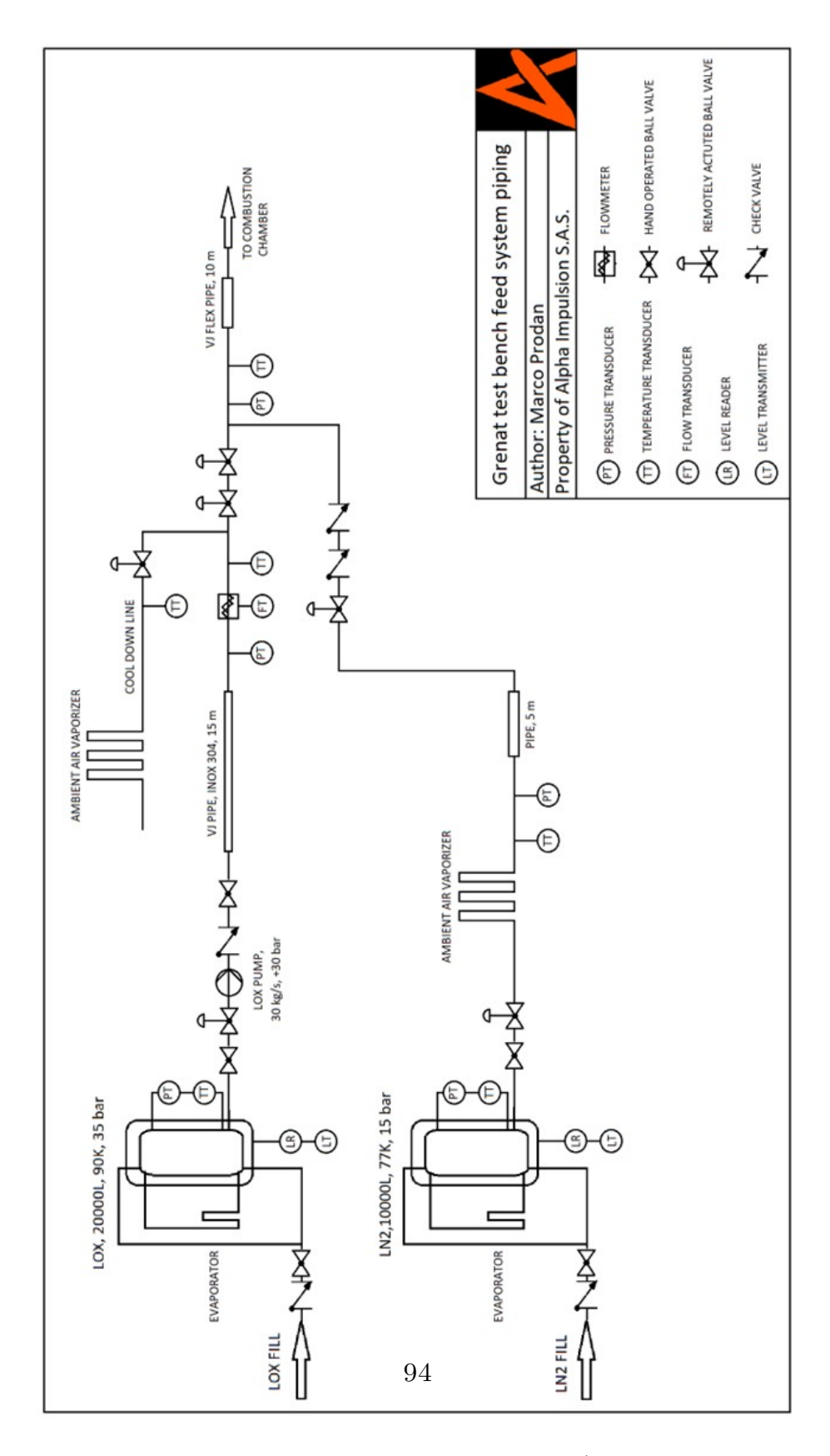


Figure 3.34: PFD of the pump pressurized feed system (Credits: Alpha Impulsion)

Table 3.9: Main feed system components (blowdown configuration; alternative values in parentheses for pump system)

Name	Description	Quantity
LOX tank + PB unit	20,000 L, 90 K, 65 bar (15–35 bar)	1
$LN_2 tank + PB unit$	2,000-10,000 L, 77 K, 15 bar	1
LOX evaporator	30 kg/s capacity	1
LN_2 evaporator	Gas generation for purge	1
Cryogenic pump	$(10-30 \text{ kg/s}, \Delta P = 30-50 \text{ bar})$	(1)
Vacuum-jacketed pipe	Main LOX line, rigid section	1 set
	(15 m)	
Flexible VJ pipe	Terminal section of main feed line	1 set
	(10 m)	
Normal pipe	Secondary and purge lines (10 m)	1 set
Hand-operated ball valve	Manual isolation	4(5)
Remote-operated ball valve	Automated isolation	6
Check valve	Backflow prevention	4(5)
Level measurement	/	2
Flowmeter	/	1
Pressure sensor	/	5
Temperature sensor	/	6

3.7 Acquisition and Control

During the preliminary design phase developed within this project, the acquisition and control system was only defined at a conceptual level and not fully developed. The detailed design of this subsystem — including the data acquisition architecture, signal conditioning, and control logic — was instead addressed in the second case study carried out later by the company.

Data Acquisition

The test bench will require a set of sensors to monitor key parameters such as thrust, pressure, and temperature. Thrust will be measured using load cells mounted on the engine support arms, with configurations adaptable to either axial-only or multi-axis measurement in case of thrust vector control implementation. Pressure and temperature sensors will be distributed along the feed system and near the combustion chamber, while level and flow sensors will monitor the tank conditions. The selection, calibration, and data acquisition chain will be finalized in the

subsequent design phase.

Electrical Power Supply

A dedicated 40 kW three-phase power line is foreseen to feed the control, acquisition, and auxiliary systems of the test bench. The supply operates at 400 V and approximately 72 A per phase, protected by MCCB-type circuit breakers rated for 100 A. Copper cables of 25–35 mm² cross-section ensure acceptable voltage drop and safe operation, with grounding resistance maintained below 1 Ω . If required, a 50–63 kVA transformer can be added to stabilize or adapt the supply voltage. Load balancing and switchgear configuration will be verified during the electrical integration phase.

3.8 Final Considerations

The development of this test bench represented my first direct experience in the design of complex cryogenic and propulsion-related ground systems. This work guided the entire theoretical and technical research presented in Chapter 2 and served as the foundation for understanding the main design methodologies applied throughout this thesis. The preliminary design phase required several months of study and iteration, reaching a complete conceptual definition of the structural and fluid systems before being concluded due to the transition to a second case study, as requested by the company. The following case study continues this work, addressing in a more detailed and integrated way those aspects — such as acquisition, control, and system automation — that were only outlined in the present chapter.

Chapter 4

Case study n.2: the Slab Burner test bench

4.1 Overview of the project

The slab burner test bench is a small-scale test rig developed to investigate, with high resolution, the regression rate of the solid fuel grain in a hybrid autophage rocket motor. The facility is conceived to reproduce the local thermo-fluidic conditions experienced at the fuel surface and to provide accurate, repeatable measurements of mass regression under controlled oxidizer flow conditions.

4.2 Specifications and operative requests

The slab burner test bench shall satisfy the following functional requirements:

- 1. provide mechanical support for the trapezoidal combustion chamber;
- 2. accept and operate a piston mechanism to insert and remove the solid fuel grain;
- 3. supply oxidizer to the chamber in gaseous form (GOX) with controlled mass flux profiles;
- 4. measure the thrust produced by the motor with appropriate load cell instrumentation;
- 5. acquire temperatures and pressures at all relevant locations in the system for transient and steady measurements;

- 6. provide inlet cooling for the combustion chamber, capable of operating with either water or liquid oxygen as required by specific tests;
- 7. safely discharge combustion products to a controlled exhaust environment.

4.3 Configuration and preliminary concept of the structure

The design request includes the following input data and boundary conditions:

- dimensions of the combustion chamber and of the fuel grain to be tested;
- fluid interfaces (type and thermodynamic state);
- measurement requirements (quantities and locations);
- operative interfaces, identifying what must be controlled or actuated;
- planned operational process (test type, duration, and repetition rate).

For reasons of simplicity, safety, transportability, and ease of access, the structure is designed as a metallic tubular frame mounted on a wheeled cart. The combustion chamber and the insertion piston are installed on top of this frame. The cart runs on rails and transfers all forces generated by the motor to a load cell assembly that measures the resulting thrust.

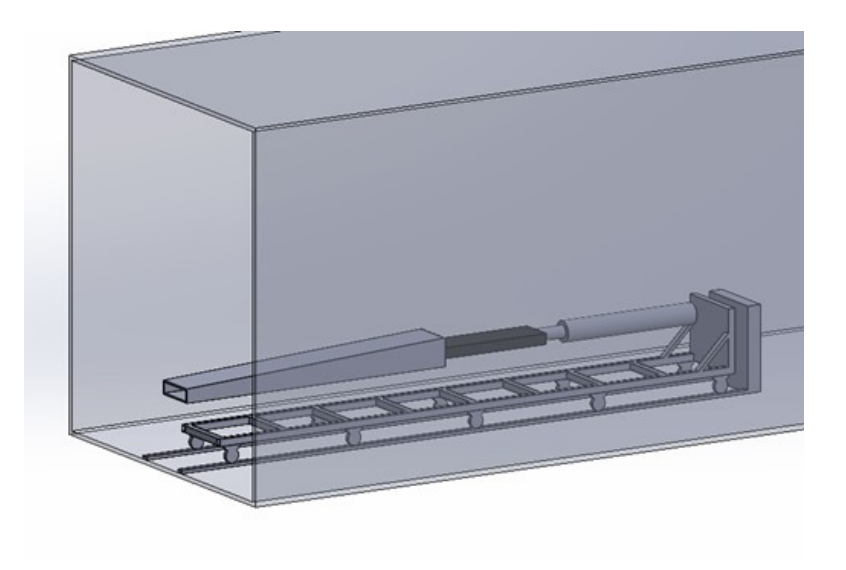


Figure 4.1: preliminary CAD model of the configuration for the thest bench (credits: Alpha Impulsion)

The entire system is housed inside a 20 ft (6 m) shipping container, with one open side that allows the exhaust gases to exit safely. A water deluge system can optionally be implemented at the container exit to suppress residual flames and mitigate heat effects. The current configuration does not yet include the mounting structure for the combustion chamber and piston, which will be introduced in a subsequent design iteration.

In general terms, the structure will require the following quantities of materials:

- 14–16 m of square steel tubing (approximately 50×50 mm) for the cart frame and mounting points of the combustion chamber and piston;
- 10 m of steel rail;
- two steel plates (approximately 400×400 mm) positioned on both sides of the load cell; these could alternatively be constructed from the same tubing, though potential deformation under load must be considered;
- one 20 ft container;
- a set of wheels mounted under the cart.

4.3.1 Structure weight estimation

An estimation of component masses is essential to define the sizing of the rails and to assess loads transmitted to the container base. Table 4.1 summarizes the approximate mass distribution.

Table 4.1: Estimated component masses for the slab burner test bench

Item	Description	Quantity	Weight [kg]
Steel tubes for structure	50×50 mm, 4 mm thick	15 m	82
Linear actuator	(reserved) kN, $0-60 \text{ mm/s}$	1 unit	100-150
Combustion chamber	Steel, $\rho = 8000 \text{ kg/m}^3$	$0.0328~\mathrm{m}^3$	up to 300
Fuel grain	HDPE, $\rho = 960 \text{ kg/m}^3$	0.001875 m^3	36
TOTAL			500-550

From these estimates, the rails must be capable of supporting approximately 250–275 kg per side with minimal rolling friction. The punctual load on each wheel depends on the total number of wheels; assuming five per side, the expected local load is around 50–55 kg per wheel, although this value may vary depending on the mass distribution along the test bench.

4.4 Subsystems

4.5 Fluids feed system

The design process begins from the fluid feeding subsystem, following an approach analogous to that adopted for the previous case study.

The feed system interfaces with the mobile cart through three main connections:

- 1. Gaseous oxygen (GOX) feeding, implemented via a flexible hose to minimize mechanical load transmission to the structure;
- 2. **Coolant feeding**, either water or liquid oxygen (LOX), using a similar flexible hose arrangement;
- 3. **Ignition fluid feeding**, dedicated to initiating combustion at the test start.

Three primary operating configurations have been evaluated, summarized in Table 4.2.

Table 4.2: Operating configurations of the slab burner fluid subsystem

Operating mode	Oxidizer	Coolant
1	GOX from tank	Water
2	GOX from tank	LOX from tank
3	GOX from evaporated cooling LOX	LOX from tank

The first configuration provides the simplest operational setup, relying only on gaseous oxygen and water tanks. Transitioning to cryogenic operation, with LOX storage and the use of evaporated LOX as oxidizer, introduces greater complexity in both design and operation. However, it also enables:

- 1. testing of the LOX cooling and handling subsystems;
- 2. reduction of storage volume requirements, since LOX density is considerably higher than that of GOX.

Nitrogen is also integrated in the system, serving for purging operations and, in cryogenic configurations, for pipe pre-cooling when available in liquid form (or gaseous purging otherwise).

The main design specifications for the feed system, beyond the fluid types, are summarized as follows:

• LOX/GOX mass flow rate: 2.7 kg/s;

- Inlet pressure at injection head: 40 bar;
- LOX storage pressure maintained above 40 bar to remain in supercritical conditions.

Three preliminary process flow diagrams (PFDs) have been prepared to represent the three operating configurations. These diagrams were developed under the following assumptions:

- 1. gases are supplied in blowdown mode, as standard tanks provide pressures around 200 bar, well above the 40 bar required for testing;
- 2. LOX nominal storage pressure is set to 60 bar to compensate for pressure losses during phase change and vaporization;
- 3. only the most relevant valves and sensors are represented, as detailed instrumentation and control design will be addressed in subsequent iterations.

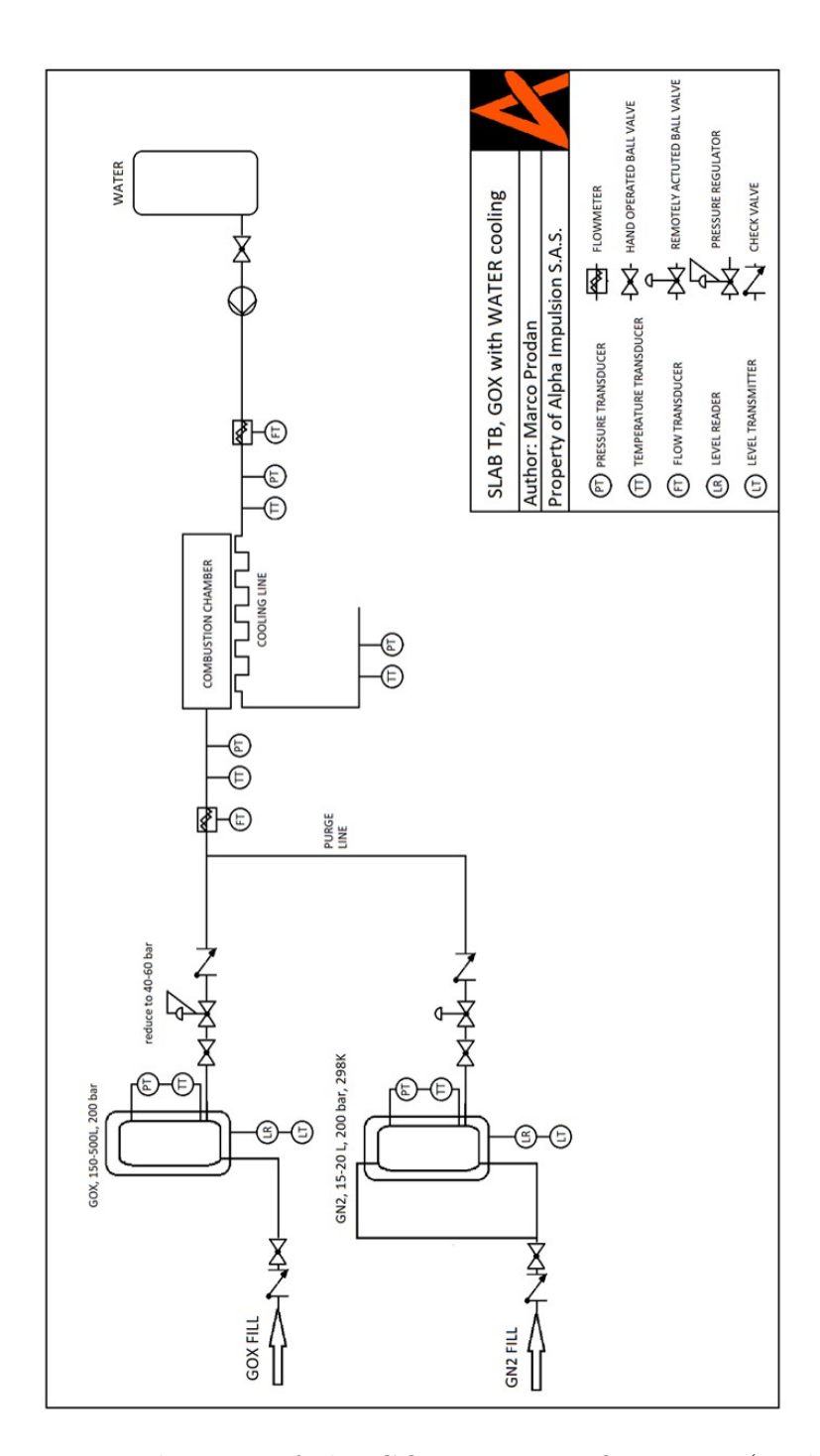


Figure 4.2: PFD diagram of the GOX-water configuration (credits: Alpha Impulsion)

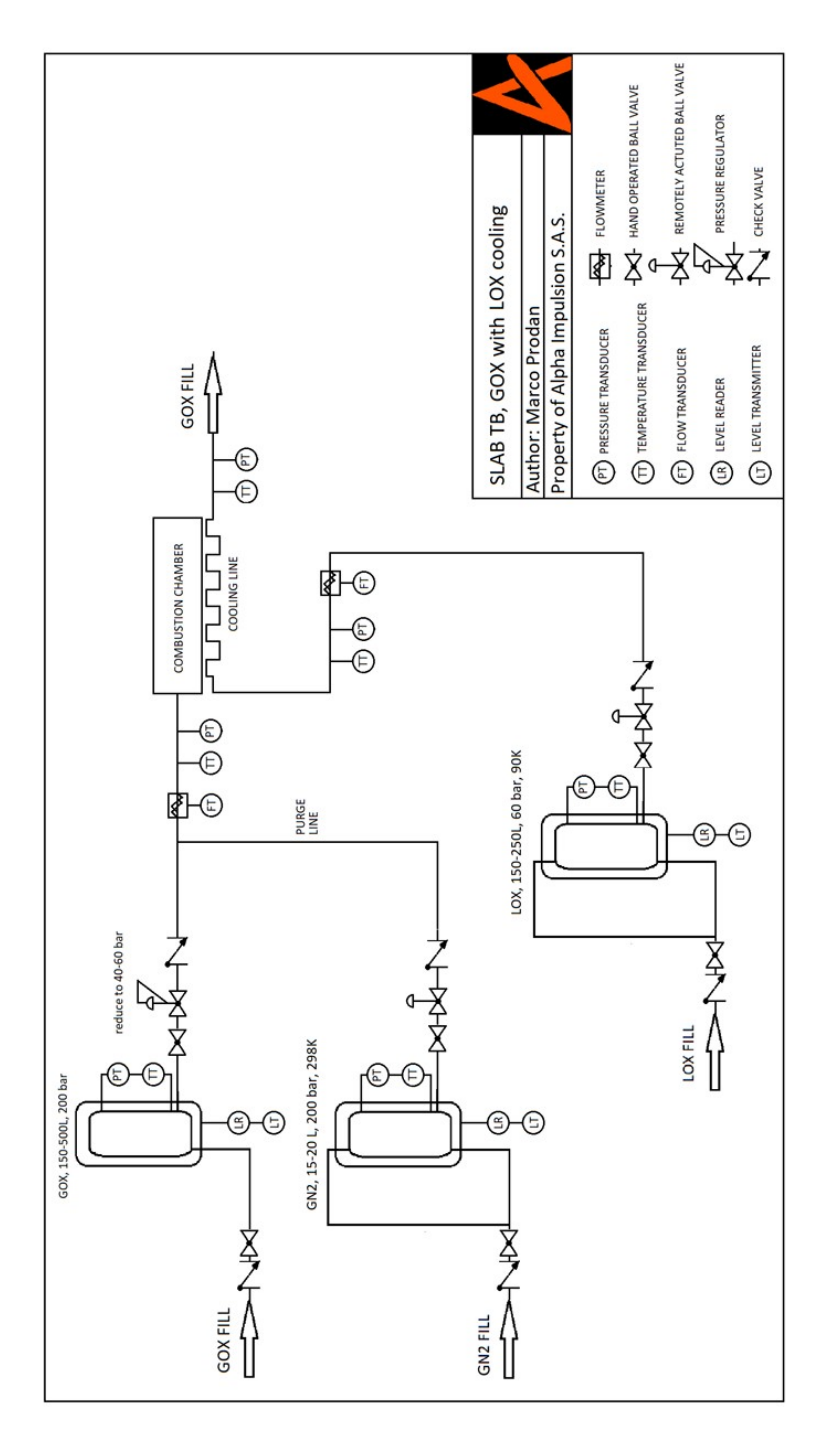


Figure 4.3: PFD diagram of the GOX-LOX configuration (credits: Alpha Impulsion)

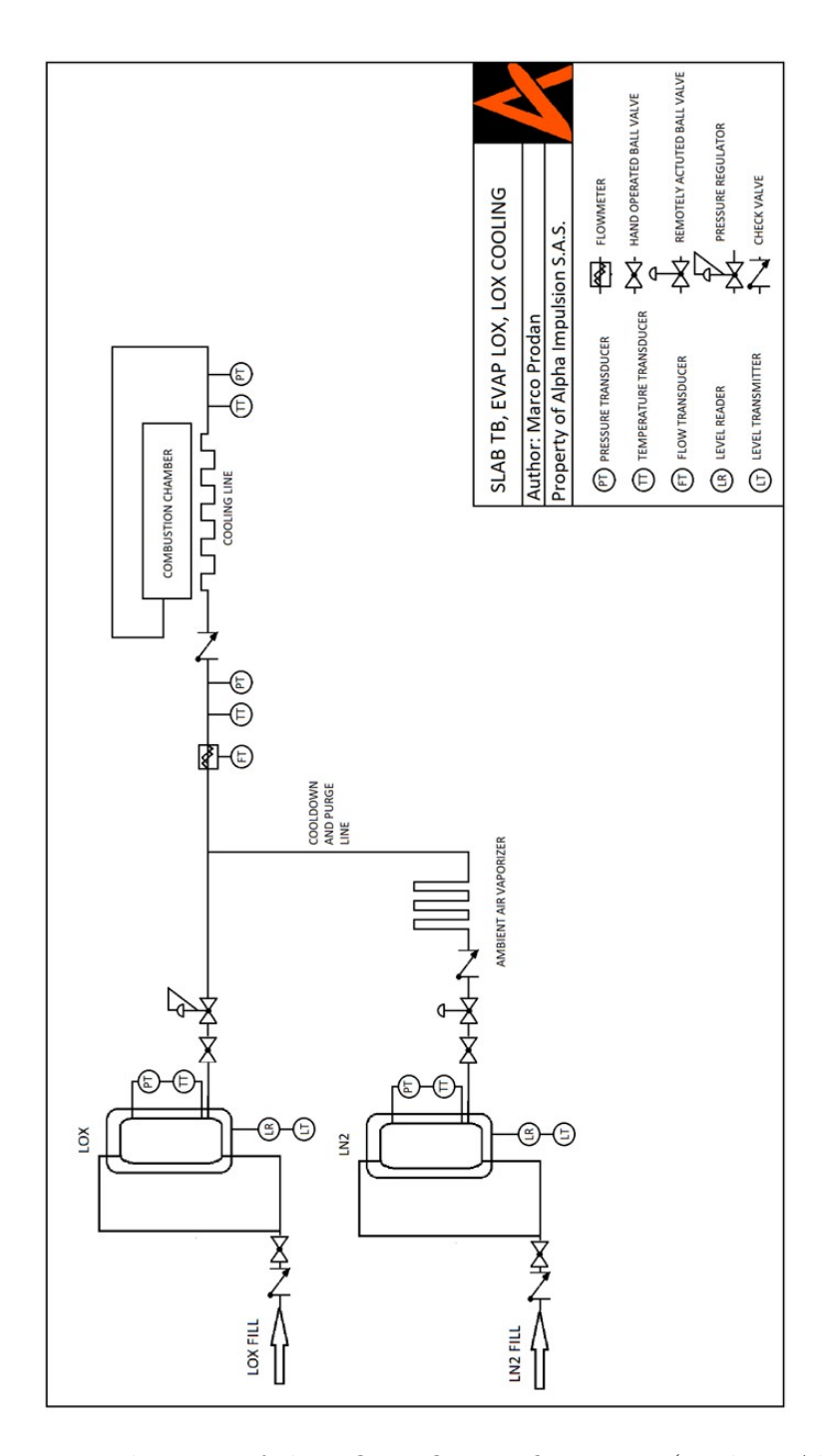


Figure 4.4: PFD diagram of the LOX-LOX configuration (credits: Alpha Impulsion)

4.5.1 Specific subsystem considerations

Following the analysis of the three preliminary configurations, several considerations can be made regarding specific components of the fluid system, in particular:

1. Tank selection and sizing:

- determination of the total volume of gaseous oxidizer required to perform a given number of tests;
- determination of the total volume of liquid oxygen required for a defined test campaign, including the choice of storage and pressurization strategy among the available options.
- 2. Valve selection and pipe sizing;
- 3. Sensor selection and compatibility;
- 4. Safety devices and operational procedures.

4.5.2 GOX and GN₂ storage system

Considering the test bench configuration and the temporary nature of its installation, the most reasonable solution is to employ standard high-pressure cylinder racks rather than a single dedicated vessel. This choice reduces cost and lead time, minimizes engineering and certification needs, and enables the use of rental services (e.g., Linde, Air Liquide). All sizing below is based on this assumption.

High-pressure GOX is typically stored at 200 bar in standard cylinders of 10, 20, 40, 50, 60, or 90 L. Delivery at 40 bar corresponds to a fivefold expansion at test conditions, reducing the storage volume requirement. GOX and GN₂ cylinders are usually rated for a MAWP of approximately 300 bar.

Oxygen storage sizing case For a single test requiring 27 kg of GOX, assuming storage at 200 bar and discharge at 40 bar, the equivalent gas volume is approximately 77 L. Accounting for blowdown, a minimum of about 96 L is required to preserve pressure margin.

This estimate assumes isothermal expansion, while the 10 s test duration suggests some cooling during blowdown; in the adiabatic limit the final temperature would drop toward 188 K (-85° C), but heat exchange with ambient reduces the effect.

The plots report the GOX required for one test and the capacity for two reference cases:

- 1. a cylinder pack composed of 10 units of 50 L each (total 500 L);
- 2. the volume for a weekly campaign of three tests.

Blowdown sizing formula To calculate the minimum cylinder volume at 200 bar required to deliver the necessary oxidizer at 40 bar in blowdown mode (isothermal approximation):

$$V_{200 \,\text{bar}} = \frac{V_{\text{required}} \times P_{\text{outlet}}}{P_{\text{initial}} - P_{\text{final}}} \tag{4.1}$$

where $V_{200\,\text{bar}}$ is the equivalent gas volume at 200 bar, V_{required} the demand at the outlet condition, P_{outlet} the operating pressure (40 bar), P_{initial} the storage pressure (200 bar), and P_{final} the minimum allowable pressure (40 bar).

		GOX cylinders at 200 bar calculations		
		need vol of GOX @40 bar, 25°C	385,7143 L	
baı	1 TEST	corresp to vol of GOX @200 bar, 25°C	77,14286 L	
500		delta P (p tank-p output)	160 bar	
AT.		cylinder vol min to do blowdown (@200 bar)	96,42857 L	
OXYGEN CYLINDERS AT 200 bar	IRS			
N N N		N TESTS with set volume of	gas available	
-	N TESTS	Volume available	500 L	
l S		n tests	5 test	
GE/				
8		VOLUME needed for set amount of tests		
	N TESTS	n tests	3 test	
		Volume needed	289,2857 L	

Figure 4.5: results of calculations for the quantity choice of 200 bar GOX cylinders

Case for dimensioning the nitrogen storage

 GN_2 is used for purging and interrupting combustion by displacing oxygen in lines and chamber. The relevant purge volume is the sum of feed-line and chamber volumes. GN_2 is stored at 200 bar and injected after O_2 valve closure following the strategy below.

Purging strategy and operational logic To limit mechanical and thermal stress, internal pressure is allowed to decay to ~ 10 bar before nitrogen injection. A balance is maintained between faster dilution (higher purge pressure) and reduced loads/costs (lower pressure).

Factors to consider

- Purge volume = pipes + chamber.
- Effective purging typically requires 5–7 exchanges.
- Higher purge pressure shortens time but increases stress and certification burden.

• Lower pressure simplifies design but may extend purge duration.

Possible approaches

- 1. Decay to ~ 10 bar, then GN_2 at ~ 12 bar (baseline).
- 2. Immediate high-pressure GN_2 (faster but mechanically harsher; generally discouraged).

Calculations The total purge volume equals the sum of line and chamber volumes. Assuming 5 exchanges, the nitrogen requirement is:

Table 4.3: Estimated nitrogen volume required for purging operations

Component	Geometry / Assumption	Volume [m ³]	Notes
Oxygen feed lines	1.5 in diameter, 4 m length	0.0044	Stainless steel tubing
Combustion chamber	Internal volume	0.0200	
Total system volume		0.0244	_
		0.122	Equivalent purge volume

Residual oxygen mass at valve closure

The trapped oxygen mass at 40 bar with total internal volume $0.024,5\,\mathrm{m}^3$ and density $\sim 52\,\mathrm{kg/m}^3$ is:

$$m_{\rm O_2} = 52 \,\mathrm{kg} \,\mathrm{m}^{-3} \times 0.024,5 \,\mathrm{m}^3 \approx 1.274 \,\mathrm{kg}.$$
 (4.2)

Estimated oxygen depressurization time from 40 bar to 10 bar With initial $\dot{m} = 2.7 \, \text{kg/s}$ and linearized decay, $\dot{m}_{\text{avg}} \approx 1.35 \, \text{kg/s}$ gives:

$$t_{\rm blowdown} \approx \frac{1.27 \,\mathrm{kg}}{1.35 \,\mathrm{kg/s}} \approx 0.94 \,\mathrm{s}.$$
 (4.3)

Assumption on purge duration The purge duration is chosen to ensure at least one full volume exchange of the feed line. Considering a line internal volume of $V_{\text{line}} = 1225 \text{ L}$ (at 1 bar) and a nitrogen volumetric flow rate $\dot{V}_{\text{N}_2} = 122.5 \text{ L/s}$, the complete exchange time is:

$$t_{\text{exchange}} = \frac{V_{\text{line}}}{\dot{V}_{\text{Na}}} = \frac{1225}{122.5} \approx 10 \,\text{s.}$$
 (4.4)

Hence, a 10 s purge guarantees one full line flushing, which is sufficient for routine operations. Longer purges (30–50 s) may be adopted for initial system conditioning or oxygen service.

Calculation of required GN₂ mass flow rate during purge Assuming a 10 s purge:

$$\dot{V}_{N_2}(1 \text{ bar}) = \frac{1225 \text{ L}}{10 \text{ s}} = 122.5 \text{ L/s}, \qquad \dot{V}_{N_2}(200 \text{ bar}) = \frac{122.5}{200} = 0.6125 \text{ L/s}.$$
 (4.5)

A target GN₂ mass flow $\sim 0.15 \, \mathrm{kg/s}$ is adopted.

Final tanks choice

To ensure approximately one week of operation:

- 1. GOX racks are available as 10×50 L with manifold and common regulator;
- 2. single cylinders are typically 50 L;
- 3. full-campaign gas on site increases cost/space; a weekly refill for GOX with full-campaign GN_2 is a practical compromise.

Final configuration: one 10×50 L GOX rack and two 50 L GN₂ cylinders. Parameters:

Table 4.4: Storage and operating parameters for oxygen and nitrogen systems

Parameter	GOX	$\overline{\mathbf{GN}_2}$
Storage solution	10×50 L cylinder rack	$2 \times 50 \text{ L cylinders}$
Vessel pressure [bar]	200	200
Total volume at storage pressure [L]	500	100
Vessel temperature [K]	298	298
Output pressure (after regulator) [bar]	40 – 50	10–16
Output mass flow rate [kg/s]	2.7	0.15

4.5.3 LOX storage and implementation for cooling

LOX storage supplies the coolant prior to evaporation to GOX. To remain supercritical during gas generation and meet injection conditions, delivery at ≥ 40 bar must be ensured either by tank pressure, a booster/compressor, or a blowdown vessel. The choice reflects feasibility, safety, and cost.

LOX tank calculations

Adopting the small dewar + bulk pressurization option, the LOX mass per test equals the injected GOX mass. Three tests are considered for a weekly design horizon. Residual LOX (heel), boil-off, and pressurization consumption are included.

Table 4.5: Estimated LOX and GOX volumes required for weekly test operations

Parameter	Value	Unit / Notes
Volume needed	360.0 23.7	L of GOX L of LOX
Density (at 90 K, 1 bar) Density (at 300 K, 1 bar) Phase conversion ratio	$ \begin{array}{c} 1140 \\ 1.43 \\ \frac{1140}{1.43} \approx 797 \end{array} $	$\begin{array}{c} \rm kg/m^3 \\ \rm kg/m^3 \\ - \end{array}$
Tank minimum volume	85.2	L

Considering margins and operational losses, a $100\,\mathrm{to}\ 150\,\mathrm{L}$ dewar is indicated and aligns with available rental sizes.

Considerations on LOX to GOX evaporation

Ideal-gas scaling suggests high pressure with heating; practically, evaporators deliver gas near tank pressure at near-ambient temperature. Meeting 40 bar GOX may thus require higher tank pressure or downstream boosting.

Final layout

The storage vessels have been positioned to ensure efficient and safe operations: their location allows straightforward access for cylinder replacement and routine maintenance, while remaining shielded from the exhaust plume and hot gases released during firings. The stand-off distance to the test article and the flame path has been selected to reduce risk in off-nominal scenarios and to comply with safety margins adopted for the bench layout. Piping routes minimize length and bends and limit the number of penetrations through the container structure, thereby improving integrity, reducing leak points, and simplifying inspection.

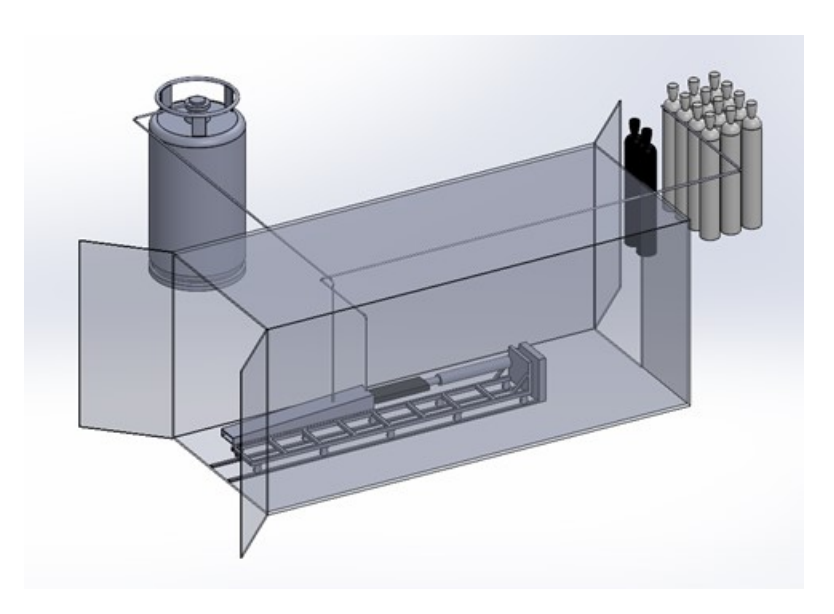


Figure 4.6: CAD model of a preliminary configuration of LOX dewar, GOX and GN2 tanks (credits: Alpha Impulsion)

4.5.4 Pipes, valves, and sensors

Following the definition of the main components of the feed system—the storage tanks—attention is now directed to the delivery process of the fluids toward the combustion chamber and the cooling system, ensuring that all parameters are properly controlled. This subsystem must perform several fundamental tasks to guarantee operational reliability, precision, and safety. These include:

- 1. Controlling the flow path of the fluids;
- 2. Regulating pressure and mass flow rate to meet test conditions;
- 3. Ensuring safety against potential emergency scenarios such as overpressure or leaks;
- 4. Acquiring relevant thermofluidic parameters through sensors to continuously monitor system status.

From this point onwards, the evaluated configuration considers GOX and GN2 cylinders in combination with a LOX dewar. A preliminary schematic representation of the main system layout is shown in Figure 4.7, illustrating the integration between feed lines, control valves, sensors, and safety devices.

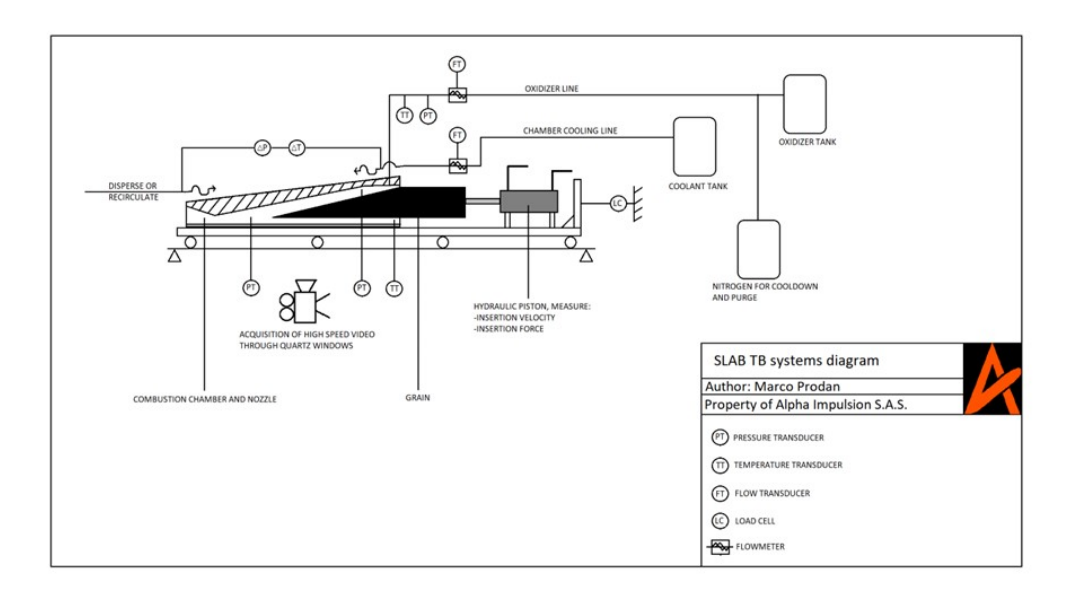


Figure 4.7: Preliminary schematic of the fluid feed system, including control and measurement components (Credits: Alpha Impulsion)

Pipe size selection for feed lines

The sizing of the feed lines for gaseous oxygen (GOX), gaseous nitrogen (GN_2), and liquid oxygen (LOX) follows the same methodology and calculation approach discussed in Chapter 2, where the detailed derivations of pressure losses and flow characteristics are reported. In this section, only the most relevant results and design choices are summarized.

Gaseous oxygen line For the gaseous oxygen delivery, the main design parameters are:

- Mass flow rate: $2.7 \,\mathrm{kg \, s^{-1}}$;
- Pressure: 40 bar;
- Pipe material: Stainless steel AISI 304/316;
- Maximum acceptable pressure drop: 0.2 bar over a 5 m section.

Two pipe diameters were considered for evaluation. For a 2 in internal diameter ($52\,\mathrm{mm}$), the computed flow velocity is approximately $25\,\mathrm{m\,s^{-1}}$, corresponding to a moderate risk level for oxygen service. Pressure losses, obtained through the Darcy–Weisbach equation with the Swamee–Jain friction factor correlation, result in approximately $5.99\,\mathrm{kPa\,m^{-1}}$. Increasing the diameter to $2.5\,\mathrm{in}$ ($65\,\mathrm{mm}$) reduces the pressure loss to about $2.93\,\mathrm{kPa\,m^{-1}}$, with a lower velocity of roughly $15.8\,\mathrm{m\,s^{-1}}$. Although the larger pipe size increases costs and fitting complexity, it provides better safety margins and lower erosion risk.

Final choice: 2.5 in (DN65) piping, oxygen-certified per ASTM A269 and cleaned according to ASTM G93, consistent with CGA G-4.4 and ISO 7291 standards.

Gaseous nitrogen purge line The nitrogen purge line was dimensioned to safely and quickly displace residual oxygen during shutdown operations. From previous calculations, the required nitrogen mass flow rate is about $0.43\,\mathrm{kg\,s^{-1}}$, corresponding to a volumetric flow of approximately $85\,\mathrm{L\,s^{-1}}$ at 10 bar and $25\,^{\circ}\mathrm{C}$. Considering mechanical constraints and recommended flow velocities (below $20\text{-}25\,\mathrm{m\,s^{-1}}$), the following options were evaluated:

- 1 in (DN25): excessive velocity, $> 25 \,\mathrm{m \, s^{-1}}$;
- 1.5 in (DN40): optimal balance, $\approx 13.5 \,\mathrm{m \, s^{-1}}$;
- 2 in (DN50): lower velocity but unnecessarily higher cost.

The corresponding pressure loss for the 1.5 in line is below $1.5 \,\mathrm{kPa}\,\mathrm{m}^{-1}$, which is negligible over the 5 m section. This diameter was therefore selected as the best compromise between efficiency, cost, and simplicity.

Liquid oxygen line For the LOX feed system, the following operating conditions were considered:

• Mass flow rate: $2.7 \,\mathrm{kg}\,\mathrm{s}^{-1}$;

• Temperature: 90 K;

• Pressure: 50 bar.

Assuming incompressible, steady, turbulent flow, pressure losses were computed via the Darcy–Weisbach equation using typical LOX properties at 90 K. Three diameters were evaluated:

Table 4.6: Pressure losses and flow velocity in candidate LOX lines

Diameter [in]	Velocity [m/s]	Pressure loss $[kPa/m]$	
1.0	24.9	0.79	
1.5	11.1	0.52	
2.0	6.2	0.39	

The 1.5 in line provides the best trade-off between hydraulic performance and cost: it ensures moderate flow velocity $(11 \,\mathrm{m\,s^{-1}})$ and acceptable losses while avoiding the weight and expense of larger diameters.

Final choice: 1.5 in (DN40) for the LOX feed system.

Summary of feed line parameters

Important consideration on oxygen line pressure drop The summarized data in the tables above include all relevant parameters for the sizing of the feed lines. Although the pressure drop in the gaseous oxygen line has been reduced by adopting a larger diameter, it remains significant; therefore, the total pipe length will be minimized, and the outlet pressure from the regulator slightly increased to compensate for frictional losses.

Table 4.7: Summary of feed line sizing for gaseous systems (GOX and GN₂)

Parameter	GOX line	\mathbf{GN}_2 purge line
Fluid	Gaseous O_2	Gaseous N ₂
Mass flow rate [kg/s]	2.7	0.43
Pressure (operating) [bar]	40	10
Temperature [°C]	25	25
Suggested pipe size	2.5" (DN65)	1.5" (DN40)
Internal diameter [mm]	65	40
Average flow velocity [m/s]	≈ 15.8	≈ 13.5
Pressure loss [kPa/m]	2.93	1.5 (est.)
Pipe material	SS AISI 304/316	SS AISI 304/316
Impingement risk	Medium-low ($v < 20 \text{ m/s}$)	Negligible
Critical references	CGA G-4.4, ISO 7291	CGA G-4.4

Table 4.8: Summary of feed line sizing for liquid oxygen (LOX)

Parameter	LOX line
Fluid	Liquid O ₂
Mass flow rate [kg/s]	2.7
Pressure (operating) [bar]	50
Temperature [°C]	-90
Suggested pipe size	1.5" (DN40)
Internal diameter [mm]	40
Average flow velocity [m/s]	≈ 11.1
Pressure loss [kPa/m]	0.52
Pipe material	SS AISI 304/316
Impingement risk	None
Critical references	CGA G-4.4, ASTM A269

4.5.5 Valve Sizing

To ensure proper sizing of the regulators and valves for both oxygen and nitrogen circuits, the flow coefficient (C_v) was evaluated under their respective operating conditions of pressure, temperature, and mass flow rate. The results below summarize the required coefficients for each configuration.

Table 4.9: Required C_v for pressure regulators

Gas	MFR [kg/s]	Inlet p [bar]	Outlet p [bar]	Req. C_v
Oxygen	2.7	200	40	5.77
Nitrogen	0.43	200	15	0.94

Table 4.10: Reference C_v values for valve and component sizing

Gas	Component Type	Assumed Pressure Drop [bar]	Required C_v
Oxygen	Control Valve	1.0	8.54
Oxygen	Check Valve	0.2	19.09
Nitrogen	Control Valve	0.5	2.56
Nitrogen	Check Valve	0.1	5.73

For the liquid oxygen feed circuit, the same calculation approach was applied. The following table summarizes the required flow coefficients for the main components.

Table 4.11: Calculated C_v for liquid oxygen components

Component	Pressure Drop [bar]	Pressure Drop [psi]	Required C_v
Pressure Regulator	15	217.6	2.54
Control Valve	1	14.5	9.83
Check Valve / Other	0.2	2.9	22.01

List of Required Components The following table summarizes the main components required for each fluid line. With reference on the preliminary PFD diagram, more information on the components is added and will be included in a more detailed PFD diagram. The selection includes all major flow control, safety, and protection devices, sized according to the operating pressures, temperatures, and pipe diameters previously defined. The subsequent step in the design process is to choose real components that satisfy the requested performance.

Table 4.12: Summary of required components for each fluid line

Subsystem	Component Desc.	Nominal Size	Pressure Rating [bar]
COVI	Hand and solenoid valves (ambient tem- perature)	2½"	60
GOX line	Check valve (ambient temperature)	2½"	60
	Relief valve	2½"	60
	Burst disk	2½"	80
	Particulate filter	2½"	60
	Flashback arrestor	$2\frac{1}{2}$ "	60
\mathbf{GN}_2 line	Hand and solenoid valves (ambient tem- perature)	1/2"	20
	Check valve	1½"	60
	Relief valve	1½"	20
	Burst disk	$1\frac{1}{2}$ "	30
LOX line	Hand and solenoid valves (cryogenic, 90 K)	1½"	60
	Check valve (cryogenic, 90 K)	1½"	60
	Relief valve (cryogenic, 90 K)	1½"	60
	Burst disk (cryogenic, 90 K)	1½"	70

4.5.6 Ignition line

The following paragraph is based on the work of my fellow colleague Alessandro Troni, whom I shared the experience at Alpha Impulsion with. [70] The ignition system requires a dedicated fuel line for kerosene (or equivalent). A compact tank feeds an automotive-grade pump to deliver the required flow at controlled pressure. Injection pressures are typically high (100–200 bar) to promote adequate atomization; in direct-injection layouts, high-pressure fuel pumps are employed to supply the injector(s) at chamber inlet conditions.

Two pump architectures are commonly considered:

Table 4.13: Direct-injection pump types for ignition fuel systems

Type	Operating principle and notes	Typical pressure
Piston pump	Reciprocating piston compresses fuel to high pressure; good metering accuracy and dynamic control	100–200 bar (up to 250 bar)
Gear pump	Meshing gears dis- place fuel with simple mechanics; lower me- tering precision than piston pumps	up to 100–150 bar (application-dependent)

Design parameters adopted for the slab-burner ignition line are:

- mass flow rate: 22–33 g/s;
- total mass per ignition sequence: 200 g;
- fuel: kerosene (reference density 800 kg/m³).

The injection line layout includes a mass-flow meter for closed-loop regulation of the pump and a non-return valve downstream of the pump to prevent backflow during transients. Figure 4.8 illustrates the proposed arrangement.

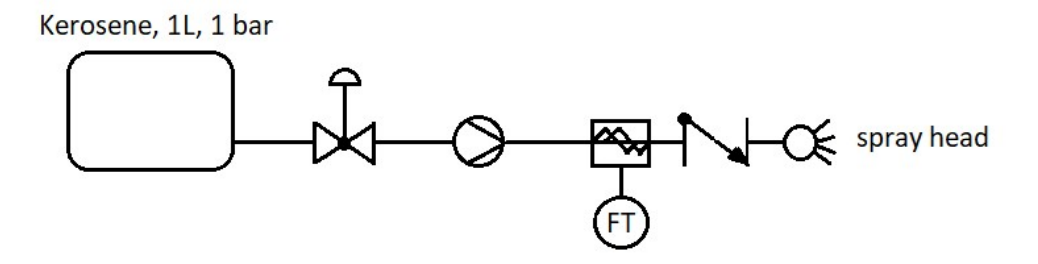


Figure 4.8: Preliminary schematic of the ignition fuel line with tank, high-pressure pump, flow meter, injector, and non-return valve (Credits: Alpha Impulsion)

4.5.7 Acquisition System interfaces

The acquisition system provides continuous monitoring of the main thermodynamic parameters in the test bench, including pressure, temperature, mass flow rate, and liquid levels. The sensors are selected according to the expected operational conditions, covering both cryogenic and ambient regimes, as well as high-temperature measurements in the combustion chamber.

Further details on sensor selection, calibration procedures, and data acquisition hardware will be presented in the dedicated control and acquisition chapter.

4.5.8 Water Deluge System

A water distribution circuit is implemented for three main purposes:

- 1. hydrostatic and pressure testing of piping systems;
- 2. pre-cooling of lines and components before LOX operation;
- 3. external water deluge for flame and heat suppression near the nozzle exit.

The system consists of a 500 L water tank, a pump capable of delivering approximately 2 kg/s, distribution piping, and a control valve. Depending on the configuration, the water line can be connected to:

- the fluid network for pressure testing,
- the cooling loop to simulate cryogenic operation using water,
- a dedicated set of sprayers positioned around the nozzle exit for flame damping.

4.5.9 Final Configuration of the Feed System

The preliminary configuration of the complete feed system is defined once all components, operating parameters, and safety features are consolidated in a detailed P&ID diagram.

Key updates from the previous design iteration include:

- 1. integration of the ignition fuel line for kerosene injection;
- 2. inclusion of all safety and relief devices;
- 3. final sizing of valves and piping sections;
- 4. definition of tank operating conditions;
- 5. integration of the full sensor network;
- 6. addition of the water deluge, cooling, and testing system.

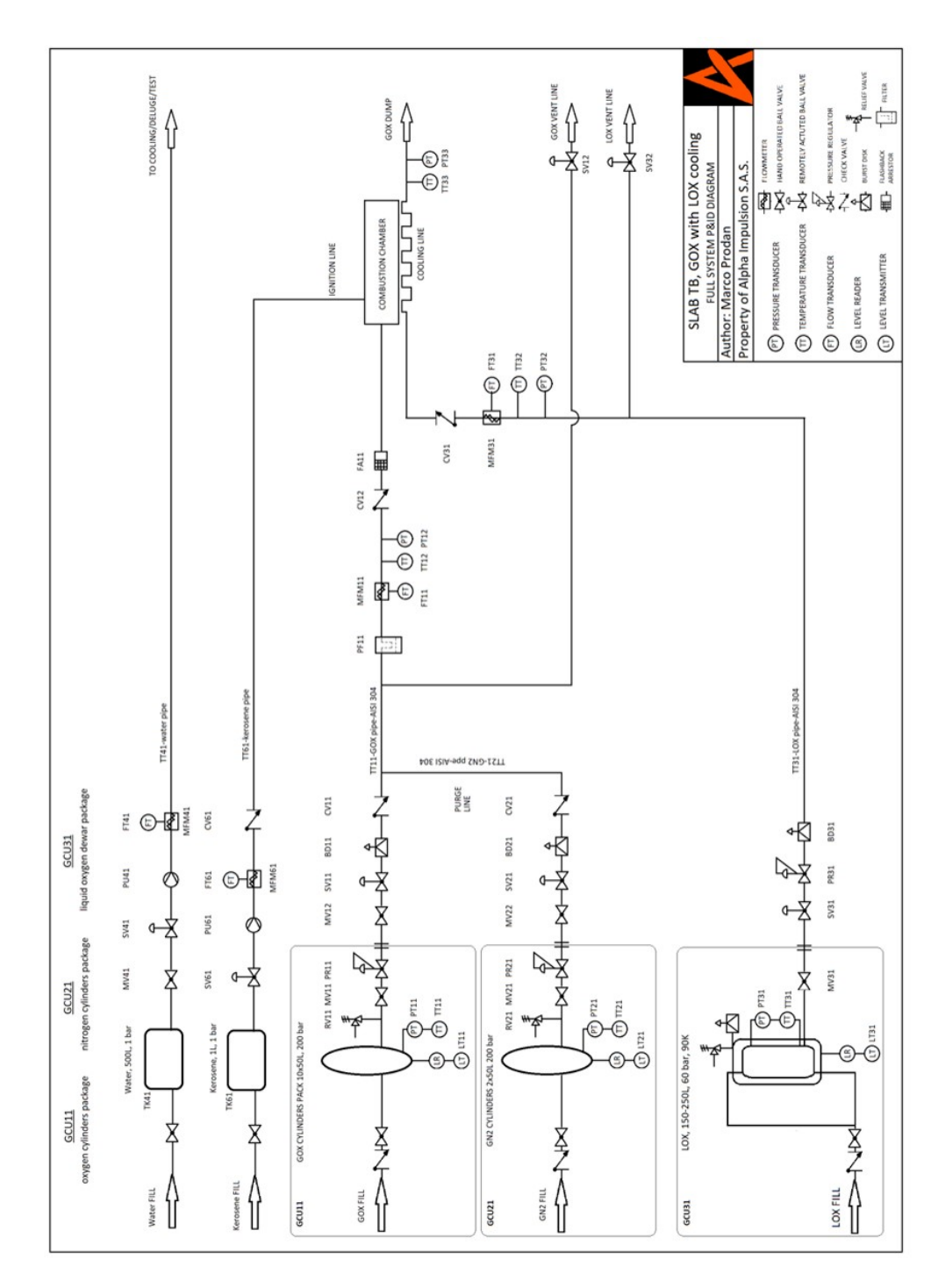


Figure 4.9: PID diagram of the feed system preliminary design (credits: Alpha Impulsion)

4.6 Acquisition System

The acquisition and control system provides both supervision and command of the test bench. Operators can manage:

- 1. the feed and fluid systems;
- 2. the insertion and actuation mechanisms;
- 3. the safety and emergency shutdown procedures.

At the same time, the system displays in real time the main monitored quantities, including pressures, temperatures, mass flow rates, fluid levels, thrust, and combustion chamber parameters.

A load cell rated for up to $10\,\mathrm{kN}$ is installed to measure the thrust produced by the engine. The acquisition chain also synchronizes all measurements for consistent time correlation between signals.

4.6.1 Control and Data Flow Architecture

The architecture integrates analog and digital acquisition channels with remotely actuated components such as valves and regulators. Each actuator requires a control signal, power line, and position feedback. Spare channels are included to allow future expansion of sensors or actuators. A video monitoring subsystem records the combustion through quartz windows using thermal and high-speed cameras.

The main data acquisition frequencies are:

• temperature: 500 Hz;

• pressure: 1000 Hz in the combustion chamber, 500 Hz in piping;

• thrust: 1000 Hz.

4.6.2 Measurement and Video Equipment

The system includes both traditional sensors and optical diagnostic tools:

- Thermal cameras (e.g., FLIR series) for surface temperature mapping and cooling performance verification;
- **High-speed cameras** (e.g., Phantom series) to capture ignition and combustion transients;
- Both are installed in shielded housings and connected via standard HDMI, USB, or Ethernet interfaces.

4.6.3 Standard Sensors and Outputs

Table 4.14 summarizes the transducers installed on the test bench and their signal types.

Table 4.14: Summary of transducers and signal types in the acquisition system

Sensor Type	Measured Quantity / Application	Signal Type
Temperature sensors	Measure temperatures in tanks, pipes, and combustion chamber	Analog (current or voltage)
Pressure sensors	Record pressures in tanks, lines, and chamber	Analog (current or voltage)
Mass flow meters	Measure oxidizer and coolant flow	Digital (Modbus, CAN, or Ethernet)
Level sensors	Monitor LOX and LN_2 tank levels	Digital (discrete or fieldbus)
Load cell	Measure thrust up to 10 kN	Analog (strain-gauge bridge)
Thermal cameras	Record surface temperature distributions	Digital (video stream)
High-speed cameras	Capture transient combustion events	Digital (Ethernet/BNC data stream)

All sensors are rated for the expected temperature and pressure ranges of the test bench and are integrated within the overall control and safety logic.

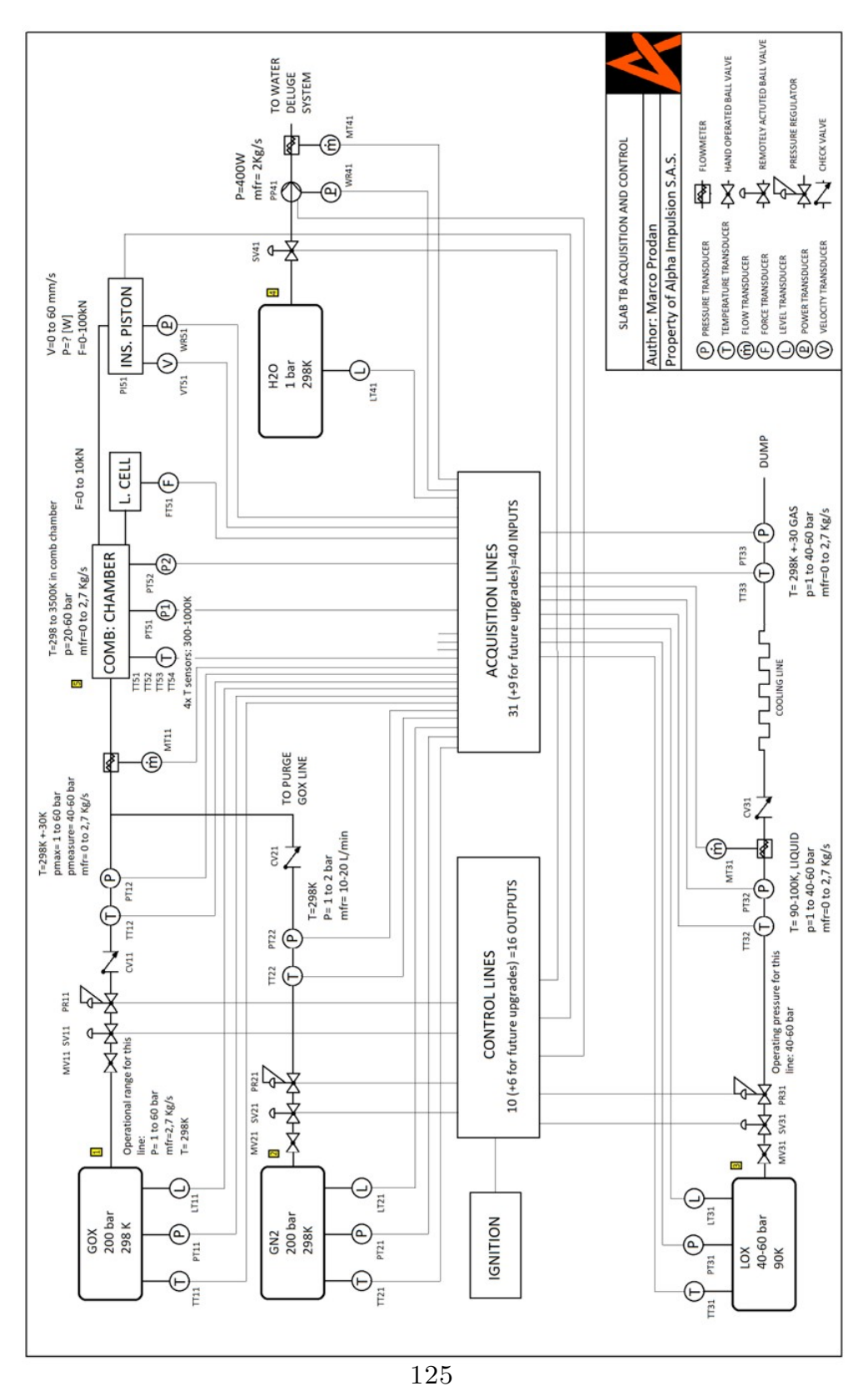


Figure 4.10: diagram of the acquisition system control and command connections (credits: Alpha Impulsion)

N	code	category	item name	description	provider reference	quantity	identif.	IN/OUT
				for now jjust alibaba one with				
23		acquisition	cryo mfm	doubled price	<u>link</u>	1	MT31	input
24		acquisition	Load cell	2-10kN link		1	FT51	input
				0-3Kg/s, operative conditions: 298K, 0-				
25		acquisition	gox mass flow meter	60 bar	omega	1	MT11	input
				1-60 bar, precise in the range 40-60,			PT12;	
26		acquisition	pressure sensor gox	T=298K+-30K, 1kHz	omega	2	PT33	input
							TT12;	
27		acquisition	temperature sensor gox	298+-30K, 500Hz	omega	2	TT33	input
				1-2 bar, T=298K+-30K, 1kHz PXM419-				
28		acquisition	pressure sensor gn2	010BGI	omega	1	PT22	input
29		acquisition	temperature sensor gn2	298+-30K, 500Hz	omega	1	TT22	input
				1-60 bar, precise in the range 40-60,				
30		acquisition	pressure sensor lox	T=90K+30K, 1kHz	omega	1	PT32	input
31		acquisition	temperature sensor lox	90+30K, 500Hz	omega	1	TT32	input
				1-60 bar, precise in the range 40-60,				
			pressure sensor combustion	operative temeprature T=298K to			PT51;	
32		acquisition	chamber	3500K(less realistically), 1kHz	omega	2	PT52	input
							TT51	
			temperature sensor	300 to 1000K, to place outside the			a	
33		acquisition	combustion chamber	combustion chamber, on walls, 500Hz	omega	4	TT54	input
34		acquisition	level sensor gox tank	defined by tank provider		1	LT11	input
35		acquisition	pressure sensor gox tank	defined by tank provider		1	PT11	input
36		acquisition	temperature sensor gox tank	defined by tank provider		1	TT11	input
37		acquisition	level sensor gn2 tank	defined by tank provider		1	LT21	input
38		acquisition	pressure sensor gn2 tank	defined by tank provider		1	PT21	input
39		acquisition	temperature sensor gn2 tank	defined by tank provider		1	TT21	input
40		acquisition	pressure sensor LOX tank	defined by tank provider		1	PT31	input
41		acquisition	temperature sensor LOX tank	defined by tank provider		1	TT31	input
42		acquisition	piston voltage	output from piston (see datasheet)		1	VT51	input
43		acquisition	piston power	output from piston (see datasheet)		1	WR51	input
44		acquisition	level sensor water tank	scale or indirect read from mfm		1	LT41	input
45		acquisition	level sensor LOX tank	defined by tank provider		1	LT31	input
46		acquisition	water pump power	output from pump		1	WR41	input
47		acquisition	mass flow meter water	2 kg/s water pump	<u>link</u>	1	MT41	input
				ACQUISIZIONE/ELABORAZIONE				
		acquisition	TELECAMERA OTTICA	IMMAGINI?		1		input/out
				ACQUISIZIONE/ELABORAZIONE				
		acquisition	TELECAMERA TERMICA	IMMAGINI?		1		input/out
			IGNITION					output
							SV11	output
							PR11	output
							SV21	output
							PR21	output
							SV31	output
							PR31	output
							SW41	output

Figure 4.11: breakdown of input/output of the system (credits: Alpha Impulsion)

4.7 Integration and final considerations

The design activity carried out for the slab burner test bench led to a comprehensive preliminary configuration of the system, integrating structural, fluidic, and control subsystems into a coherent concept. At the current stage, the main outcomes of the study include the structural layout of the container-based bench, a defined configuration of the fluid feed systems, and a preliminary control and acquisition network scheme. These elements together establish a solid foundation for the subsequent detailed design and industrial implementation.

The fluid system design has been completed up to the level of defining the operative parameters, pressure and flow requirements, and the preliminary component sizing. The next step, which lies beyond the scope of this thesis, consists in the detailed selection and procurement of components. This phase requires close collaboration with suppliers to compare specifications, costs, and delivery conditions, leading to the final choice of tanks, pipes, valves, sensors, regulators, and other critical parts. This process was initiated and partially developed during the author's internship experience at *Alpha Impulsion*, where significant time was dedicated to supplier contact, quotation analysis, and compatibility verification. However, due to confidentiality reasons and the industrial nature of the information, the related material is not reported in this document.

The control and acquisition system configuration, including the mapping of all measurement and actuation channels, is also finalized to the level required for external development. The diagrams and functional descriptions prepared as part of this work provide the necessary basis for future collaboration with specialized automation companies, which will implement the complete control interface and data acquisition architecture. Discussions with several potential suppliers have already started, but the detailed engineering and integration activities exceed the boundaries of the present study.

As for the broader considerations introduced in Chapter 2, this project has focused primarily on the systems engineering aspect of the slab burner bench. While the mechanical integration, safety validation, and operational testing phases remain to be completed, the current outcome successfully defines the technical and functional framework of the bench. In conclusion, the work establishes a robust preliminary design that can now evolve into the detailed engineering and realization phases, serving as a practical reference for future developments within the hybrid autophage propulsion research program.

Chapter 5

Comparison between the two case studies

General design approach. The design processes of the two test benches differ significantly, primarily due to the disparity in their scale, complexity, and objectives. While both projects share the same methodological foundation, the slab burner bench benefited from the experience acquired during the development of the larger launcher test bench, allowing a more refined definition to be reached within a shorter timeframe. The launcher bench, conversely, represents a large-scale infrastructure, requiring a longer and more detailed engineering phase, especially in the integration of multiple subsystems and the management of operational constraints.

Safety considerations. Safety plays a crucial role in both designs, though its implementation scale differs substantially. The launcher test bench, given its higher operating pressures, larger fluid storage volumes, and greater overall energy involved, demands a more extensive analysis of operational safety and redundancy measures. Additional attention is required to implement fail-safe systems, emergency shutdown logic, and protective barriers to ensure safe handling of cryogenic and pressurized fluids. The slab burner bench, while still subject to the same safety principles, involves lower energy levels and simpler configurations, thus allowing for a more streamlined and easily monitored system without compromising safety.

Structural and functional philosophy. The slab burner test bench is intentionally conceived as a compact, modular, and transportable platform. Its design prioritizes simplicity, flexibility, and rapid modification, enabling frequent adjustments and reconfigurations for experimental purposes. In contrast, the launcher bench requires a much longer design and realization process due to the size and

complexity of its subsystems. The involvement of specialized engineers and designers is essential to ensure proper performance and compliance with structural, cryogenic, and operational requirements.

Environmental impact. The environmental characteristics of the two test benches also differ significantly, mainly as a consequence of the vast difference in fluid flow rates and power levels involved. The launcher bench, with its high-thrust engines and large quantities of cryogenic propellants, requires extensive exhaust management and noise mitigation systems. The slab burner bench, on the other hand, has a much smaller environmental footprint, limited mainly to controlled gaseous emissions and localized heat and noise effects, allowing for safer operation in confined or semi-mobile installations.

Measurement and acquisition systems. The two benches have distinct measurement focuses according to their experimental objectives. The slab burner test bench, designed specifically to study the regression rate of the hybrid autophage grain, centers its acquisition system on precise control of the feeding system and high-resolution monitoring of combustion chamber parameters. It also integrates video-based diagnostics—such as high-speed and thermal cameras—as a key part of the measurement process. In contrast, the launcher bench prioritizes the measurement of thrust and the evaluation of engine behavior in autophage mode, emphasizing the assessment of global propulsion performance rather than local regression phenomena.

Insertion mechanisms. A fundamental difference between the two designs lies in the insertion system. In the launcher configuration, the insertion mechanism is based on a screw-driven system integrated into the motor, similar to the expected flight configuration. Any limitations in this system directly influence engine performance and are therefore part of the natural experimental scope. In the slab burner bench, however, the insertion process is treated as a controlled variable: it is performed by a high-power piston capable of overcoming the fuel's mechanical resistance and ensuring the desired advancement rate of the grain within the combustion chamber. This approach minimizes interference between the insertion system and the combustion process, leading to more consistent and measurable results.

Thrust measurement systems. The differences in insertion methods are reflected in the design of the thrust measurement systems. In the launcher test bench, the entire motor assembly is mounted on dedicated support arms equipped with load cells that record the total thrust. This configuration allows vectorial measurements and ensures sensitivity to possible misalignments or lateral thrust

components. Conversely, in the slab burner bench, the thrust produced must be isolated from the piston's mechanical influence. For this reason, the entire assembly is mounted on a rail-guided cart that transfers the generated force to a load cell through a reaction plate. The rail system, designed to minimize friction, ensures accurate force transmission, while the dissipative losses are later modeled and compensated for in data analysis. Although the magnitude of the forces is smaller, thrust remains a fundamental measurable parameter for validating experimental performance.

Summary. Overall, while both test benches share common design principles and are part of the same hybrid propulsion research effort, they differ substantially in purpose, scale, and implementation complexity. The launcher bench represents a full-scale infrastructure aimed at validating propulsion systems for orbital applications, whereas the slab burner bench serves as a flexible, cost-effective research tool to deepen understanding of combustion and regression processes under controlled laboratory conditions.

Chapter 6

Conclusions and Future Developments

Conclusions

This thesis presented the design and preliminary development of two experimental infrastructures aimed at testing hybrid autophage rocket motors. The principal goal was to establish a coherent methodology for the conception of test benches, combining the design of structural, fluidic, control, and acquisition systems into a unified framework. The approach was applied to two complementary case studies—the large-scale launcher test bench and the smaller slab burner rig—which differ significantly in complexity, scale, and functional objectives. This dual analysis made it possible to validate the design logic under distinct operational conditions, providing a consistent yet flexible methodological base.

The work led to the definition of a complete design process that begins with requirement identification and continues through subsystem configuration, safety assessment, and system integration. Both case studies resulted in coherent architectures, in which each subsystem — from tanks and feed lines to the acquisition and control systems — was dimensioned and characterized according to the specific needs of the respective test configuration. Particular attention was devoted to safety, operational feasibility, and environmental considerations, as these aspects are crucial in cryogenic and high-pressure testing environments. The result is a solid conceptual design framework that can guide the realization of both small-scale and large-scale hybrid propulsion testing infrastructures.

Limitations of the Work

While the results obtained represent a comprehensive foundation for further development, this study remains within the boundaries of a preliminary design phase. Several simplifying assumptions were introduced to make the problem tractable and to focus on the overall system integration rather than on the detailed engineering of each component.

The structural design, for instance, has not yet been verified through finite element analysis or experimental validation. Similarly, the thermodynamic and fluid-dynamic models used for sizing the tanks and pipelines — including blowdown calculations and cryogenic evaporation processes — were based on idealized assumptions that will require refinement with more advanced numerical simulations. Safety and automation logics were defined at a conceptual level, outlining the control philosophy but without yet implementing full redundancy or fail-safe mechanisms. In addition, the economic aspects were treated qualitatively, while the actual procurement and cost optimization phase would need to be addressed in collaboration with industrial partners and suppliers.

Despite these limitations, the thesis provides a robust methodological foundation and a set of design references that can be directly employed as a starting point for the detailed engineering phase. The outcomes achieved — particularly the integration of cryogenic and high-pressure systems within modular test infrastructures — already represent a significant step toward the operational realization of hybrid propulsion testing facilities.

Future Developments

Future developments of this work will naturally progress toward the detailed design and practical implementation of the proposed systems. The next step will consist in completing the structural analyses, refining the mechanical layout, and finalizing the component selection based on direct consultation with suppliers. This phase will also involve a more accurate modeling of tank sizing and blowdown behavior, taking into account non-isothermal gas expansion, real-gas properties, and heat transfer with the environment. These refinements will ensure that the theoretical assumptions made during the preliminary design are validated and optimized for real operation.

Once the detailed design is completed, the construction and commissioning of the test benches will represent the first opportunity for experimental validation. Through static firing campaigns and controlled testing, it will be possible to verify the effectiveness of the feed systems, evaluate the performance of the acquisition architecture, and refine the regression-rate measurement methodology. Particular emphasis will be placed on the slab burner rig, which, due to its simplicity and modularity, offers the ideal platform for iterative testing and model validation. The data collected from these campaigns will provide valuable insight for improving numerical models of hybrid autophage combustion and for validating the design choices made in this study.

From a broader perspective, future work could also focus on expanding the acquisition and control system toward real-time data management and advanced safety automation, possibly including hardware-in-the-loop simulations. Environmental and safety analyses could also be deepened, extending to exhaust management, noise reduction, and risk assessment in cryogenic environments. Finally, the methodologies developed here could be adapted and scaled to other hybrid or semi-cryogenic propulsion systems, ensuring continuity between laboratory-scale research and large-scale testing infrastructures.

Final Remarks

In summary, this thesis established a structured and replicable approach to the design of hybrid rocket engine test facilities, bridging the gap between theoretical research and experimental realization. By integrating multidisciplinary aspects — from cryogenic feed systems to data acquisition and safety management — the work provides a complete reference framework for future test bench development. The methodologies, results, and design strategies presented here represent not an endpoint, but a foundation upon which future engineers and researchers can build more advanced, detailed, and experimentally validated test systems, contributing to the ongoing evolution of hybrid and autophage propulsion technologies toward full operational maturity.

Bibliography

- [1] Shamim Rahman, Bartt Hebert, Mark Glorioso, and Richard Gilbrech. «Rocket Propulsion Testing at Stennis Space Center: Current Capability and Future Challenges». In: 39th AIAA/ASME/SAE/ASEE Joint Propulsion Conference and Exhibit. July 2003. ISBN: 978-1-62410-098-7. DOI: 10.2514/6.2003-5038 (cit. on pp. 2, 3).
- [2] NASA. Stennis Space Center. Accessed: 2025-10-02. 2025. URL: https://www.nasa.gov/stennis/ (cit. on pp. 2, 6, 16, 31, 53, 55).
- [3] DLR German Aerospace Center. Test Facilities Department. Accessed: 2025-10-02. 2025. URL: https://www.dlr.de/en/ra/about-us/departments/test-facilities (cit. on pp. 2, 31, 55).
- [4] Wolfgang Kitsche. Operation of Cryogenic Rocket Engines. Berlin, Germany: Springer, 2021. ISBN: 978-3-030-73500-3. DOI: 10.1007/978-3-030-73501-0 (cit. on pp. 2, 9, 14, 16, 18, 20, 24, 27, 53-55).
- [5] Anders Hansson. «Book Review: Fundamentals of Hybrid Rocket Combustion and Propulsion». In: *The Aeronautical Journal* 112.1131 (Mar. 2008). Review of Chiaverini & Kuo (eds.), *Fundamentals of Hybrid Rocket Combustion and Propulsion*, AIAA, 2007, pp. 178–179. DOI: 10.1017/S0001924000087443 (cit. on pp. 5, 14).
- [6] George P. Sutton and Oscar Biblarz. Rocket Propulsion Elements. 9th ed. Hoboken, NJ: John Wiley & Sons, 2017. ISBN: 978-1-119-39217-8 (cit. on pp. 5, 6, 12, 14, 27, 28, 30, 32, 33, 35, 47, 51, 55).
- [7] Martin Gros, Marius Celette, and Dylan de Lima Viana. «Hybrid Autophage Propulsion for Space Launch Vehicles: A Promising Concept». In: *Proceedings of the 74th International Astronautical Congress (IAC)*. HAL Id: hal-04704331. Baku, Azerbaijan: International Astronautical Federation, Oct. 2023. URL: https://iafastro.directory/iac/paper/id/78100/summary/ (cit. on p. 8).

- [8] Fawaz Mustafa. «Autophage Propulsion». PhD Thesis. PhD thesis. University of Glasgow, Sept. 2022. URL: http://theses.gla.ac.uk/id/eprint/82858 (cit. on p. 8).
- [9] Yousef Haik and Tamer Shahin. *Engineering Design Process*. 2nd ed. Stamford, CT: Cengage Learning, 2010. ISBN: 978-0-495-66816-6 (cit. on p. 14).
- [10] CEN European Committee for Standardization. EN 1992-1-1: Eurocode 2: Design of Concrete Structures Part 1-1: General Rules and Rules for Buildings. Brussels: CEN. 2004 (cit. on p. 17).
- [11] Randall F. Barron. *Cryogenic Systems*. 2nd ed. Oxford University Press, 1985. ISBN: 978-0195035671 (cit. on pp. 18–20, 24, 25, 27–33, 35, 47).
- [12] H. P. Edwards and W. H. Avery. Cryogenic Propellant Technology. Tech. rep. NASA, 1966 (cit. on pp. 18, 19).
- [13] Jack W. Ekin. Experimental Techniques for Low-Temperature Measurements: Cryostat Design, Material Properties and Superconductor Critical-Current Testing. Oxford University Press, 2006. ISBN: 978-0-19-857054-4 (cit. on pp. 18, 19).
- [14] G. H. Kinchin and R. S. Pease. *Cryogenic Engineering*. Academic Press, 1971. ISBN: 978-0124078508 (cit. on p. 19).
- [15] Jaroslaw Polinski. *Materials in Cryogenics*. Tech. rep. Lecture notes, CERN Cryogenics Course 2010. Geneva, Switzerland: CERN European Course in Cryogenics, 2010. URL: https://indico.cern.ch/event/90787/session/1/attachments/1093424/1559936/Materials_in_Cryogenics.pdf (cit. on pp. 20–23).
- [16] T. D. Bostock and R. G. Scurlock. Low-Loss Storage and Handling of Cryogenic Liquids. Springer, 2019. DOI: 10.1007/978-3-030-10641-6 (cit. on pp. 24, 25, 27).
- [17] H. W. Marsh. «Design of Cryogenic Storage Tanks for Industrial Applications». In: ASTM Special Technical Publication. ASTM International, 1962 (cit. on pp. 24, 25).
- [18] W. Johnson. Development Path for Cryogenic Insulation Systems. Tech. rep. NASA, 2019. URL: https://ntrs.nasa.gov/api/citations/20190027327/downloads/20190027327.pdf (cit. on pp. 24, 25).
- [19] R. H. Perry and D. W. Green. Perry's Chemical Engineers' Handbook. 9th ed. McGraw-Hill, 2019. ISBN: 978-0-07-183408-7 (cit. on pp. 27-33, 47, 48, 85, 87).
- [20] Cryogenic Vessels Gas/Materials Compatibility. International Organization for Standardization, 2017 (cit. on pp. 27, 29–33, 37, 44, 47, 48).

- [21] Oxygen Pipeline and Piping Systems. Compressed Gas Association, 2019 (cit. on pp. 27, 30–33, 38, 39).
- [22] Oxygen Pipeline and Piping Systems. Tech. rep. Doc 13/20. European Industrial Gases Association (EIGA), 2020 (cit. on pp. 27, 28, 30, 32, 33, 37, 47, 48, 86, 87, 90).
- [23] Recommended Practice on Static Electricity. National Fire Protection Association, 2019 (cit. on pp. 27, 30–32).
- [24] Standard Practice for Selection and Use of Materials for Oxygen-Enriched Environments. ASTM International, 2020 (cit. on pp. 27, 30–32).
- [25] Standard for the Design and Fabrication of Ground Support Equipment. NASA, 2016 (cit. on pp. 27, 30–32).
- [26] Standard Practice for Cleaning Methods and Cleanliness Levels for Material and Equipment Used in Oxygen-Enriched Environments. ASTM International, 2020 (cit. on pp. 27, 30, 31, 40).
- [27] Gas Cylinders Refillable Seamless Steel Gas Cylinders Part 1: Normalized Steel Cylinders. International Organization for Standardization, 2019 (cit. on p. 28).
- [28] Gas Cylinders Refilling Stations and Bundles for Compressed Gases Inspection and Testing. International Organization for Standardization, 2010 (cit. on pp. 28, 40).
- [29] Standard Guide for Designing Systems for Oxygen Service. ASTM International, 2013 (cit. on p. 38).
- [30] M. Van Dyke and A. Clark. *Materials for Oxygen Service: Ignition and Combustion Behavior*. Technical Memorandum NASA/TM-2014-217911. NASA, 2014 (cit. on p. 38).
- [31] Cryocomp, Inc. How To Specify a Cryogenic Valve The Basics. Accessed 2025-10-07. 2025. URL: https://www.cryocomp.com/how-to-specify-a-cryogenic-valve/ (cit. on pp. 41, 45).
- [32] Parker Hannifin Corporation. Cryogenic Valves Catalog Parker Bestobell. Accessed 2025-10-07. Parker. 2025. URL: https://www.parker.com/content/dam/Parker-com/Literature/Instrumentation-Products-Division/Catalogs/Cryogenic-Valves-for-Industrial-Gas-Applications.pdf (cit. on pp. 41, 42, 45).
- [33] Parker Hannifin Corporation. Cryogenic Check Valves Parker Bestobell. Accessed 2025-10-07. Parker. 2025. URL: https://ph.parker.com/us/en/product-list/cryogenic-check-valves (cit. on p. 42).

- [34] Parker Hannifin Corporation. Cryogenic Safety Relief Valves Parker. Accessed 2025-10-07. Parker. 2025. URL: https://ph.parker.com/br/en/product/cryogenic-safety-relief-valve/cwt20rr17n00 (cit. on p. 43).
- [35] Ramen Valves. Oxygen Degreased Valves: A Critical Safety Measure. Accessed 2025-10-07. 2024. URL: https://www.ramenvalves.com/uncategorized/oxygen-degreased-valves-a-critical-safety-measure/(cit. on p. 44).
- [36] Lake Shore Cryotronics, Inc. DT-670 Series Silicon Diode Temperature Sensors. Accessed 2025-10-07. Lake Shore Cryotronics. Westerville, OH, USA, 2023. URL: https://www.lakeshore.com/products/dt-670-series-diodes (cit. on p. 47).
- [37] Omega Engineering, Inc. PR-10 Series Precision Platinum Resistance Temperature Detectors (RTDs). Accessed 2025-10-07. Omega Engineering. Norwalk, CT, USA, 2023. URL: https://www.omega.com/en-us/temperaturemeasurement/rtd-sensors/pr-10-series/p/PR-10-2-100-1-8-6-E (cit. on p. 47).
- [38] Beckhoff Automation. EtherCAT Technology Overview. Accessed: 2025-10-03. 2022. URL: https://www.ethercat.org/en/technology.html (cit. on p. 51).
- [39] Siemens AG. PROFINET Industrial Ethernet System Description. Accessed: 2025-10-03. 2020. URL: https://new.siemens.com/global/en/products/automation/profinet.html (cit. on p. 51).
- [40] S. Pereira. Fieldbuses for Process Control: Engineering, Operation, and Maintenance. ISA International Society of Automation, 2005. ISBN: 9781556178696 (cit. on p. 51).
- [41] Vinod Kumar, P. Krishnan, and N. Rajesh. «Effect of Various Deflectors on Acoustic Load Distribution during Rocket Vehicle Launch». In: *International Journal of Engineering Research & Technology (IJERT)* 2.6 (2013), pp. 867–870. URL: https://www.ijert.org/research/effect-of-various-deflectors-on-acoustic-load-distribution-during-rocket-vehicle-launch-IJERTV2IS60867.pdf (cit. on p. 53).
- [42] Jai S. Sachdev, Vineet Ahuja, Ashvin Hosangadi, and Daniel C. Allgood. «Analysis of Flame Deflector Spray Nozzles in Rocket Engine Test Stands». In: AIAA/ASME/SAE/ASEE Joint Propulsion Conference & Exhibit (2010). AIAA 2010-6972 (cit. on pp. 68, 78).
- [43] P. L. Hensarling. *Test Facilities Capability Handbook*. Tech. rep. NASA NTRS. NASA / NTRS, 2007 (cit. on p. 69).
- [44] Structures to Resist the Effects of Accidental Blast (UFC 3-340-02). Tech. rep. UFC 3-340-02, WBDG. U.S. Department of Defense, (cit. on p. 70).

- [45] JJ Hansen / Sun Devil Rocketry. Student Design of a Bipropellant Liquid Rocket Engine and Test Stand. Sun Devil Rocketry design report. (cit. on p. 70).
- [46] A. R. Meghavath. «Design of a State-Of-The-Art Test Facility for Rocket Engines». In: —. DivA portal thesis. 2022 (cit. on pp. 70, 76).
- [47] «Pressure-impulse blast response of steel ISO containers». In: (—). Study on blast behavior of ISO containers (cit. on p. 71).
- [48] EN 1993-1-1: Eurocode 3 Design of steel structures General rules and rules for buildings. 2005 (cit. on pp. 74, 77, 78).
- [49] NAFEMS Ltd. Best Practice Guide: Finite Element Analysis of Structural Components. Tech. rep. 2020 (cit. on p. 74).
- [50] DIN 1025-2: Hot rolled steel I and H sections Dimensions, masses, sectional properties. 2011 (cit. on p. 75).
- [51] EN 1993-1-2: Eurocode 3 Design of steel structures Structural fire design. 2005 (cit. on pp. 76, 78).
- [52] ArcelorMittal. Material data sheet: S235JR structural steel. https://steelsection.com/s235jr/. 2024 (cit. on p. 76).
- [53] ThyssenKrupp Materials. S235 and S355 mechanical properties. https://www.thyssenkrupp-materials.co.uk. 2024 (cit. on p. 76).
- [54] George E. Totten. Handbook of Mechanical Alloy Design and High Temperature Properties. CRC Press, 2013 (cit. on pp. 76, 78).
- [55] ASM International. ASM Handbook Volume 1A Properties and Selection: Irons, Steels, and High-Performance Alloys. 2020 (cit. on pp. 76, 78).
- [56] MSC Software. NASTRAN 2018 User Guide Linear Static and Thermal Analysis. 2018 (cit. on p. 76).
- [57] D. Anderson and J. Hall. «Design of Reusable Rocket Test Structures for University-Scale Engines». In: *AIAA Propulsion Conference*. 2021 (cit. on p. 76).
- [58] EN 1992-1-1: Eurocode 2: Design of Concrete Structures Part 1-1: General Rules and Rules for Buildings. Brussels, Belgium, 2004 (cit. on p. 80).
- [59] CEB-FIP Model Code for Concrete Structures. Lausanne, Switzerland: Comité Euro-International du Béton, 1978 (cit. on p. 80).
- [60] Chart Industries. Vacuum Insulated Piping (VIP) Systems Technical Overview. https://www.chartindustries.com. 2023 (cit. on pp. 84, 90).
- [61] ISO 21010: Cryogenic vessels Gas/materials compatibility. 2017 (cit. on pp. 84, 86).

- [62] Emerson. Micro Motion Coriolis Meters for Cryogenic Liquids. https://www.emerson.com. 2024 (cit. on p. 84).
- [63] CGA G-4.4: Oxygen Pipeline Systems. Tech. rep. Compressed Gas Association, 2013 (cit. on p. 84).
- [64] HEROSE GmbH. Cryogenic Valves for Industrial Gases and LOX Service— Catalog. https://www.herose.com. 2024 (cit. on p. 84).
- [65] Flow of Fluids Through Valves, Fittings, and Pipe (Crane TP-410). Crane Co. 2018 (cit. on p. 85).
- [66] NIST. Thermophysical Properties of Oxygen. https://webbook.nist.gov/chemistry/ (accessed 2024). 2024 (cit. on p. 85).
- [67] George P. Sutton and Oscar Biblarz. *Rocket Propulsion Elements*. 9th. Wiley, 2017 (cit. on pp. 85, 89).
- [68] Nikkiso ACD. Cryogenic Pumps for LOX/LIN/LNG Product Overview. https://www.nikkisocryo.com. 2024 (cit. on p. 89).
- [69] Barber-Nichols. Cryogenic Pumps and Turbo Pumps LOX Applications. https://www.barber-nichols.com. 2024 (cit. on p. 89).
- [70] Alessandro Troni. «Preliminary design of a hybrid autophage engine test bench». Master's Thesis. Milan, Italy: Politecnico di Milano, 2025 (cit. on p. 119).